Porosity and permeability in the Graminia Formation, Upper Devonian Winterburn Group in the Germain Field, northeastern Alberta

by

Meghan Emilie Black

A thesis submitted in partial fulfillment of the requirements for the degree of

Master of Science

Department of Earth and Atmospheric Sciences

University of Alberta

Abstract:

The Upper Devonian Graminia Formation (Winterburn Group) found in the Germain field of northeastern Alberta includes the Blueridge Member (Frasnian) and the Upper Graminia Member (Famennian). A green silty-shale paleosol overlies the formation in this area. The bitumen-bearing dolostones of this formation are divided into Facies A, B, C, D, E, and F based on mineralogy, fabric, and cement types. Facies A, B, C, and E are formed of very finely to finely crystalline dolomitic siltstones to silty dolostones that are variably cemented with calcite and dolomite. Facies D is a green silty-shale bed that lies between Facies C and E. Facies F is a powdered dolomite cemented with bitumen.

The sediments of the Blueridge Member were deposited during a third order regression in an inner-ramp setting. The sediments of the Upper Graminia Member were deposited during a fall in sea level that caused the ramp to shallow into the peritidal to supratidal zone. The precise timing and formation of dolomite is not known, but is thought to be sabhka-related based on the depositional framework. Facies F (powdered dolomite) may have been produced by diagenetic changes associated with a period of karst/exposure. Porosity values range from 3 to 40% and average permeability values range from 5 to 450 md. The main types of porosity are intergranular/intercrystalline (very common), vuggy (common) and fracture (rare). The permeability is controlled by the intergranular/intercrystalline pores and fractures. The porosity and permeability values do not display any predictable patterns across the Germain Field.

Acknowledgements:

Thank you to Laricina Energy Ltd. for giving me the opportunity to pursue this project and allowing me to view and sample their cores. I would like to recognize and thank Kent Barrett for his guidance, mentorship and support while I worked at Laricina and as I completed this thesis.

This thesis would not have been possible without my supervisor, Dr. Brian Jones, who provided me with the opportunity to attend graduate school and believed in me from the beginning. I want to thank him for the mentorship, guidance, many lessons in grammar and writing, all of the edits, and for teaching me so much about carbonate sedimentology and the scientific process. Thank you also to the Carbonate Research Group for all of the coffee, ideas and help with my research and graduate courses; Hongwen Zhao, Joshua Thomas, Alexandra Der, Rong Li and Ting Liang.

Thank you to all of the people who were instrumental on the technical end of this thesis; George Braybrook (U of A SEM Lab), Diane Caird (U of A XRD Laboratory), all of the wonderful people at New Horizon Core Storage Ltd. and AGAT Laboratories, and everyone in the University of Alberta Department of Earth and Atmospheric Sciences.

This thesis would never been completed without out the love, major support and financial backing from my parents, Susan and Cameron. Thank you also my sister, Shannon; my Grandpa, Dr. Donald Black; my Nana, Rissa Ayris; my "fairy godmother," Llana Nakonechny; and to all of my Aunts, Uncles and cousins. A special thanks to my Great Aunt Val, who I sadly lost during my time at U of A while writing this thesis; I know she would have been very proud to see me finish.

Finally, thank you to all of my friends, colleagues and all of the people who assisted me over the years in various ways and throughout all the stages of this thesis. Thank you to Dr. Robert Luth, Dr. Jillian Parboosingh, Dr. Octavian Catuneanu, Joanne Dolan, Jamie Robbins, Sharon and Tony Robbins, and Dennis Price. THANK YOU!

Table of Contents:

List of Tables and Figures:

Tables:

Figures:

CHAPTER 1: INTRODUCTION

Recently, there has been great success in exploiting the bitumen in the McMurray Formation, thus much attention has been drawn to investigating other bitumen targets. One bitumen target is the Devonian Grosmont Formation, the second largest bitumen reservoir in Alberta (Machel et al. 2012). Extraction of the bitumen from this formation has not been viable until recently when specific technology, such as steam-assisted gravity drainage (SAGD), was developed that made it possible to exploit this resource. Companies such as Laricina Energy Ltd. (Laricina) have been working with new technology and successfully extracting bitumen from the Grosmont Formation and Cretaceous Grand Rapids Formation.

Laricina is one of many companies using SAGD techniques to extract the highly viscous to solid bitumen from formations such as the Grosmont Formation. This process involves drilling two parallel horizontal boreholes. One borehole is used to inject steam into the targeted formation and the second is used to collect the bitumen and pump it to the surface. The steam that is injected into the upper horizontal borehole leg heats the surrounding bitumen, substantially lowering its viscosity, essentially rendering it a mobile liquid. Gravity then draws the liquid down and into the lower of the two borehole legs. The bitumen is then extracted via pumping action to the surface.

In some cases, the process is mitigated with the use of a solvent, such as propane. Solvents are added to the steam in order to decrease the amount of heat required to mobilize the bitumen which increases the overall bitumen recovery. Additional techniques, including enhanced solvent extraction incorporating electromagnetic heating or ESEIEH (pronounced: “easy”) are still being developed and piloted.

Successes with the use of SAGD has allowed for the investigation of other bitumen targets with similar reservoir characteristics. Preliminary investigation of the Upper Devonian Graminia Formation of the Winterburn Group has shown that is has very similar characteristics to the Grosmont Formation and thus warrants more investigation.

Objectives

It is important to understand the two primary key characteristics of a potentially good reservoir with respect to these bitumen plays; porosity and permeability. These are integral to fully estimating the economic potential and viability of a target; more specifically, what causes and controls them. Therefore, the main focus of this study will be to examine the porosity and permeability of the rocks in the Graminia Formation by investigating the stratigraphy, deposition, sedimentation, and diagenesis.

Study Area and Data Set

The study area is located in the northeast plains area of Alberta, Canada, approximately 130 km southwest of the city of Fort McMurray. This area, known as the Germain Field, is owned by Laricina (Fig. 1.1). The Germain Field consists of seventy-one sections spread over

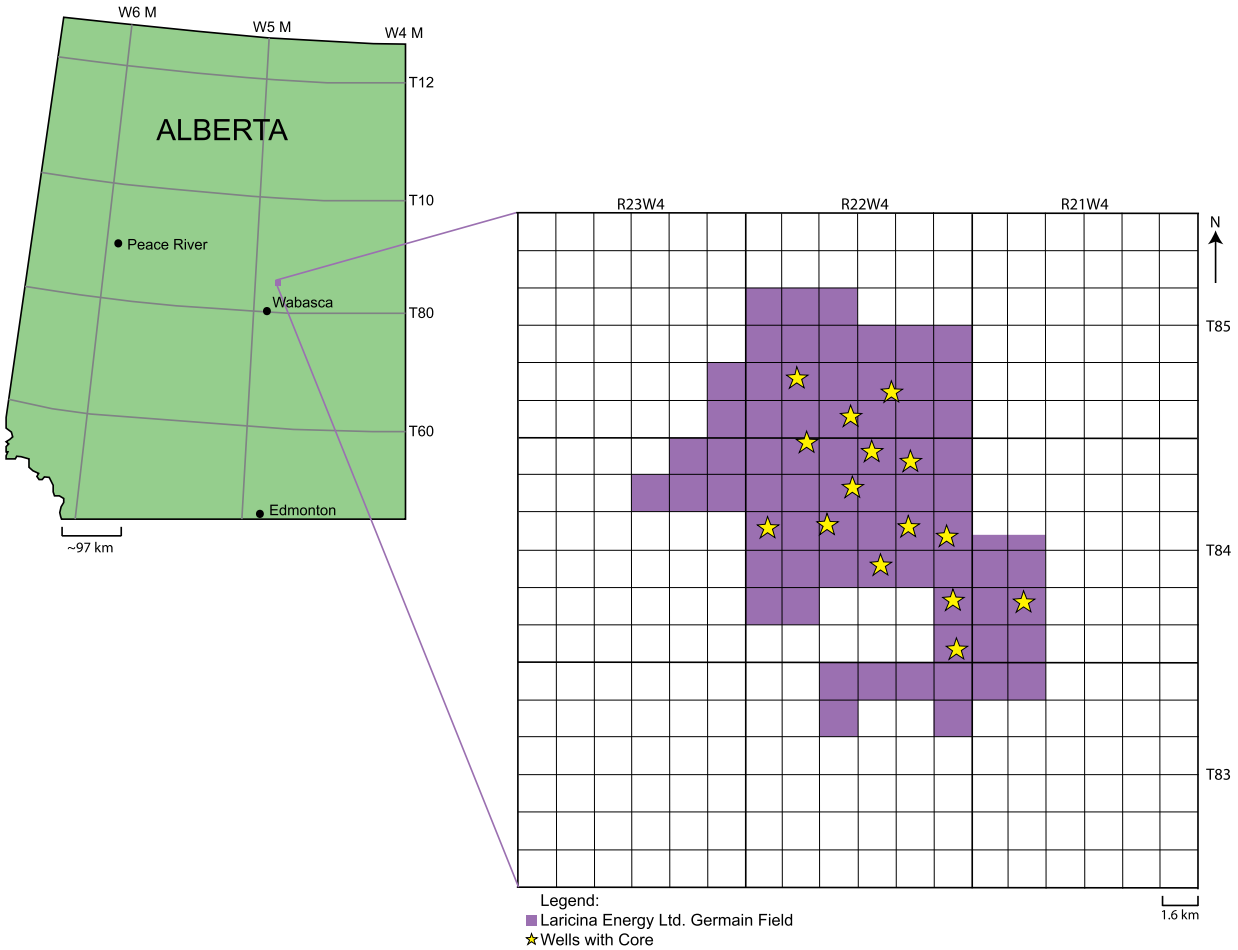

Figure 1.1: The area of study; the Germain Field and its location within northeastern Alberta.

townships 83 to 85 and ranges 21W4 to 23W4. This study investigates the stratigraphic section which includes the Graminia Formation (Upper Graminia Member and the Blueridge Member), which belong to the Devonian Winterburn Group. As of December 8, 2011, five-hundred and eighty-eight wells had been drilled in this area. Only thirty-seven of these wells, however, penetrate into the Graminia Formation, and of these wells, core is only available from fifteen wells (Fig. 1.1). Laricina has graciously allowed for the viewing and sampling of all fifteen of these cores in the area as well as the use of the porosity and permeability data from the routine core analysis run by AGAT Laboratories. Fifty-six thin sections and twenty-two scanning electron microscopy (SEM) mounts were made from samples taken from the fifteen wells. These cores and samples were observed and documented to allow for the understanding of the depositional and diagenetic fabrics.

Raster well logs from the fifteen wells were scrutinized for specific signatures that indicated stratigraphic contacts, degree of porosity and permeability, and were compared to the data obtained from the cores, thin sections, and SEM. The key fifteen well logs contain Gamma Ray and Density/Neutron porosity logs.

Methodologies

This study focused primarily on the porosity and permeability from core samples taken from the Graminia Formation. Cores were observed and logged, noting dominant and accessory lithologies, colours, textures, crystallinity and size, allochemical content, trace fossils, diagenetic fabrics, and/or cements. Further, visual estimations of hydrocarbon staining, types of porosity and permeability and their estimated percentage values, as well as the type, degree and orientation of fracturing were made. From these cores, samples for x-ray diffraction (XRD), SEM and thin sections were selected based on macroscopic porosity and textural features. Included in the SEM analysis was the energy dispersive x-ray (EDX) analysis system that was used to semi-quantitatively identify mineralogy via elemental peak analysis. The porosity and permeability values from the routine core analysis previously performed by AGAT Laboratories for Laricina were used for statistical purposes.

The XRD analyses provided additional information on the lithology of the rock. Specifically, it was used to help differentiate the various types of non-carbonate minerals present in the rocks of the Graminia Formation. Samples weighing a few grams were ground using a mortar and pestle into a fine powder, with an individual grain size of no more than 10 μm. The powders were then mounted on zero-background silicon plates and loaded into and subsequently analyzed on the Rigaku Powder X-Ray Diffractometer at the University of Alberta X-Ray

X-Ray	Cobalt tube (38kV/38mA)	I. Monochromator	CBO
Goniometer	Ultima IV (ADS)	C. Monochromator	Not Used
Attachment	Auto Sample Changer (10 samples)	Counter	D/teX Ultra
Sample-Spin	None	Scan Mode	Continuous
Filter	K-beta Filter	Scan Speed	2.000 deg./min
Division Slit	2/3 degree	Scan Axis	2ɵ/ɵ
Division H.L. Slit	10mm	Theta Offset	0.0000 deg.
Scintillator Slit	Open	Sampling Width	0.0200 deg.
Recording Slit	8.00mm	Scan Range	5.0000 to 90.0000 deg
		Repeat Count	1

Table 1.1: Conditions for the Rigaku Powder X-Ray Diffractometer.

Diffraction Laboratory. This machine is equipped with a cobalt tube, graphite monochromator and scintillation detector under the conditions listed in Table 1.1. Results were obtained and compared to the International Centre for Diffraction Data (ICDD) database and the Inorganic Crystal Structure Database (ICSD) via the use of the Jade 9.0 software. This software was able to match the peak patterns given by the samples with known minerals and identify the corresponding mineralogy of the sample.

SEM was used to examine micro-porosity, permeability, fracturing, identify the relationships of grains to cements as well as some basic mineralogy and the fabric and texture of the sample. Samples selected for SEM analysis were no larger than 1 cm high and 1.5 cm in diameter and were coated in gold using the Xenosput XE2000 to increase the conductivity of the sample prior to examination under the SEM. The samples were analyzed using the JEOL 6301F (Field Emission Scanning Electron Microscope). This machine provided the opportunity to take high-resolution digital images at magnifications ranging from 25 x to 25,000 x. Semi-quantitative elemental analysis was also available within the set up via a PGT X-ray analysis system (res. 135 eV). This was completed using the IMIX program to determine the specific elemental content in the samples.

Samples that exemplified the macroscopically visible characteristics of the different styles and types of porosities, permeabilities and fabrics of the Upper Graminia and Blueridge Members were selected and made into thin sections for closer examination.

The samples selected for thin sectioning were impregnated with blue epoxy to highlight porosity prior to cutting of the thin sections. Afterwards, half of each thin section was stained with alizarin red and potassium ferricyanide to easily differentiate between calcite from dolomite, and high-ferroan calcite or dolomite (2% or greater Fe), from low-ferroan (can be up to 2% Fe) bearing calcite or dolomite, respectively. If calcite is present, the alizarin red will stain

it red, making it very easy to differentiate between these two minerals. Potassium ferricyanide indicates calcite or dolomite crystals that are high in ferrous iron (Fe^{2+}); high-ferroan dolomite will be stained blue and high-ferroan calcite, in combination with the alizarin red stain, will be stained purple. This characteristic cannot be determined without the use of staining and will support the understanding of the diagenesis of the sample. The other half of the thin section was kept unstained so it could be compared with the stained half.

The porosity and permeability values from the routine core analysis were compared with those estimated from the thin sections and SEM samples. Samples were analyzed as per the 1998 "Recommended Practices for Core Analysis Methodologies," written by the Exploration and Production Department of the American Petroleum Institute. The sample values were also used in the statistical analysis of the different facies to determine any trends. The values used were the depth of the sample, the maximum gas permeability value (k_{max}) and the porosity (Φ). The values were appraised for correctness using the core analysis quality control report included with the Routine Core Analysis. Laricina selected the samples and the depths previous to this study, so some of the wells were not as heavily sampled as others and not all the wells had all facies sampled. Likewise, these samples were not also necessarily the same as those used for the thin section, XRD and SEM analyses. Thus, the degree of sampling does not necessarily reflect the quality of the core.

Previous Work

The literature on the Winterburn Group is meagre and is even more limited with respect to specific formations and members. Switzer et al. (1994) mentioned that no significant hydrocarbon reserves had been assigned to this interval and inferred that this was related directly to the lack of published articles available regarding the Graminia Formation. The Winterburn Group is generally only mentioned in studies regarding the Devonian interval at a provincial, basin-wide scale (e.g., Burrowes and Krause 1987; Moore 1988; Morrow and Geldsetzer 1989; Dix 1990; Stoakes 1992; Wendte 1992a, b; Switzer et al. 1994; Potma et al. 2001) or as part of a small field study (i.e., Geological Staff, Imperial Ltd. 1950; Andrichuk and Wonfor 1953, 1954; Storey 1953; Belyea 1954a, b; Workman 1954; Belyea 1955; Belyea and McLaren 1957). Specifically, the Graminia Formation is commonly only named for completeness sake, in the background or introduction sections in other literature on other Winterburn Group strata (e.g., Stearn 1987; Weissenberger 1994; McLean and Klapper 1998) and not investigated further.

There are only two publications that specifically address the Graminia Formation and Blueridge Member. These are: "The Blue Ridge Member of the Graminia Formation" by

Choquette (1955) and “Lithology, biostratigraphy and geochemistry of the Upper Devonian Graminia Formation, central Alberta” by Meijer Drees et al. (1998).

Nomenclature

The original nomenclature for the Winterburn Group was proposed by the Geological Staff of the Western Division of Imperial Oil Limited in 1950. They defined the Winterburn Formation as part of the Minnewanka Group, which included the Nisku Member, Calmar Member, and the Graminia Member. The Winterburn Formation was elevated to Group status by Andrichuk and Wonfor (1954), and consequently, the Nisku Member, the Calmar Member, and the Graminia Member were each elevated to formation status.

The Blueridge Member was officially designated by Choquette (1955) when the wildcat well, 5-14-058-5W5, began producing oil out of this interval which was previously misidentified (e.g., Geological Staff, Imperial Ltd. 1950; Andrichuk and Wonfor 1953, 1954; Storey 1953; Belyea 1954a, b; Workman 1954; Belyea 1955) as part of the Nisku Formation.

The first time that the informal ‘Graminia Silt’ member is mentioned is by Warren and Stelck (1954). Choquette (1955) acknowledged that the upper boundary of this member “is marked by a change from prominent siltstones of the top of the Graminia to the massive dolomite” but did not specifically name this siltstone unit. He did, however, label it is as the ‘Graminia Silt’ on the log correlations. There is sporadic use of the term ‘Graminia Silt’ throughout the literature until recently, when some authors, such as Switzer et al. (1994), chose to call it the ‘Upper Graminia’ member. This removes the genetic significance of the previous name. This study proposes that the formal name for this unit be the Upper Graminia Member.

Stratigraphy

The Winterburn Group (Fig. 1.2) in the Germain Field includes the Nisku Formation, Calmar Formation, and Graminia Formation. The Graminia Formation is comprised of the Blueridge Member and the Upper Graminia Member. The Winterburn Group rests conformably on the Upper Ireton Formation. The Upper Devonian Winterburn Group is capped by a major disconformity that represents the significant hiatus from the Carboniferous through to the Albian (Cretaceous). Specifically, the disconformity is overlaid by an unnamed green paleosol that is most likely of Cretaceous age which is overlain by the Wabiskaw Member of the Clearwater

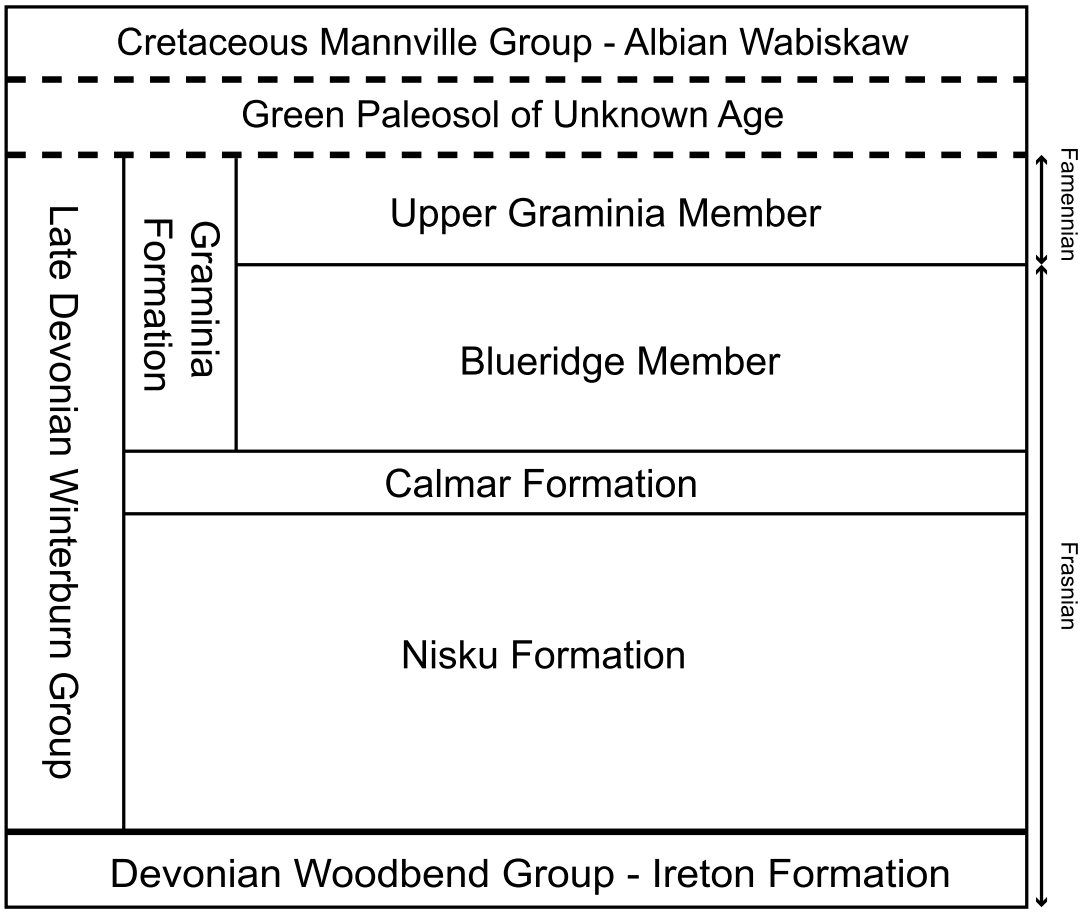

Figure 1.2: Stratigraphy of the Upper Devonian Winterburn Group within the Germain Field, northeastern Alberta.

Formation (Mannville Group). This inference of age is based on coal-filled rootlets observed in the paleosol that are similar to the coal seams often observed at the base of the Wabiskaw Member in the Germain Field. Preliminary research has indicated that this paleosol is unique to the Germain Field as there is no mention of it in the literature. The McMurray Formation is absent in the Germain Field.

In the Germain Field, all units in the Winterburn Group are stratigraphically conformable. The contact between the Blueridge Member and Upper Graminia Member is gradational. The contact between the Upper Graminia Member and the Blueridge Member is thought to be the boundary between the Frasnian and Famennian based on multiple biostratigraphic studies (e.g., Sorauf and Pedder 1986; Stearn 1987; Goodfellow et al. 1989; Weissenberger 1994; McLean and Klapper 1998; Meijer Drees et al. 1998; Bond and Wignall 2008; John et al. 2010). The Frasnian-Famennian boundary is highly significant because it marks one of the most significant extinction events of the Phanerozoic. Although it has been intensely studied, the lack of fossils in the Upper Graminia Member and Blueridge Member make exact dating difficult.

Lithostratigraphy

The Nisku Formation in the Germain Field is a massive, finely crystalline dolostone with low porosity. The porosity is primarily pin-point vugs, brachiopod molds and thin fractures that are typically lined with calcite and filled with green silty shale. The Nisku Formation is easily identified on borehole logs based on a low gamma ray signature (Fig. 1.3). The average thickness is unknown because wells in the Germain Field did not penetrate into the Nisku Formation, or did not penetrate through the whole thickness of the formation.

There is an abrupt and distinct contact observed between the Nisku Formation and Calmar Formation in the Germain Field. The heavily bioturbated dolomitic, argillaceous silty-sand of the Calmar Formation is relatively more radioactive than the other rocks in the Winterburn Group and easily identified on a borehole log based on the high gamma ray signature (Fig. 1.3). The Calmar Formation has very low porosity and permeability and it has an average thickness of 4 m throughout the study area.

In the Germain Field, the contact between the Calmar Formation and the Blueridge Member is gradational. The Blueridge Member is comprised of porous, interbedded, silty, finely crystalline dolostones and fractured, very finely crystalline, massive dolostones. There are poorly preserved brachiopod and gastropod fragments, and other allochems, including ooids and peloids. Fractures and pores tend to be fully or partially cemented with calcite and dolomite, respectively. Some sections contain a bioturbated aspect; however, no specific trace fossils have been identified. The Blueridge Member has a similar borehole signature as the Nisku Formation, with a low gamma ray reading (Fig. 1.3). The average thickness of the Blueridge Member in the study area is 24 m.

The contact between the Blueride Member and Upper Graminia Member in the Germain Field is gradational. The base of the Upper Graminia Member is characterized by a 3 to 8 m thick section of high gamma ray readings above the low gamma ray signature of the Blueridge Member (Fig. 1.3). The Upper Graminia Member in the Germain Field is characterized by interlaminated, green-gray siltstones and shales with fine grained, variably silty dolomitic sandstones. The laminae are devoid of fossils, but appear bioturbated; however, there are no recognizable trace fossils. The top of the Upper Graminia Member can be difficult to identify on borehole logs because it is variable and can have a very similar signature to the overlying paleosol. The average thickness of the Upper Graminia Member in the study area is 14 m.

There is a green-gray silty to shaley paleosol in the area in many, but not all, wells. The paleosol has an average thickness of 11 m, but the thickness varies from 0 m to 19 m across the Germain Field. The paleosol is very difficult to identify on gamma ray borehole logs because of its variably radioactive nature.

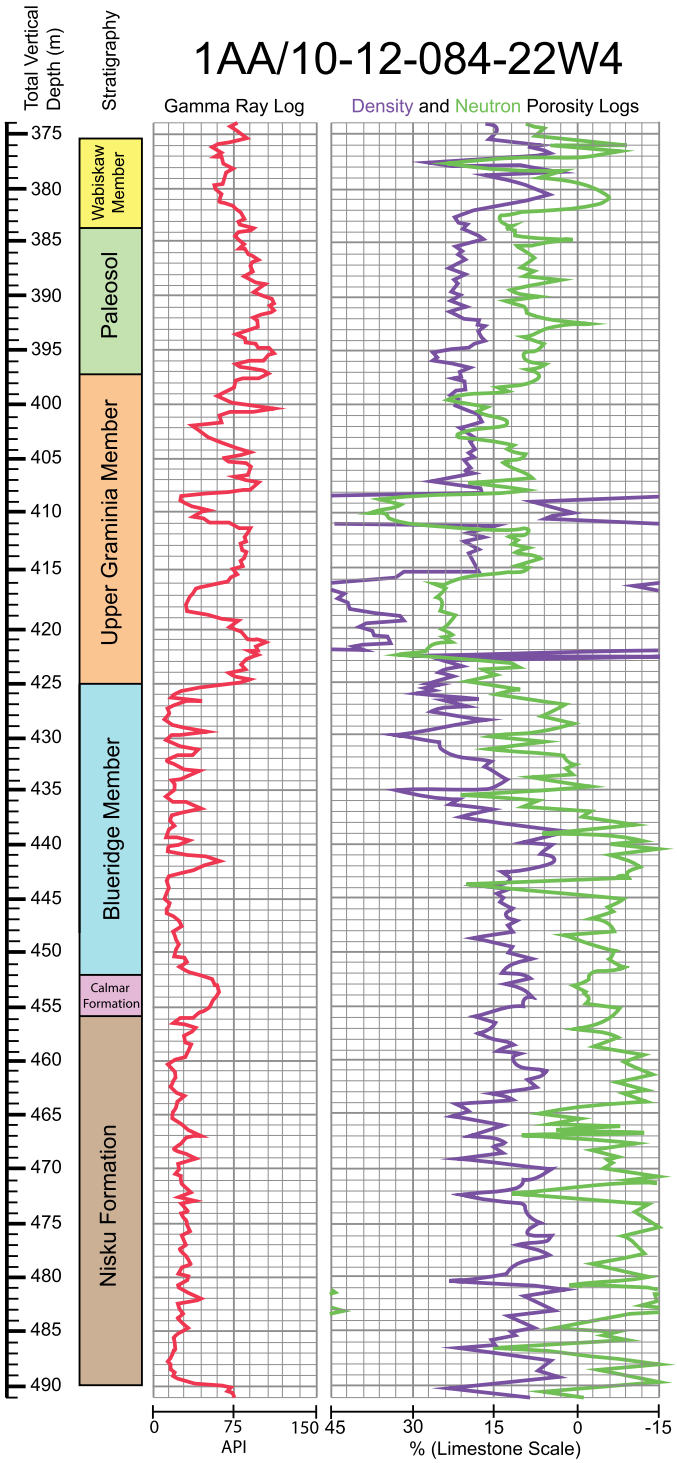

Figure 1.3: Lithostratigraphy and characteristic well log signatures of the upper Devonian Winterburn Group strata.

CHAPTER 2: FACIES IN THE GRAMINIA FORMATION

There are six facies (A, B, C, D, E and F) identified in the Graminia Formation based on the mineralogy, fabric, and cement type observed in core samples. These facies will be described in the first part of the chapter and their distribution and architecture will be discussed in the second part of the chapter.

Given that the rocks are dolomitized, the facies reflect both diagenetic and original depositional fabrics. The rocks have been named using a ternary diagram (Fig. 2.1) that has dolomite, calcite, and clastic minerals at its apices. If the rock is composed of greater than 80% dolomite, it is classified as a dolostone using the scheme defined by Friedman (1965); if composed of greater than 80% calcite, then Dunham's (1962) limestone classification is used; and if more than 80% clastics, the Wentworth scale is employed. Rocks intermittent to these end-members are named as shown in Figure 2.1. Cements are described using Folk (1965) and Bathurst (1975).

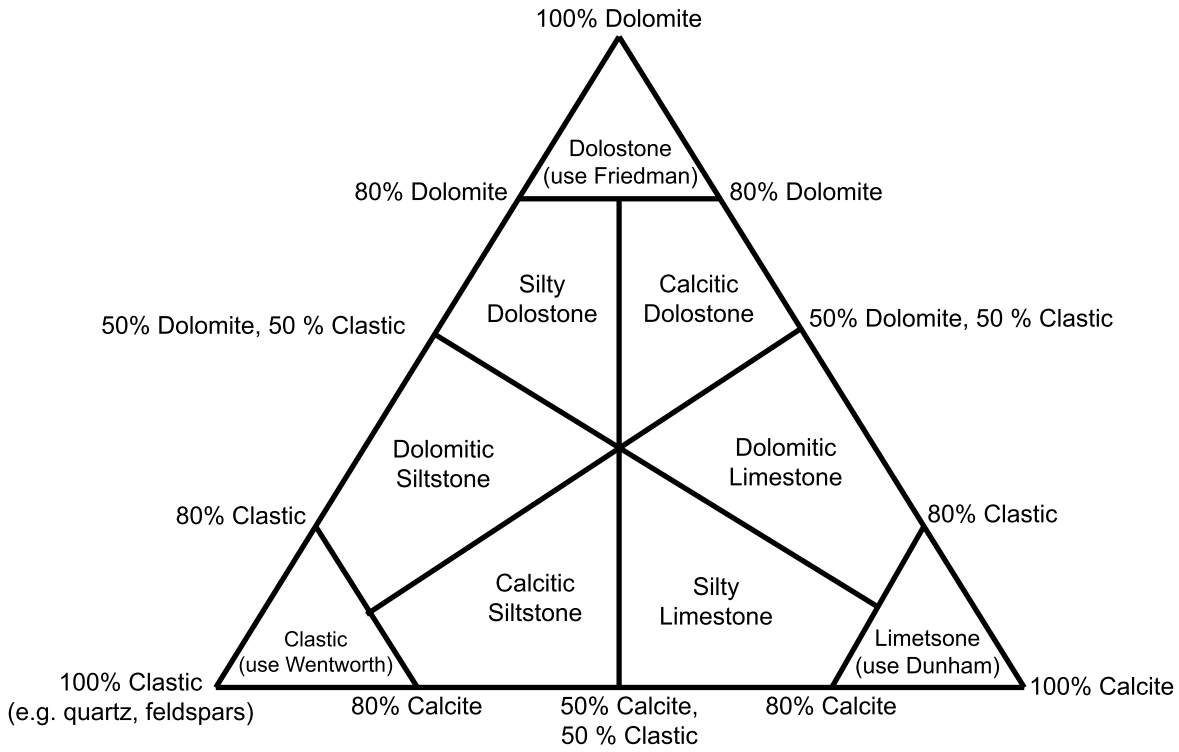

Figure 2.1: Ternary diagram implemented for naming the clastic, dolomitic and calcitic rocks of the Graminia Formation. This schematic uses siltstone as the default clastic name as all of the clastic components of these rocks specifically fall into the siltstone size of the Wentworth classification system. This ternary could also be used for clastic components that were bigger or smaller; example: dolomitic sandstone.

Facies Descriptions

Facies A

This facies, found in the upper part of the Upper Graminia Member, is formed of very finely to finely crystalline dolomitic siltstone to silty dolostone that is interlaminated/mottled (respectively) with silty shale (Fig. 2.2). This facies can appear brecciated or disrupted. This facies is divided into Facies A1 and A2 based on minor but important differences in mineralogy and crystal size.

Facies A1 is a very finely to finely crystalline dolomitic siltstone that is interlaminated with silty shale (Fig. 2.3, 2.4). The dolomitic siltstone is comprised largely of well sorted, subangular to subrounded quartz grains with an average grain size of 30 μm and very finely to finely crystalline (<100 μm to 250 μm), low-ferroan dolomite grains. Quartz forms 50 to 80% of

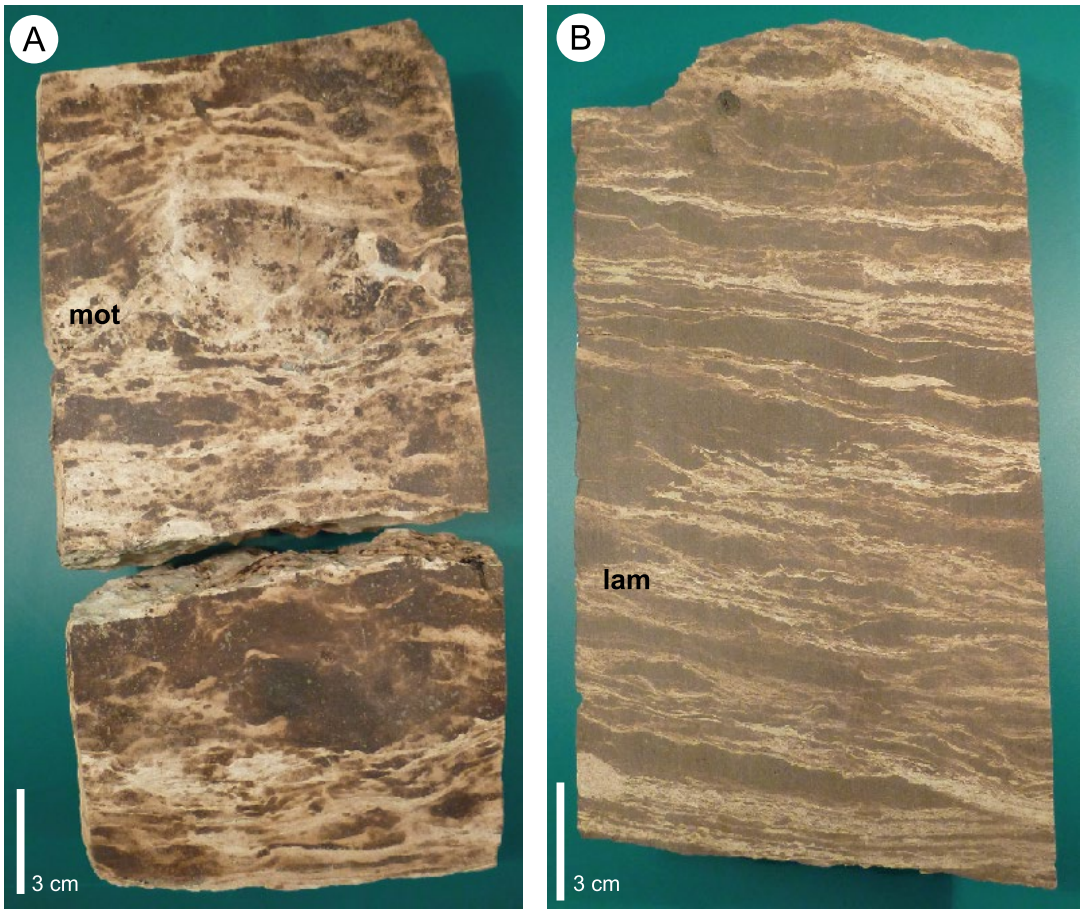

Figure 2.2: Core characteristic of Facies A. mot = mottled, lam = laminated. A) Core from 421.10 m from well 1AA/06-24-084-22W4. B) Core from 423.01 m from well 1AA/06-35-084-22W4.

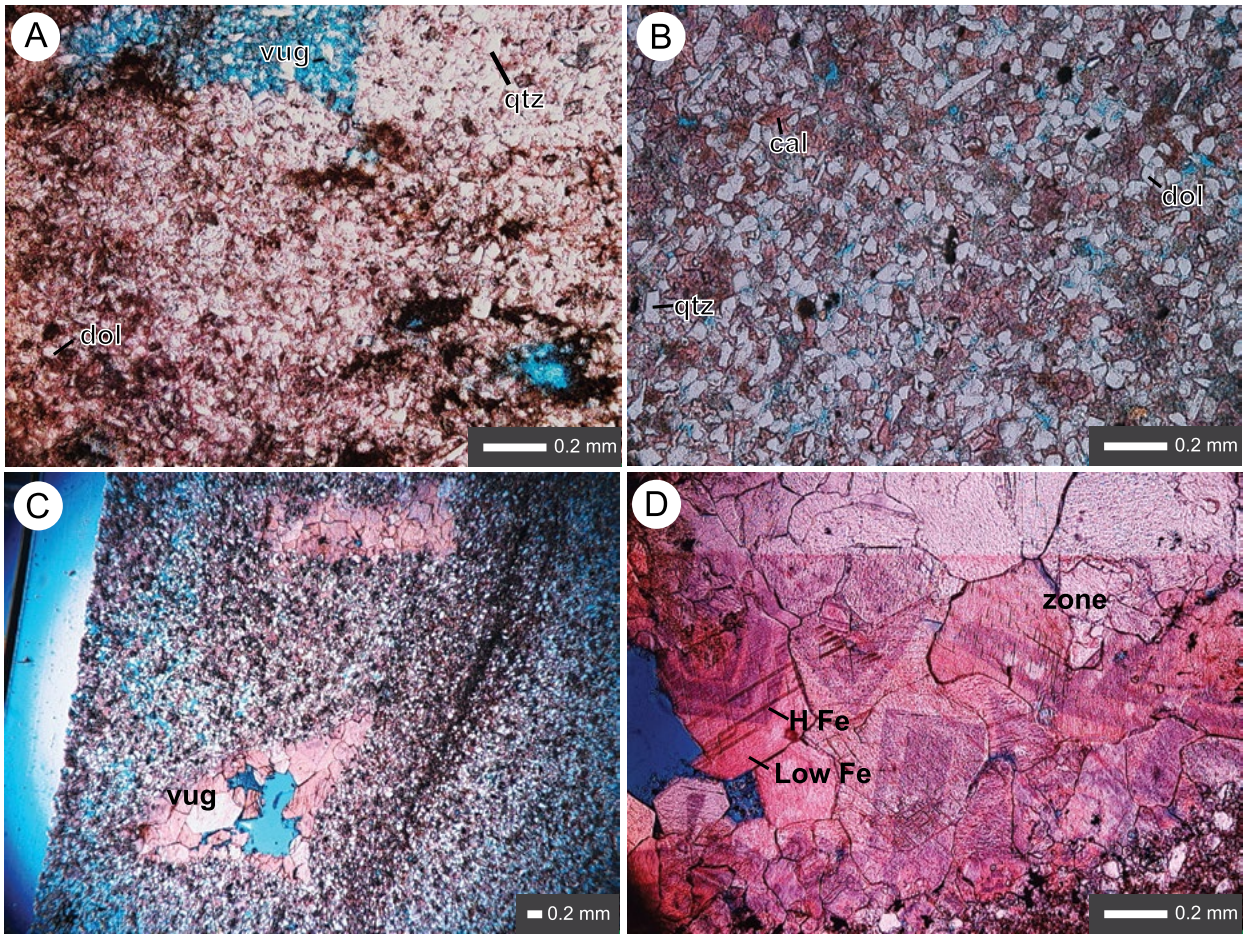

Figure 2.3: Thin sections in PPL representative of the rocks typical of Facies A. qtz = quartz; dol = dolomite; cal = calcite; vug = vuggy porosity; zone = zoned calcite cement; H Fe = high-ferroan calcite; L Fe = low-ferroan calcite. A) Facies A1; thin section from 398.49 m from well 1AA/01-10-085-22W4. B) Facies A2; thin section from 425.08 m from well 1AA/10-15-084-22W4. C) Vuggy porosity cemented with spar calcite; thin section from 425.08 m from well 1AA-10-15-084-22W4. D) Zoned spar calcite cement seen in some of the vugs; thin section from 424.66 m from well 1AA/10-15-084-22W4.

this lithology whereas dolomite forms 20 to 50%. Additionally, there are minor (<2%) amounts of biotite, muscovite, plagioclases and pyrite. There are no fossils or allochems. It is cemented by low-ferroan, sparry (<4 μm), equant calcite. The interlaminated silty green-gray shale contains muscovite, kaolinite, pyrite, quartz, and potassium feldspar. It is considered a silty shale based on average grain size and its fissile nature. The ratio of dolomitic siltstone to shale in facies A1 is approximately 1:1.

Facies A2 is a finely crystalline, silty dolostone mottled with silty shale (Fig. 2.3, 2.4). The silty dolostone is comprised of finely crystalline (100 to 250 μm) low-ferroan dolomite grains with well sorted, subangular to subrounded quartz grains with an average grain size of

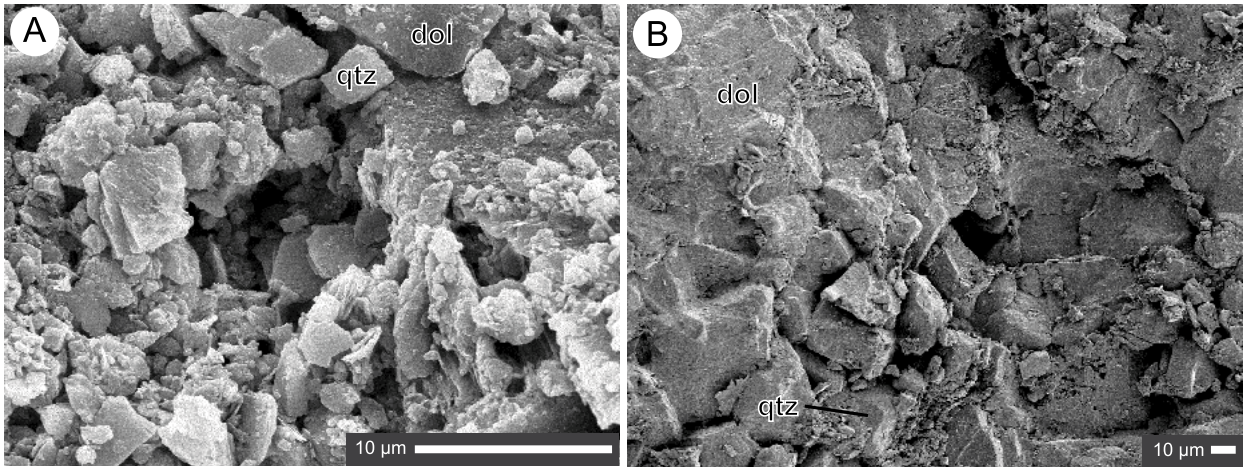

Figure 2.4: SEM images characteristic of Facies A. qtz = quartz; dol = dolomite. A) Facies A1 from 424.66 m from well 1AA/10-15-084-22W4. B) Facies A2 from 430.60 m from well 1AA/06-24-084-22W4.

40 µm. In contrast to Facies A1, dolomite dominates (50 to 65%), and quartz forms 35 to 50% of the lithology. Accessory minerals (<2%) include biotite, muscovite, and plagioclase. Pyrite is more common (5-10%) in this facies, than in Facies A1. This silty dolostone is cemented by low-ferroan, sparry, equant calcite. There are no fossils or allochems present. Although it has a bioturbated aspect, no individual trace fossils could be identified. The silty shale is the same as in Facies A1. It is, however, more common in this facies (A2) with the ratio of silty dolostone to silty shale being approximately 2:3.

The dolomitic siltstones to silty dolostones are bitumen stained, whereas the silty shales are impermeable and are not bitumen stained. Porosity in Facies A typically ranges from 3 to 39% with an average porosity of 21%. The porosity consists of intergranular porosity between the quartz and dolomite grains along with some vuggy porosity and minor fracture porosity. The intergranular space is partially cemented by micritic (>4 µm) to sparry calcite. The spherical vugs are 10 to 20 mm in diameter with most being filled with sparry calcite cement (Fig. 2.3). This results in a decreased pore size that leads to a much lower overall porosity because the open pore is decreased to a diameter of about 2 mm. Some of the calcite cement is zoned with alternating zones of high-ferroan and low-ferroan calcite (Fig. 2.3). There is also a minor contribution to the overall porosity of the facies from fracture porosity. Fractures are up to 20 mm long and 0.2 mm wide and tend to be occluded by low-ferroan, sparry equant calcite. This facies has low permeability; an average of 315 md.

Facies B

Facies B, found in the lower part of the Upper Graminia Member, is a very finely crystalline dolomitic siltstone to silty dolostone that is easily identifiable on borehole logs by its high gamma ray signature (Fig. 2.5). Although similar to Facies A, it lacks the silty shale laminae. The dolomitic siltstone to silty dolostone is comprised of well sorted, subangular to subrounded quartz grains (40 to 70%) with an average grain size of 30 µm and very finely to finely crystalline (<100 µm to 250 µm), low-ferroan dolomite grains (45 to 70%). The high potassium feldspar (orthoclase, sanidine and microcline) content (10 to 12%) of this facies is probably responsible for the high gamma ray signature. The feldspar anorthite is also present.

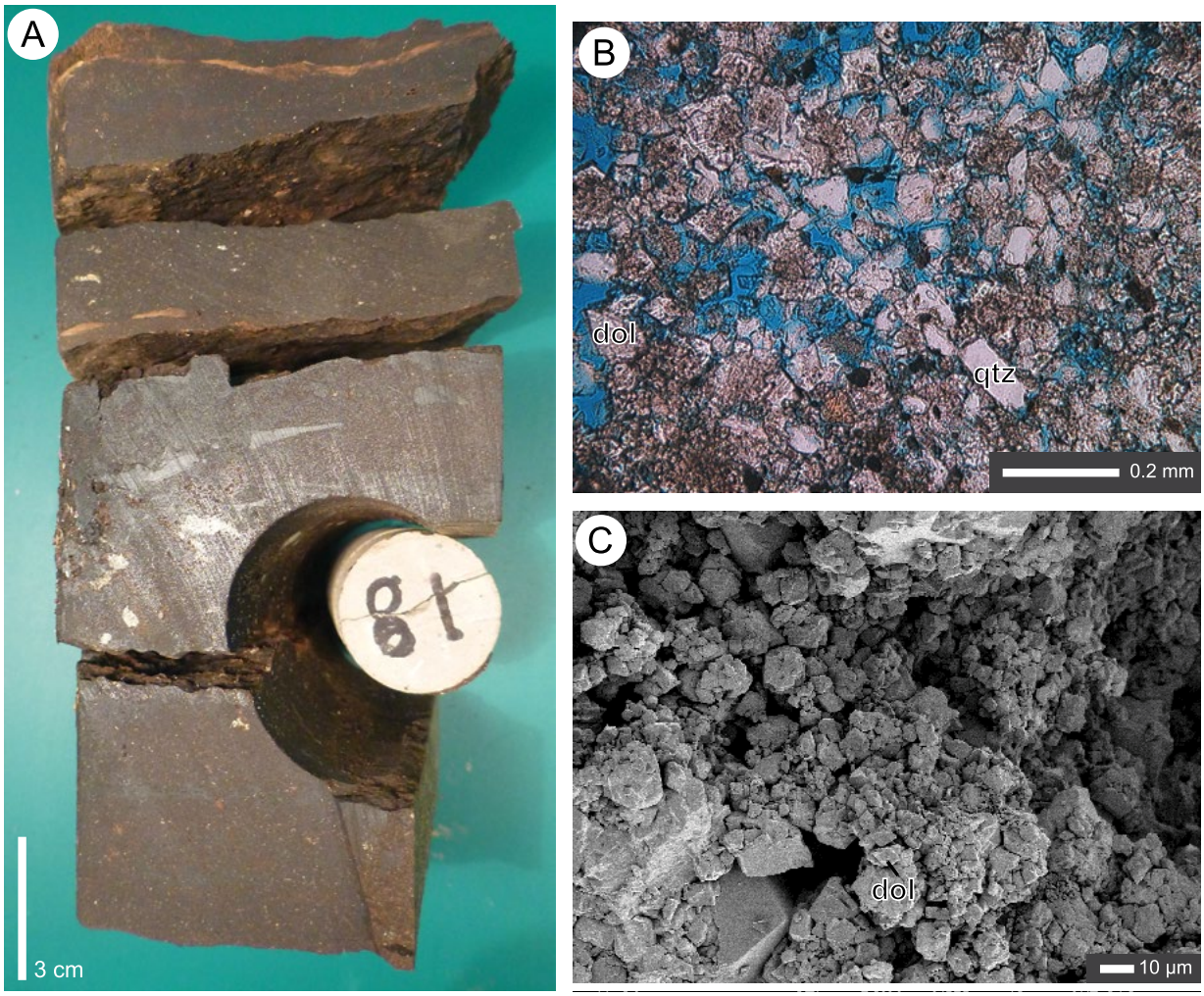

Figure 2.5: A) Core characteristic of Facies B from 422.75 m from well 1AA/06-24-084-22W4. Note that when the bitumen is removed, that the rock stays solid. B) Thin section in PPL of the rocks typical of Facies B from 416.70 m from well 1AA/10-15-084-22W4. qtz = quartz; dol = dolomite. C) SEM image of some typical rocks from Facies B from 413.33 m and from well 1AA/10-15-084-22W4.

Minor (<5%) amounts of pyrite, muscovite, and kaolinite are also present. Cement, when present, is low-ferroan, sparry, equant mosaic calcite. However, the grains in the facies appear to be completely cemented due to the heavy bitumen saturation. Note that when the bitumen is removed from the rock, the rock stays intact.

The porosity in this facies ranges from 2 to 40%, with an average porosity of 27%. The porosity is predominantly intergranular with the size and shape of the pores being controlled by the packing of the dolomite and quartz grains. This facies has moderately high permeability, with an average permeability of 450 md.

Facies C

Facies C, found in the upper part of the Blueridge Member, is a very finely crystalline silty dolostone that is variably mottled and/or interlaminated with silty shale (Fig. 2.6, 2.7). Despite the bioturbated aspect, there are no recognizable trace fossils and it is less bioturbated than Facies A2. The very finely crystalline (<100 μm) dolostone is formed of 90% low-ferroan to ferroan dolomite. Other minerals include pyrite (5 to 10%) and quartz (1 to 2%). The interlaminated silty shale is the same as in Facies A.

Poorly preserved allochems in this facies have been moderately to completely leached. Although poorly preserved, it appears that this facies originally included ooids, peloids, gastropod and brachiopod fragments (Fig. 2.8). The leached allochem molds comprise an average of 20% of the rock.

The porosity in this facies ranges from 4 to 38% with an average porosity of 21% and is dominantly comprised of moldic, vuggy porosity derived from the leached allochems. The vugs are commonly lined with finely crystalline dolomite cement (Fig. 2.8). Rarely, there is low-ferroan, sparry equant calcite filling the molds associated with the dolomitic cement. On average, 15% (range of 5 to 90%) of these vugs are filled with cement. Although the dolomite rhombs tend to be packed closely together, there are minor amounts of intercrystalline porosity in some samples. Fractures are rare in this facies. There is low permeability in this facies, averaging 275 md.

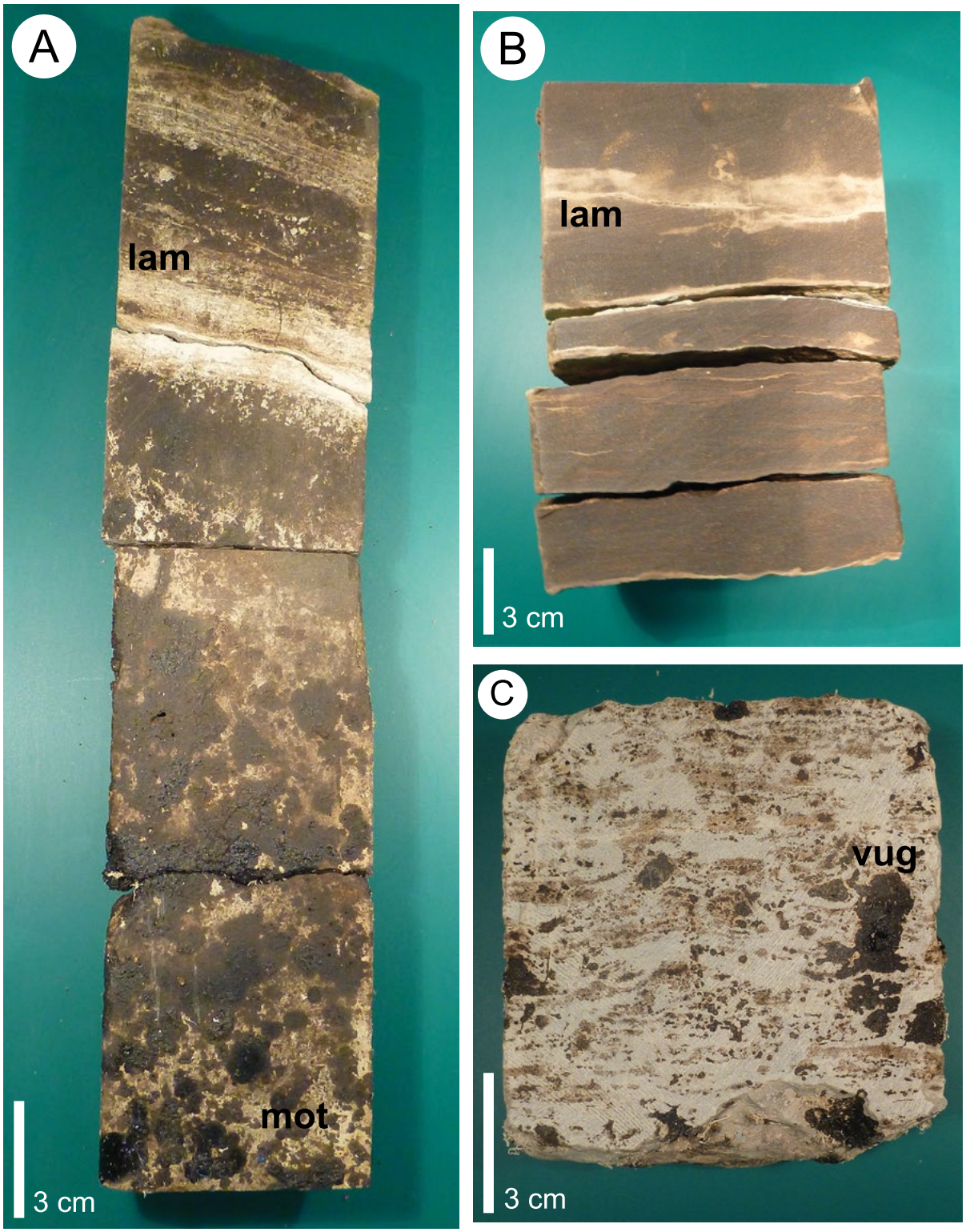

Figure 2.6: Cores characteristic of Facies C. mot = mottled; lam = laminated; vug = vuggy porosity. A) Core showing both mottled and interlaminated sections from 446.00 m from well 1AA/12-21-084-22W4. B) Core showing interlaminated section from 425.35 m from well 1AA/06-24-084-22W4. C) Core showing more mottling and very common vuggy porosity from 447.28 m from well 1AA/12-21-084-22W4.

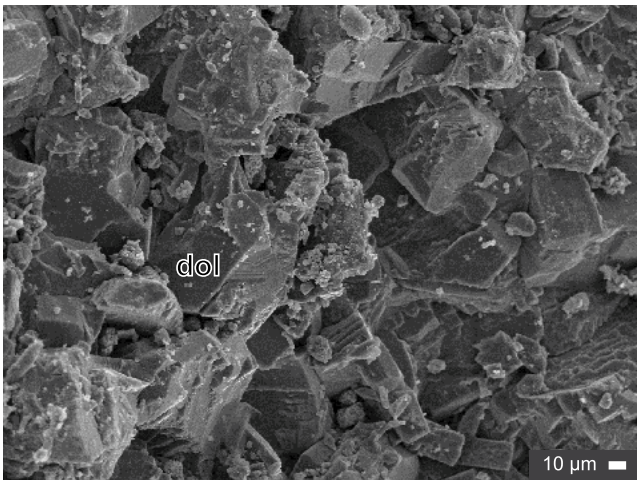

Figure 2.7: SEM image representing the characteristics of Facies C from 433.92 m from well 1AA/10-15-084-22W4. dol = dolomite.

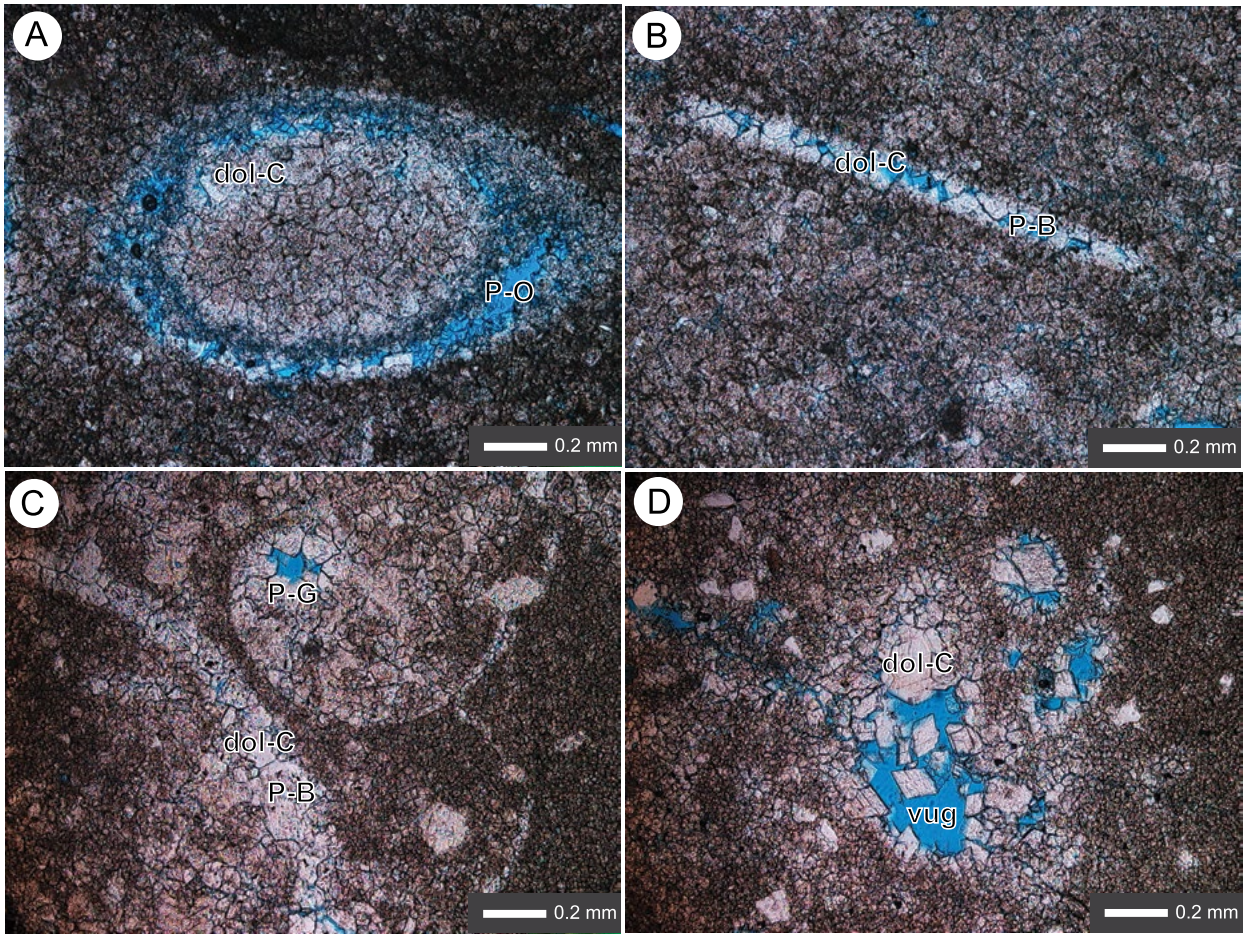

Figure 2.8: Thin sections characteristic of Facies C in PPL. P-O = pore from a leached ooid; P-B = pore from a leached brachiopod fragment; P-G = pore from a leached gastropod; dol-C = dolomitic cement; vug = vuggy porosity. A) Leached ooid lined with dolomitic cement from 439.00 m from well 100/09-04-085-22W4. B) Leached Brachiopod fragment, lined with dolomitic cement from 439.00 m from well 100/09-04-085-22W4. C) Leached Gastropod fragment, lined with dolomitic cement from 423.84 m from well 1AA/12-21-084-22W4. D) Vuggy porosity with rhombic dolomitic cement from 434.15 m from well 1AA/06-24-084-22W4.

Facies D

Facies D is a green-gray laminated silty-shale bed, 1 to 2 m thick that is found in the middle of the Blueridge Member (Fig. 2.9). Like Facies B, it easily identified on borehole logs by its high gamma ray signature, which probably reflects its high potassium-bearing mineral content. This facies, like the silty shale in Facies A, is formed of silt to clay sized grains of muscovite, kaolinite, pyrite, quartz, and potassium feldspar along with 2 to 15% very finely to finely crystalline (<100 μm to 250 μm), low-ferroan dolomite.

The facies has very low porosity, from 4 to 16%, with an average of 10%; and very low permeability, generally about 5 md.

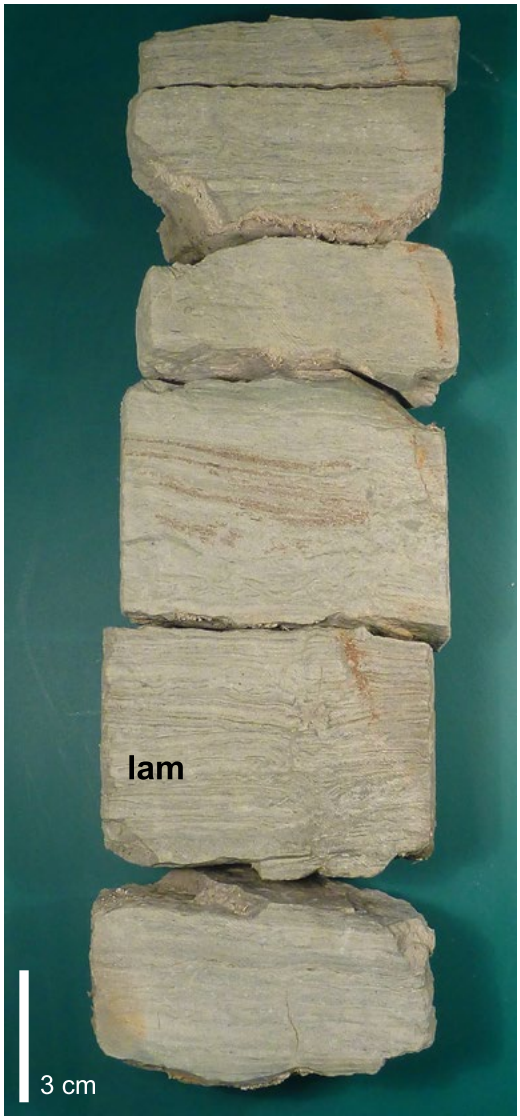

Figure 2.9: Core characteristic of Facies D from 447.48 m from well 1AA/12-21-084-22W4. lam = laminated.

Facies E

This facies, typically found in the lower half of the Blueridge Member, is a highly fractured, very finely crystalline, variably silty dolostone (Fig. 2.10, 2.11). The dolomite is low-ferroan, very finely crystalline (<100 μm) and forms ≥90% of this facies. Other components include subangular to subrounded quartz grains (~5%) with an average grain size of 30 μm, pyrite, and calcite. The dolostone is cemented with low-ferroan, sparry calcite.

There are poorly preserved allochems present in this facies. There are much fewer allochems present in this facies than in Facies C, comprising an average of about 10% of the total rock. The allochems have been moderately to completely leached. Although poorly preserved, it appears that this facies originally included ooids, peloids, gastropod, and brachiopod fragments, similar to Facies C (Fig. 2.12). There are rare preserved sections of *Syringopora* sp. (Fig. 2.10).

Most of the porosity in this facies, which ranges from 4 to 37% with an average of 17%, is associated with the fractures. There is also some vuggy and intergranular porosity. The fractures, which are 2 to 15 cm long and 2 to 10 mm wide, form an interconnected network. Many of the fractures are partially filled (20 to 50%) with low-ferroan equant, sparry calcite (Fig. 2.12). The spherical to oval vugs are from 0.5 to 6 mm in diameter and do not contribute substantially to the overall porosity, as they tend to be filled (50 to 80%) with ferroan and low-ferroan, sparry equant calcite. Much of this calcite shows zoning, alternating high-ferroan and low-ferroan calcite (Fig. 2.12). There is limited intergranular porosity as the dolomite grains are well cemented with low-ferroan, sparry calcite. The permeability of this facies is low, averaging 200 md.

Facies F

Facies F, found throughout the Blueridge Member, is a very finely crystalline, poorly cemented dolostone that is typically saturated with bitumen. The bitumen often acts as the cement in this facies and when the bitumen is removed, the rock becomes a dolomite powder. This dolomite powder is white-gray in colour and has the texture of flour. This facies is found in beds up to 20 cm thick interbedded with Facies C and E. This facies differs from Facies B because it is formed entirely of dolomite (Fig. 2.7), and the rock forms a powder when the bitumen is removed.

The dolomite crystals in this facies are very finely crystalline (<100 μm), typically averaging 50 μm in size. The crystals are subhedral to anhedral in shape. Accessory minerals

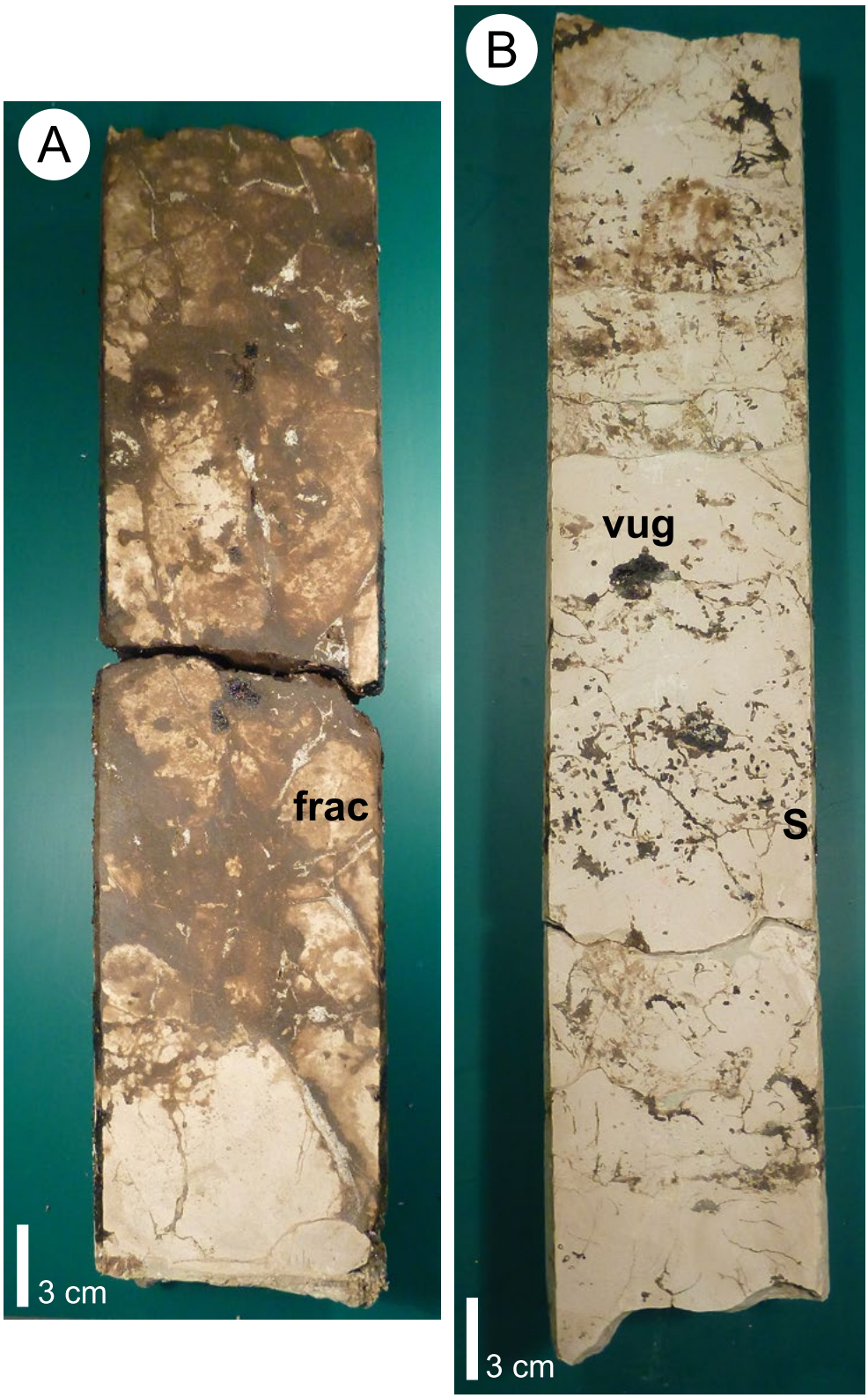

Figure 2.10: Cores characteristic of Facies E. frac = fractures; S = Syringopora sp.; vug = vuggy porosity. A) Core showing the fractured nature of Facies E; from 443.51 m from core 1AA/06-24-084-22W4. B) Core showing the vuggy porosity and *Syringopora* sp. from 452.37 m from well 1AA/06-24-084-22W4.

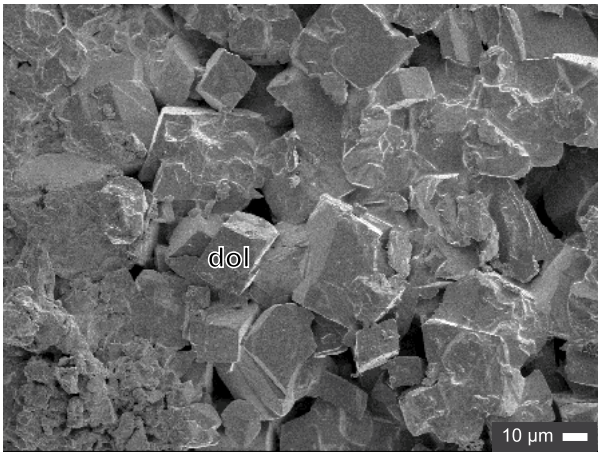

Figure 2.11: SEM image representing the characteristics of Facies E from 436.40 m from well 1AA/10-19-084-22W4. dol = dolomite.

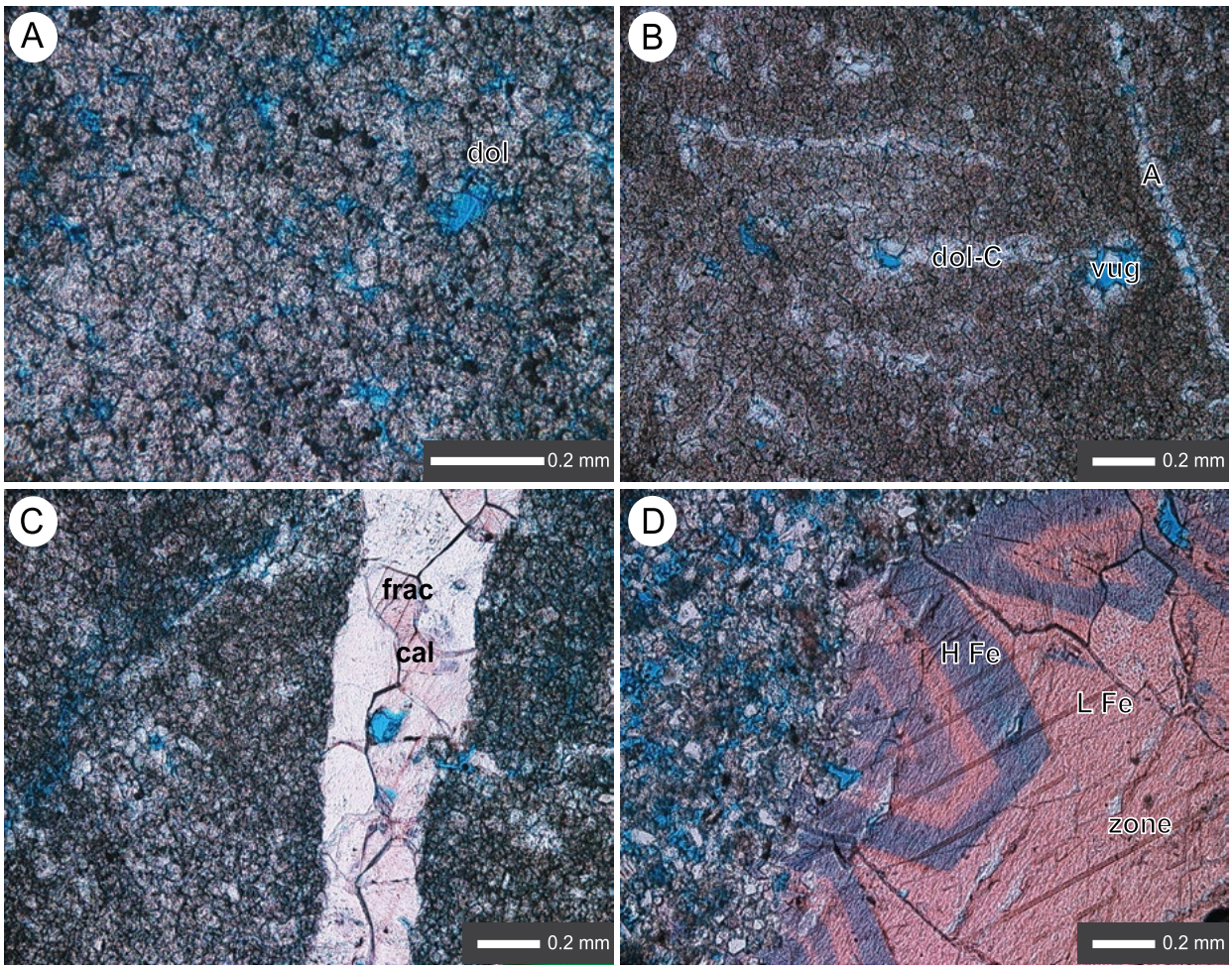

Figure 2.12: Thin sections characteristic of Facies E in PPL. dol = dolomite; vug = vuggy porosity; A = leached allochem; dol-C = dolomitic cement; frac = fracture; cal = calcite; zone = zoned calcite cement; H Fe = high-ferroan calcite; L Fe = low-ferroan calcite. A) Typical matrix in the rocks of Facies E from 443.00 m from well 1AA/06-24-084-22W4. B) Leached allochems, lined with dolomitic cement from 446.00 m from well 1AA/06-24-084-22W4. C) A fracture filled with calcite cement from 442.45 m from well 1AA/06-24-084-22W4. D) Zoned spar calcite cement seen in some of the vugs from 432.28 m from well 1AA/10-19-084-22W4.

include minor amounts (≤1%) of potassium feldspar, pyrite, quartz, and clay minerals. The clay minerals are mostly located in the pore throats between the dolomite crystals and there is rare dolomite cement. The facies is typically 'cemented' by the bitumen in the rock.

The porosity of this facies is very high, averaging 37% (ranges from 30 to 40%). The porosity is entirely intergranular. The permeability of this facies is also very high, averaging 425 md.

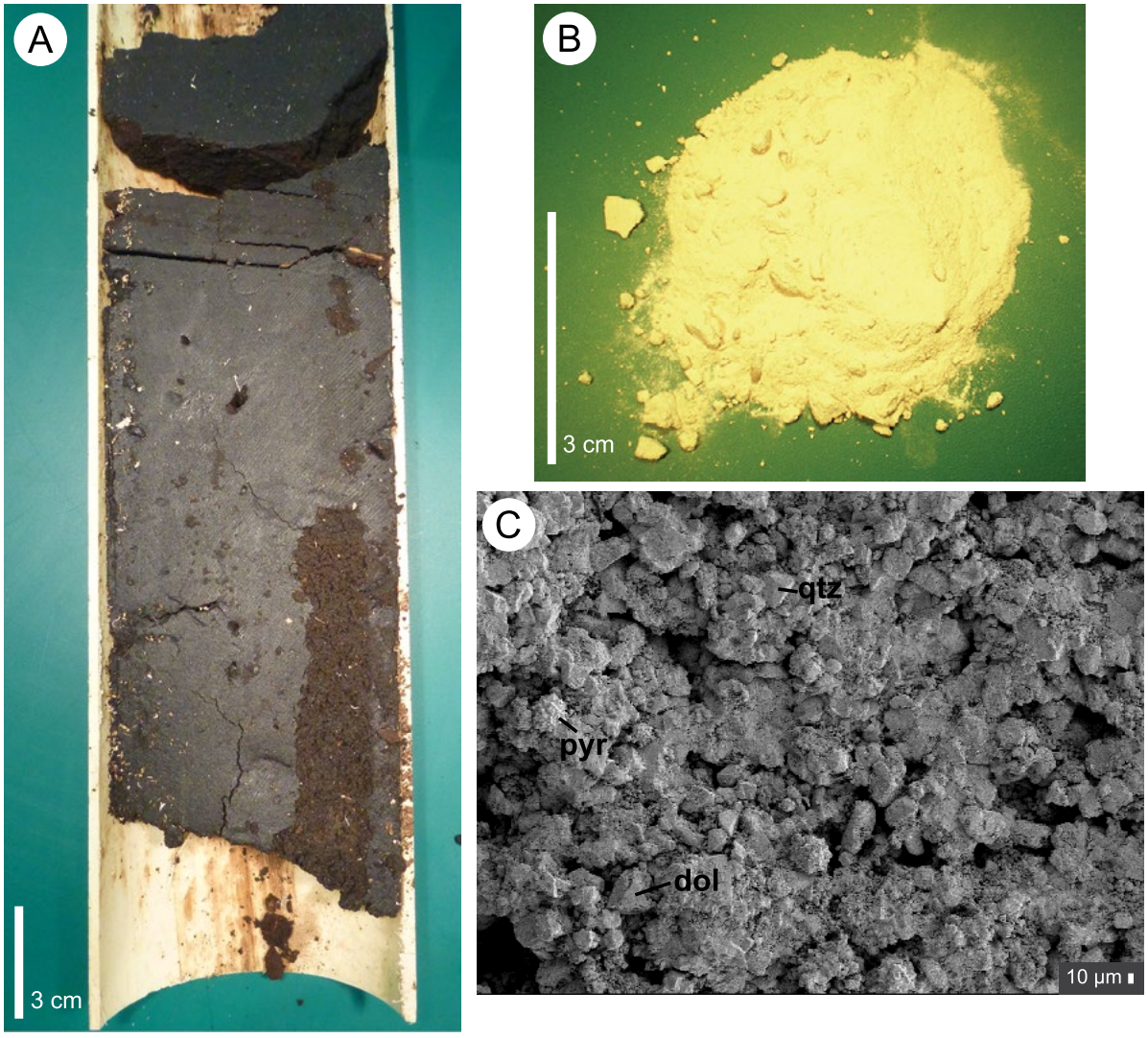

Figure 2.13: A) Core typical of Facies F from core 437.00 m from well 1AA/10-120-84-22W4. Note the saturation with bitumen and that the core cannot be removed from its sleeve. B) Core typical of Facies F when the bitumen is removed (powdered dolomite); from 438.00 m from well 1AA-10-12-084-22W4. C) SEM image of the rocks typical of Facies F from 438.00 m from well 1AA/10-12-084-22W4.qtz = quartz; pyr = pyrite; dol = dolomite.

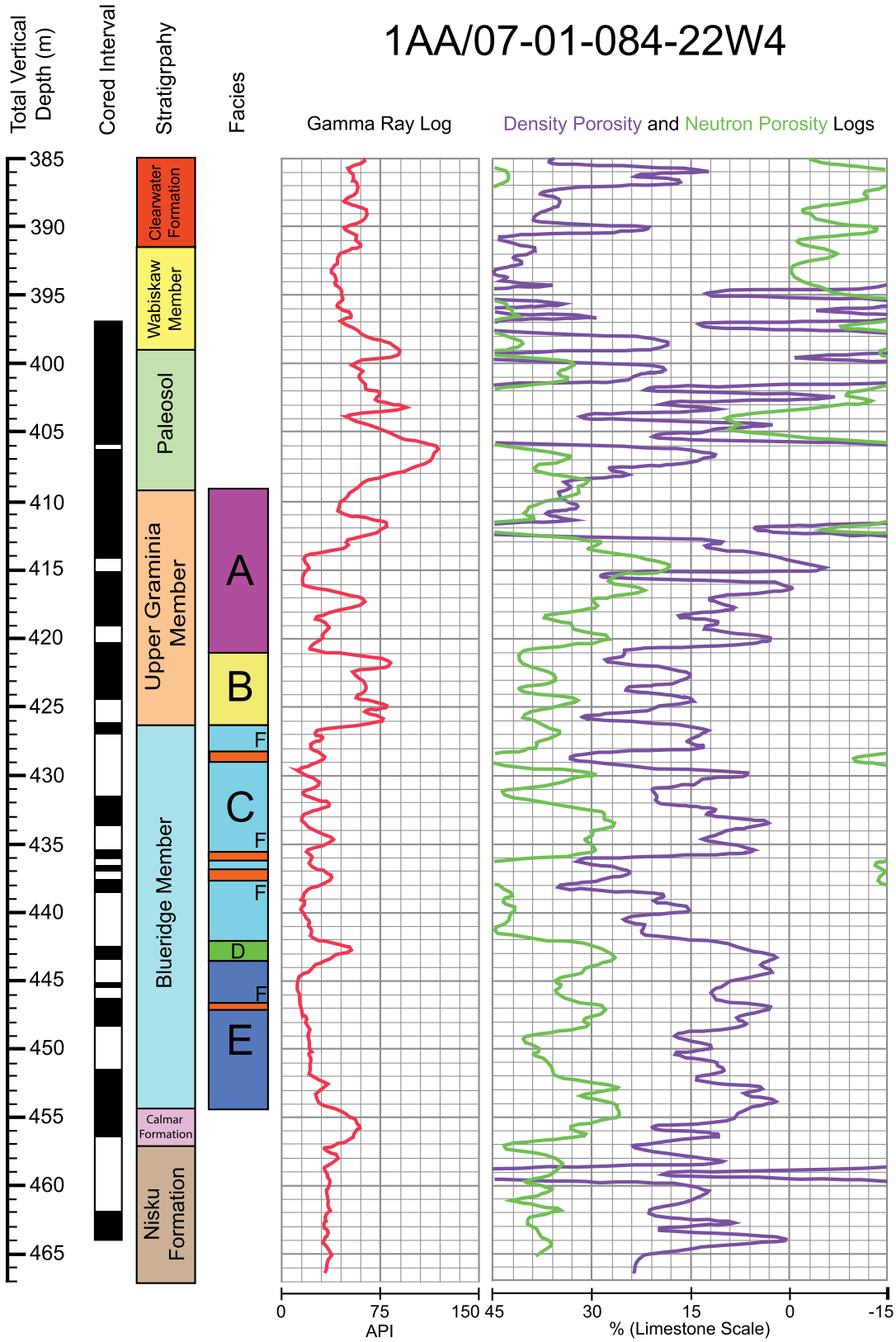

Figure 2.14: Type log showing the cored intervals, stratigraphy, facies and well log signatures of the Graminia Formation.

Facies Architecture

The logs from well 1AA/07-01-084-22W4 (Fig. 2.14), which provide the best overview of the succession, show the vertical facies architecture of the Graminia Formation in the study area. The facies occur in a regular and consistent vertical stacking pattern. At the top of the Graminia Formation is Facies A, followed by Facies B, Facies C, Facies D and Facies E in a downward succession. This order does not deviate throughout the study area (Fig. 2.15). Facies F occurs within Facies C and Facies E, when it is present, but does not correlate throughout the project area.

There is some lateral variation of the thickness of the facies (Fig. 2.15). The thickness of Facies A averages 10 m but varies from 0 to 15 m thick. Facies A displays the most variation as it thins and eventually pinches out towards the east.

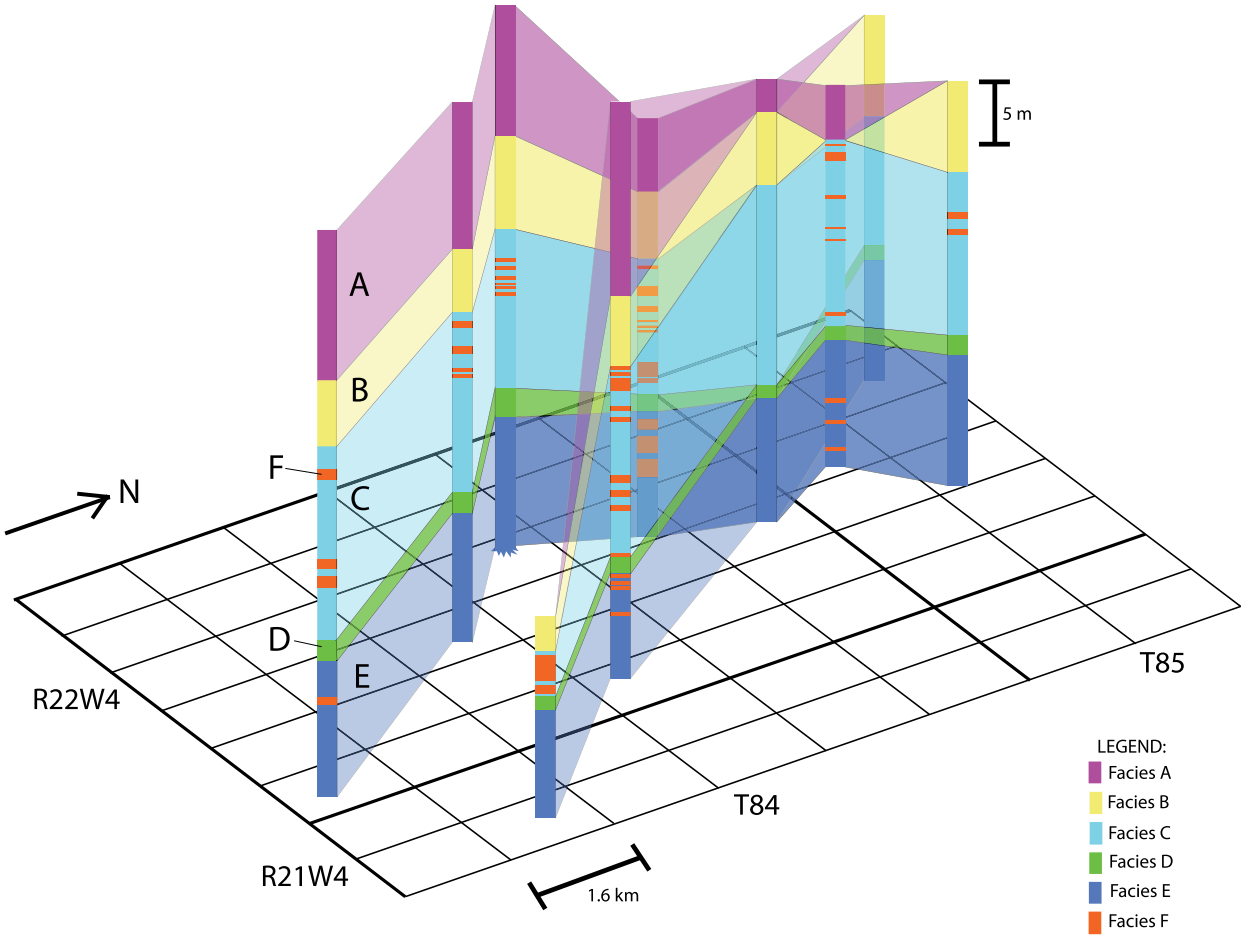

Figure 2.15: Fence diagram illustrating the lateral variation and relationships of the facies in the Graminia Formation across the Germain Field.

Facies B averages 6 m in thickness but varies from 3 to 9 m. The facies is thinnest in the southeast corner of the study area and thickest in the west-northwest. Similarly, Facies C is thinner in the southeast and thicker in the west-northwest. Facies C is also present in all of the wells in the study area. Facies C is 4 to 16 m thick with an average of 13 m.

Facies D, present in every well, is relatively uniform in thickness throughout the area. It averages 1.4 m in thickness but varies from 1.3 to 1.9 m thick.

Facies E averages 10 m thick and varies from 8 to 11 m. It is very consistent throughout the area, but does noticeably thin to the southeast.

Comparison with Other Studies

To date, the only information on the lithology, biostratigraphy and geochemistry of the Graminia Formation was provided by Meijer Drees et al. (1998) who described the formation in central Alberta in townships 55 to 66 and ranges 25W5 to 2W5, which is southeast of Germain Field. Meijer Drees et al. (1998) divided the Graminia Formation into the 'Graminia Silt,' the upper Blue Ridge, middle Blue Ridge, and the lower Blue Ridge.

The 'Graminia Silt,' as described by Meijer Drees et al. (1998), correlates with the Upper Graminia Member in the Germain Field, which includes Facies A and B. Meijer Drees et al. (1998) described the 'Graminia Silt' in their area as: "…an interbedded unit of green and greenish grey, dolomitic sandstones, siltstones and shales. The sand and siltstone beds are non-fossiliferous, have a bioturbated aspect and do not contain recognizable trace fossils."

Based on this study of the Germain area and the work of Meijer Drees et al. (1998), it appears that grain size in the 'Graminia Silt' may decrease towards the east. Meijer Drees et al. (1998) described the unit as being comprised of "dolomitic sandstone," whereas in the Germain Field, the grain size was identified as more consistent with silt-sized grains. This may be an artifact, as Meijer Drees et al. (1998) did not define the term "dolomitic sandstone" with respect to either grain size or mineralogical content. This unit thickens eastward towards the subcrop edge. The average thickness of the 'Graminia Silt' unit as described in Meijer Drees et al. (1998) is 2.9 m, whereas the Upper Graminia Member (Facies A and B) in the Germain Field is 16 m.

Meijer Drees et al. (1998) described the upper Blue Ridge unit as "…an interbedded unit of porous, peloidal dolostones; non-porous, brecciated, locally anhydritic dolostones, including a silty or sandy matrix; and non-porous, silty and locally stromatolitic dolostone." This unit does not correlate with any facies found in the Germain Field.

The middle Blue Ridge as defined by Meijer Drees et al. (1998), is characterized by "… porous, very fine to fine crystalline dolostones, including scattered, poorly preserved corals and brachiopods" with "vuggy porosity [that] is partly or completely filled with coarsely crystalline calcite or anhydrite." This is generally consistent with the Blueridge Member (Facies C and E) found in the Germain Field, except that no corals (other than the rare *Syringopora* sp. found in Facies E) or anhydrite were found in the Germain Field. The presence of anhydrite could be local to the study area of Meijer Drees et al. (1998).

Meijer Drees et al. (1998) described the lower Blue Ridge as being composed of heavily bioturbated, argillaceous, silty dolostones that decreases in thickness and grades eastward into the underlying Calmar Formation. Meijer Drees et al. (1998) hypothesized that this unit would pinch out towards the east. The Germain Field is east of the Meijer Drees et al. (1998) area and as predicted, this unit does not correlate to any units present within the Germain Field.

CHAPTER 3: DEPOSITIONAL REGIMES OF THE GRAMINIA FORMATION

Dolomitization has destroyed most of the fabrics that are needed to reconstruct the original sedimentology of the Graminia Formation and thus accurately interpret the original environment of deposition. It is, therefore, extremely difficult to ascertain the specific environments of deposition of the formation on an individual facies level. Instead, the environment of deposition is assessed from a broader perspective that deals with the stratigraphic units. The basin-wide framework will be discussed followed by a more specific look at the factors that affected deposition in the Germain Field.

Depositional Framework

Today, the Western Canada Sedimentary Basin (WCSB) is a foreland basin located throughout the Canadian provinces of northeastern British Columbia, Alberta, Saskatchewan, southwestern Manitoba and into parts of the northern United States. It includes a northeasterly trending wedge of sedimentary rocks that overlie an Archean and Proterozoic crystalline basement. It is divided into two major sub-basins; the Alberta Basin and the Williston Basin (Wright et al. 1994). These two basins are separated by a northeasterly-trending positive element, which includes the Bow Island Arch (Wright et al. 1994). The Germain Field is located within the Alberta Basin (Fig. 3.1).

During Devonian time, the WCSB was situated on the western edge of Laurussia, which was formed upon the convergence of modern day North America and Greenland in the late Silurian (Ziegler 1988). The relative position of the WCSB to the paleoequator is still a point of contention (e.g., Scotese et al. 1985; Embry 1988; Witzke and Heckel 1988) that depends largely on how the paleobiology, paleoclimatology, tectonics and/or paleomagnetic data have been integrated into the overall paleogeographic model. It is most likely that the Germain Field was located on a shallow marine ramp or shelf that was proximal to the paleoshoreline (Fig. 3.2). Witzke and Heckle (1988) and Wendte (1992a) suggested that the Germain Field was located at approximately 15°S during the middle Devonian, and by the late Devonian, plate tectonics had shifted the location of the field to a lower paleolattitude, closer to the paleoequator.

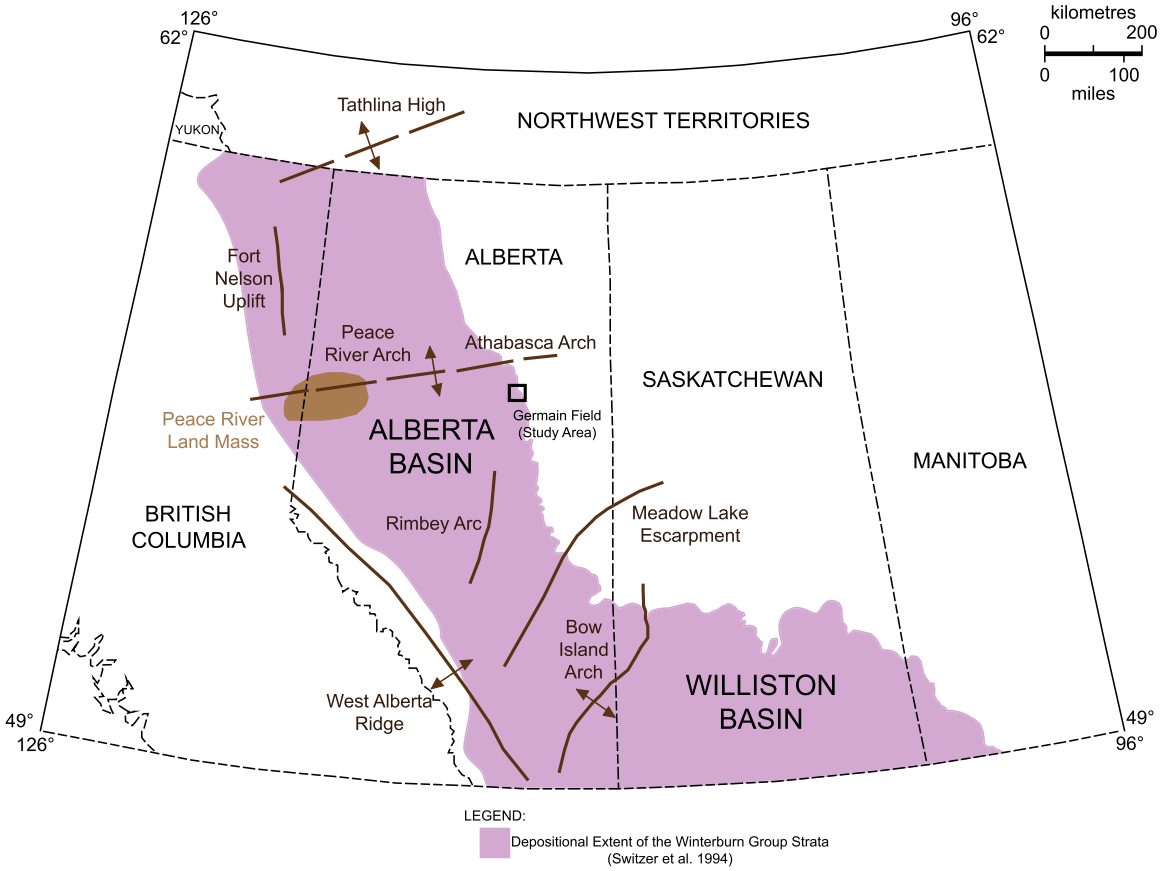

Figure 3.1: The extent of the Upper Devonian Winterburn Group in the Western Canada Sedimentary Basin and the tectonic elements; modified from Stoakes (1992), Switzer et al. (1994), and Wright et al. (1994).

The foreland basin was developed through tectonic events in the mid Jurassic to late Cretaceous and again in the late Cretaceous to Paleocene (Wendte 1992a). One of these events, the Laramide Orogeny, led to tilting, downwarping and deeper burial of the strata in the western part of the basin (Switzer et al. 1994). The deeper burial allowed for maturation and migration of hydrocarbons, which are of great economic importance today (Wendte 1992b). It also accounts for the consistent and uniform westerly dip of the Winterburn Group strata towards the center of the Williston Basin and into southwestern Saskatchewan.

The main basinal setting of the WCSB in the Devonian was a cratonic platform (Wright et al. 1994). Sediments were deposited on the cratonic platform over time and can be categorized into two stratigraphic divisions (Sloss 1963, 1988). The first division is the Sauk sequence, which contains rocks of Cambrian age and older. The second division contains three sequences of Paleozoic aged rocks: the Tippecanoe, the Kaskaskia and the Absaroka sequences. The Winterburn Group strata belong to the Kaskaskia sequence (Switzer et al. 1994).

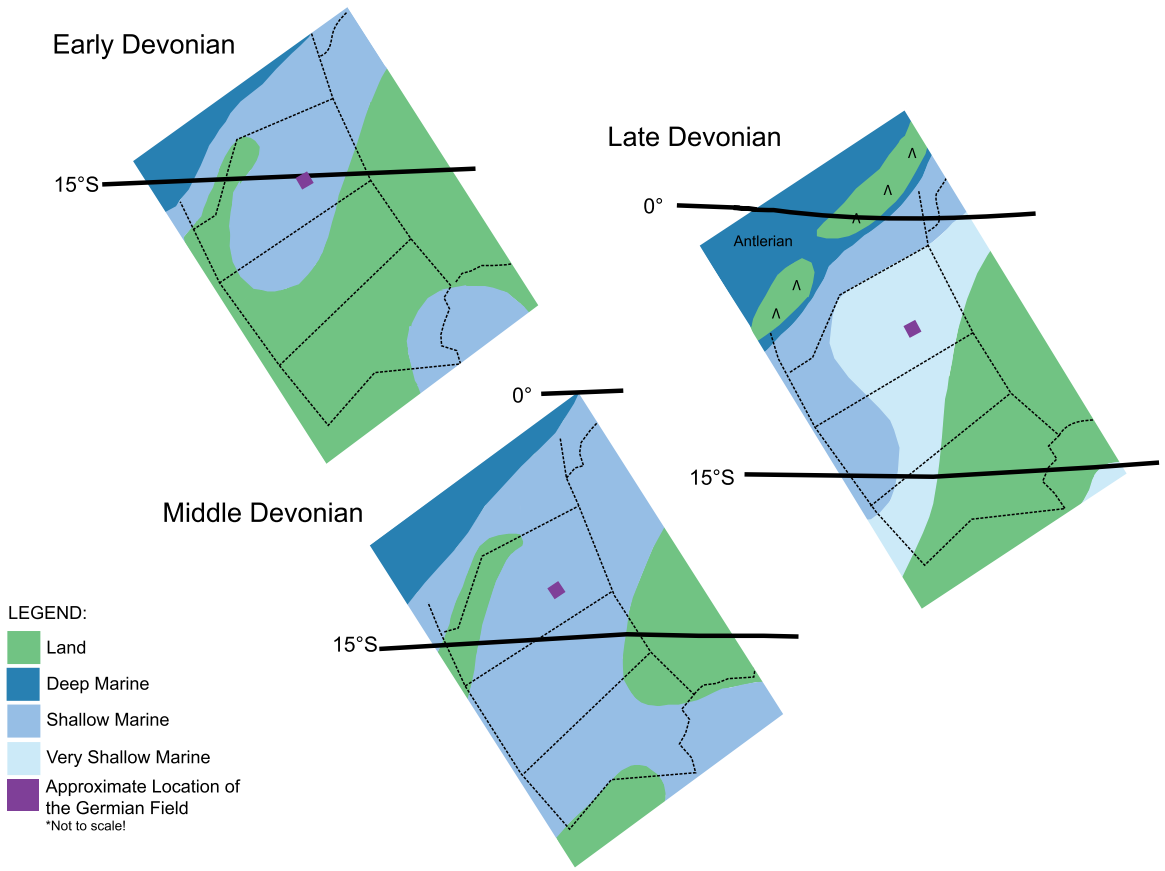

Figure 3.2: Paleogeography of the Germain Field throughout the early, middle and late Devonian; modified from Wendte (1992) and Witzke and Heckel (1988).

Alternatively, the sediments deposited on the cratonic platform can be divided into megasequences (as per Wendte 1992a, b; Stoakes 1992), which represent the sediments that are deposited over one complete transgressive-regressive cycle. Wendte (1992a, b) and Stoakes (1992) divided the Devonian sediments of the WCSB into five megasequences: the Upper Elk Point megasequence, the Beaverhill lake Megasequence, the Woodbend megasequence, the Winterburn megasequence, and the Wabamun megasequence. The sediments of the Winterburn Group are thought to have been deposited as part of the Winterburn megasequence, except for the sediments of the Upper Graminia Member (Wendte 1992b; Stoakes 1992; Switzer et al. 1994; Meijer Drees et al. 1998). The sediments of the Upper Graminia Member are thought to have been deposited as part of the Wabamun megasequence (Wendte 1992b; Stoakes 1992; Switzer et al. 1994; Meijer Drees et al. 1998).

Deposition of these sequences on the cratonic platform occurred largely on the passive margin and was controlled by recurring large scale transgressions and regressions (Kent 1994). Three inundations occurred within the basin, beginning with the first in the Cambrian, coming in from the west (Kent 1994; Wright et al. 1994). The second inundation came from the southeast

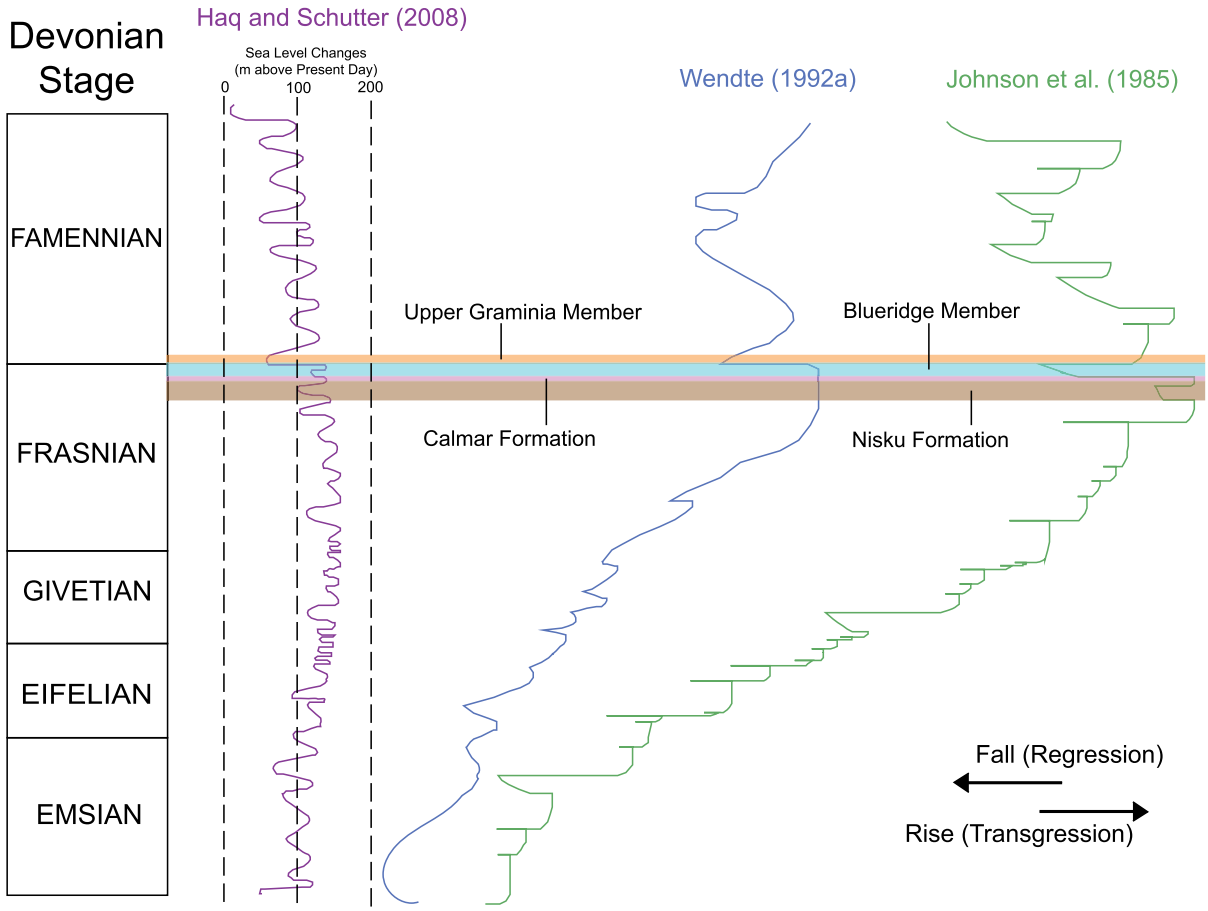

Figure 3.3: Sea level curves for the Devonian.

in the Late Ordovician and led to a prolonged period of carbonate sedimentation that ended in the Silurian (Kent 1968, 1969, 1984, 1994; Dunn 1976). The third inundation, which occurred in the Devonian, came from the northwest and spread into the interior cratonic platform through a southeast trending embayment. The embayment widened over time to become a seaway, which in turn gradually expanded into a ramp in the early Carboniferous (Geldsetzer 1988; Moore 1988; Morrow and Geldsetzer 1988; Kent 1994; Switzer et al. 1994).

The sea level curves for the Devonian (Johnson et al. 1985; Wendte 1992a; Haq and Schutter 2008) all similarly reflect an overall rise in sea level on a large scale (first order; Fig. 3.3). On a smaller scale (second order), there is an overall fall in sea level inferred over the late Frasnian and early Famennian when the sediments of the Winterburn Group were deposited (Johnson et al. 1985; Stoakes 1992; Wendte 1992a, b; Switzer et al. 1994; Haq and Schutter 2008). It is important to note that these sea level curves represent large thicknesses of rock deposited over long periods of time. The sediments of the Winterburn Group only represent a small fraction of the total thickness deposited. Thus, the curves can be difficult to interpret on such a small scale. There is also variation between the curves primarily due to scale. Haq and

Schutter (2008) and Johnson et al. (1985) presented sea level curves that reflect the global sea level, while the sea level curve that Wendte (1992a) developed is specific to the WCSB. The Germain Field is a very small area within the WCSB, so the actual sea level in that area may vary considerably from that proposed for the entire basin or globe.

The early Devonian was a period of epeirogenic uplift that resulted in significant topographic highs or cratonic arches (Fig. 3.1), including: the Peace River Arch, Athabasca Arch, Meadowlake Escarpment, Rimbey Arc, and the West Alberta Ridge (Switzer et al. 1994; Wright et al. 1994). There was also significant erosion of previously deposited strata. This uplift and erosion created a flat topographic profile at the top of the Woodbend Group strata. The sediments of the Winterburn Group were subsequently deposited on this flat surface (Switzer et al. 1994). As a result, the sediments of the Winterburn Group also have a very even distribution throughout the basin with very few areas of non-deposition (Fig. 3.1; Wright et al. 1994).

Deposition of the Winterburn Strata

Towards the end of the deposition of the sediments of the Devonian Woodbend Group, there was a third order fall in sea level (Potma et al. 2001), as reflected in the sea level curves proposed by Haq and Schutter (2008), Wendte (1992a), and Johnson et al. (1985) (Fig. 3.3). This event allowed the deep marine shales of the Upper Ireton Formation to be deposited (Switzer et al. 1994). The deposition of the sediments of the Winterburn Group marks the start of a new cycle, beginning with a third order transgression (Stoakes 1992; Potma et al. 2001).

The sediments of the Winterburn Group were deposited in the northeast corner of British Columbia, throughout most of Alberta, across southern Saskatchewan and into the southwestern corner of Manitoba (Fig. 3.1). In British Columbia, the Trout River Formation and the Kakisa Formation correlate to the Upper Graminia Member and the Blueridge Member (Fig. 3.4; Geldsetzer et al. 1993; Switzer et al. 1994). In northwestern Alberta, the Graminia Formation is present, but only consists of the Upper Graminia Member while the Blueridge Member still correlates to the Kakisa Formation (Fig. 3.4; Switzer et al. 1994; McLean and Klapper 1998). In the front ranges and foothills of Alberta, the Upper Graminia Member is related to the Sassenach Formation (Fig. 3.4; McLaren and Mountjoy 1962; Switzer et al. 1994; Weissenberger 1994; McLean and Klapper 1998). The Blueridge Member correlates to the Mount Hawk Formation and the Arcs Member of the Southesk Formation (Fig. 3.4; McLaren and Mountjoy 1962; Weissenberger 1994; McLean and Klapper 1998) in this area. In southern Alberta, the Crowfoot Formation correlates to the Upper Graminia Member and the Blueridge Member correlates to the Arcs Member of the Southesk Formation (Fig. 3.4; Belyea and McLaren 1957; Switzer et al.

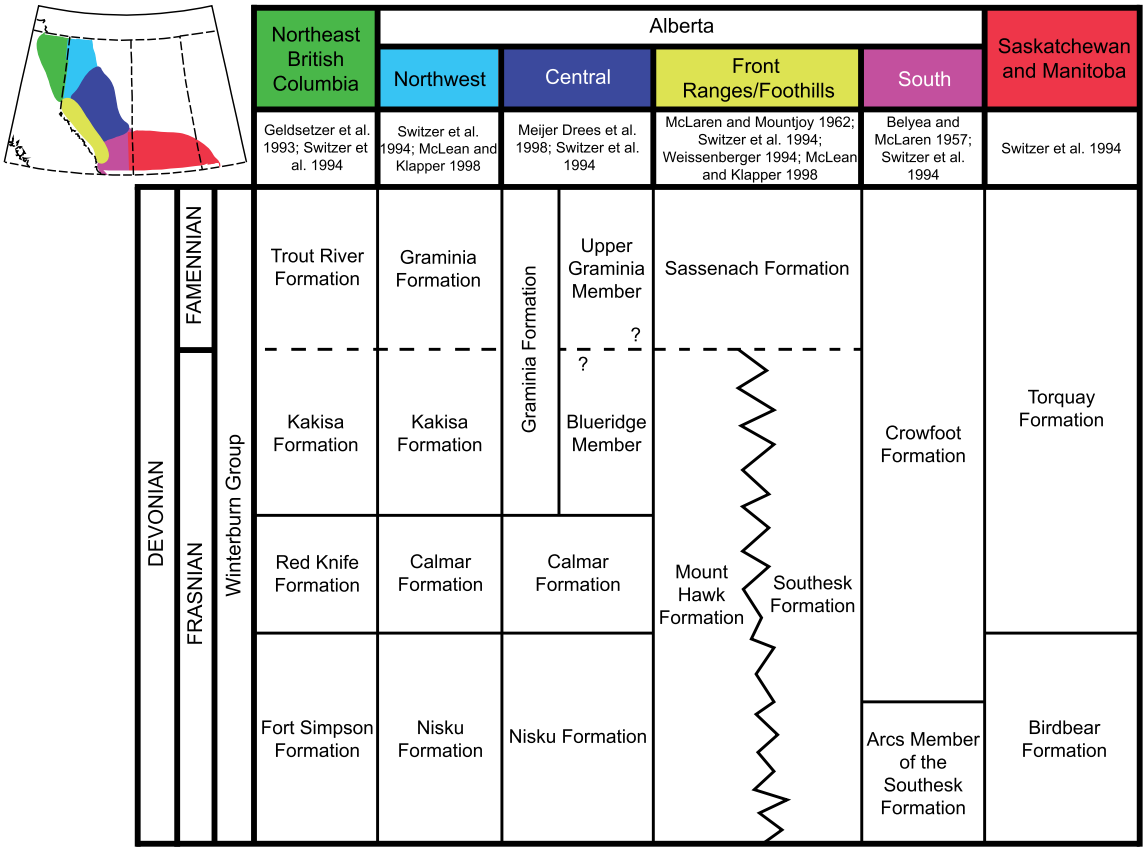

Figure 3.4: Stratigraphy of the Upper Devonian rocks across the Western Canada Sedimentary Basin.

1994). In Saskatchewan and Manitoba, the Upper Graminia Member correlates with the Torquay Formation and the Blueridge Member correlates to the Birdbear Formation (Fig. 3.4; Switzer et al. 1994).

The carbonate sediments of the Nisku Formation were deposited after those of the Upper Ireton Formation. The sediments of the Nisku Formation represent one full, third order cycle of transgression and regression (Fig. 3.3; Chevron Exploration Staff 1979; Stoakes 1992; Switzer et al. 1994; Potma et al. 2001). The sediments of the Nisku Formation were deposited primarily on a shallow marine ramp or shelf (Chevron Exploration Staff 1979; Switzer et al. 1994; Potma et al. 2001). The Nisku Formation is known for major reefal development that occurred within some areas of the basin (Chevron Exploration Staff 1979; Switzer et al. 1994; Potma et al. 2001). There was near complete, uniform filling of the basin by the end of the deposition of the Nisku Formation (Switzer et al. 1994). Due to a lack of core in the Germain Field, the Nisku Formation was not a focus of the study.

The Calmar Formation is formed of siliciclastic and carbonate sediments that have been interpreted very differently by various authors (e.g., Chevron Exploration Staff 1979; Wendte

1992b; Switzer et al. 1994; Meijer Drees et al. 1998; Potma et al. 2001). Most commonly, the sediments of the Calmar Formation are thought to have been deposited as a result of a small transgressive event which allowed for the widespread mixing of the siliciclastic and carbonate sediments (Chevron Exploration Staff 1979; Switzer et al. 1994; Potma et al. 2001). It is here that opinions diverge. The Chevron Exploration Staff (1979) thought that the input of clastic material into the sediments of the Calmar Formation was controlled by a very low rate of subsidence in the basin at the time. Conversely, Switzer et al. (1994) proposed that much of the clastic material was produced by reworking of the underlying Nisku Formation siliciclastics during the marine incursion. In some areas of the WCSB, the upper most Nisku Formation and the Calmar Formation are indistinguishable (Switzer et al. 1994). In the Germain Field, the sediments of the Calmar Formation were deposited in a deeper, mid-ramp setting, below fair weather wave base. This allowed for a combination of terrigenous clastic input, storm reworking of clastics of the underlying Nisku Formation, and bioturbation.

Following deposition of the sediments of the Calmar Formation, deposition of the sediments of the Blueridge Member (Table 3.1) commenced during a third order regression. Meijer Drees et al. (1998) and Switzer et al. (1994) agreed that in central Alberta, the sediments of the Blueridge Member were deposited on a carbonate shelf or ramp in shallow to very shallow water depths. Based on the sedimentology and allochems present, the sediments of the Blueridge Member in the Germain Field are thought to represent an inner-ramp setting. The lack of any coral build-up and the presence of robust allochems such as brachiopods and gastropods suggest turbulent wave energy (Meijer Drees et al. 1998). Anhydrite and other evaporitic minerals were observed in cored sections of the Blueridge Member in areas west of the Germain Field, suggesting that the basin was shallower westward (Choquette 1955; Meijer Drees et al. 1998).

At the end of the Frasnian, the sea level rose and sediments of the Upper Graminia Member were deposited (Table 3.1). In the Northwest Territories, Geldsetzer (1988) found a microkarst surface between the Kakisa Formation and the Trout River Formation, which are equivalents to the Blueridge Member and the Upper Graminia Member, respectively (Fig. 3.4). This implied that there was a period of subaerial exposure and thus, a discontinuity between these two members. For this reason, the Upper Graminia Member is considered to be depositionally related to the overlying Wabamun Group, but stratigraphically included in the discussion of the Winterburn Group strata because of its age. In the Germain Field, there is no evidence of such a discontinuity between the Blueridge Member and Upper Graminia Member. Instead, it is thought that the sea level fell causing the ramp in the Germain Field to shallow into the peritidal to supratidal zone. This eventually led to the subaerial exposure at the top of the Upper Graminia Member.

Facies	Stratigraphy	Deposition	Sea Level
A	Upper Graminia Member	Peritidal to supratidal	Transgression
B	Upper Graminia Member	Peritidal to supratidal	Transgression
C	Blueridge Member	Inner Ramp	Regression
D	Blueridge Member	Inner Ramp	Regression
E	Blueridge Member	Inner Ramp	Regression
F	Blueridge Member	N/A - Diagenetic	N/A - Diagenetic

Table 3.1: Summary of the deposition and the facies in the Graminia Formation.

The Frasnian-Famennian Boundary

Meijer Drees et al. (1998), Switzer et al. (1994), and Stoakes (1992) argued that the Blueridge Member and Upper Graminia Member were deposited as part of separate depositional sequences: the Winterburn megasequence and the Wabamun megasequence. The division of these two megasequences in the WCSB corresponds to the chronological transition between the Frasnian and the Famennian stages of the Devonian. The megasequence boundary also forms a disconformity and is typically marked by a lithological transition from carbonate to siliciclastic materials and a change in fauna. In the Germain Field, the deposition of the carbonate sediments of the Blueridge Member was terminated at the end Frasnian when sea level began to rise. The resulting transgression also signaled the end of the Winterburn megasequence. A new depositional sequence began with the start of the new transgressive-regressive cycle. The siliciclastic sediments of the Famennian Upper Graminia Member are therefore considered to be part of the next depositional sequence: the Wabamun megasequence.

The Frasnian-Famennian boundary represents one of the most significant global-scale extinction events of the Phanerozoic (Switzer et al. 1994). Many studies (e.g., Sorauf and Pedder 1986; Orchard 1989; Shields and Geldsetzer 1992; Weissenberger 1994; McLean and Klapper 1998) have attempted to confirm the exact ages of the Upper Graminia Member and the Blueridge Member primarily through a combination of biostratigraphy and sedimentology in order to constrain this boundary within the rock record of the WCSB. Due to a lack of fossils available for dating in the sediments and inconsistent changes in fauna along the perceived Frasnian-Famennian boundary, the exact boundary location has so far eluded scientists.

Based on sedimentology alone, as there was also a lack of fossils available for dating in the Blueridge Member and the Upper Graminia Member in the Germain Field, the sediments of the Upper Graminia Member in the Germain Field were deposited as part of the Winterburn megasequence, not the Wabamun megasequence as previously thought. There is no evidence to indicate a disconformity between the Blueridge Member and the Upper Graminia Member in the Germain Field.

CHAPTER 4: DIAGENESIS, POROSITY AND PERMEABILITY

Diagenesis

The formulation of a diagenetic history for the rocks of any formation incorporates many factors, including the stratigraphy, deposition, and the different processes that are involved in diagenesis. Despite the destruction of much of the original depositional fabric by dolomitization, there is sufficient information to understand some aspects of the evolution of the rocks in the Graminia Formation. These aspects include the vugs (very common), pervasive dolomitization, dolomitic cement (common), fractures (rare), calcite cements (very common), stylolites (very rare), and paleosol.

Dolomitization of the sediments that now form the Graminia Formation produced a thick succession of petrographically homogeneous, very finely crystalline dolostone. The dolostones of the Graminia Formation are consistent through the vertical extent of the strata and do not vary laterally throughout the Germain Field. There are also dolomitic cements that line many of the vugs in Facies C and E. It is unclear if the dolomitic cements were formed during the same phase of dolomitization as the matrix, or during a later phase. It is likely, however, that dolomitization occurred early in the post-depositional history as all of the original rock textures and fabrics have been destroyed. The dolomitization could have been formed by evaporation (sabhka model), seepage-reflux, marine mixing or thermal convection, as per the dolomitization models presented by Tucker and Wright (1990). There is no evidence to support any of these models; however, the sabhka model seems the most realistic mode of dolomitization given the presence of sulphate minerals in the Graminia Formation elsewhere in the basin (Choquette 1955; Switzer et al. 1994; Meijer Drees et al. 1998) as well as the supratidal depositional environment in which the facies of the Upper Graminia Member were deposited.

Scholle and Ulmer-Scholle (2003) demonstrated the typical stages of leaching in a carbonate rock; incipient grain leaching, moderate grain leaching, and complete grain leaching. Applying these stages, the rocks of the Graminia Formation display moderate to complete leaching of allochems (ooids, peloids, brachiopod fragments and gastropod fragments) in Facies C and E. This leaching took place before or during the dolomitization of the succession as many of the leached allochems are lined with dolomitic cement. If vugs were formed prior to dolomitization, little can be determined about their initial formation as the original fabrics have been completely obliterated, leaving just the original outline of the allochem (Tucker and Wright 1990).

Fractures occur in Facies A and E, but are more common in Facies E. They were formed

post-dolomitization. Most of the fractures are filled with calcite cement, but some remained open. These fractures may have formed during the early stages of burial diagenesis based on the presence of calcite cement and lack of dolomitic cement, as is consistent with similar examples given by Tucker and Wright (1990).

Spar calcite cement fills some of the intergranular pores, the vugs, and the fractures found in the dolostones of the Graminia Formation. In Facies A and to a lesser degree, in Facies B, the calcite cement fills the intergranular pores. Some vugs in Facies C and E are lined with dolomitic cement and filled with calcite cement. In Facies A, C and E, the calcite cement variably occludes the vuggy porosity and the fractures. Zoning in some of the calcite cement provides a record of subtle changes in the pore-fluid conditions as is commonly associated with burial diagenesis (Dickson 1966; Katz 1971; Scholle and Ulmer-Scholle 2003).

There are rare stylolites in Facies E. Tucker and Wright (1990) noted that stylolites are indicative of chemical compaction due to burial diagenesis. Timing of the burial with respect to dolomitization can generally be determined by whether or not the stylolites cross-cut the dolomite grains (Tucker and Wright 1990). It is not possible to determine if the chemical compaction occurred before or after the dolomitization in the Graminia Formation because the dolomite crystals are too small to determine if the stylolites cross-cut the individual crystals or not.

There is an apple-green-gray silty-shale paleosol overlying the Graminia Formation in many, but not all, of the wells in the Germain Field. This paleosol was recognized based on the criteria given by Wright (1992) including: biological features, colour, destratification, horizonation and boundaries, granulometrics, mineralogical assemblages, macrostructures, and micromorphology. Following deposition of the Graminia Formation, there was either hiatus in the rock record or sediments were deposited and subsequently eroded until the Albian, when the overlying Wabiskaw Member (Mannville Group) was deposited. This paleosol was probably deposited in association with a period of subaerial exposure and possibly karstification that took place sometime during this hiatus and after the rocks of the Graminia Formation were formed, buried, and diagenetically altered. The hiatus in stratigraphy suggests that the paleosol must have been formed sometime during the early Carboniferous to the early-mid Cretaceous. There is no direct evidence to suggest that the rocks of the Graminia Formation in the Germain Field were subject to any karst processes prior to the deposition of this paleosol, but there is a potential karst surface at the Frasnian-Famennian boundary between the Upper Graminia Member and Blueridge Member in other areas.

Bitumen migration likely occurred last as all of the rocks of the Graminia Formation

and some more porous sections of the overlying paleosol are stained. The source of the oil and bitumen in the Winterburn Group is still being debated. Based on the total organic carbon (TOC) values reported by Meijer Drees et al. (1998), the shales in the Graminia Formation are not source rocks. The Chevron Exploration Staff (1979) and Allan and Creaney (1991) argued that the oil and bitumen found in the Winterburn Group was generated in the lower most shales of the Cynthia Member (Nisku Formation). Fowler et al. (2001) and Stasiuk and Fowler (2004) found that in southern Alberta, the rocks of the Cynthia Member had high (up to 15%) TOC values, which means that these rocks are good potential source rocks. They also found that while these rocks could be acting as the source of hydrocarbons in southern Alberta, the rocks of the Cynthia Member in west-central Alberta are comprised of a different organic facies, which lacks the necessary organic content to produce hydrocarbons. Fowler et al. (2001) and Stasiuk and Fowler (2004) predicted that these non-productive rocks extend into northeastern Alberta, and thus are likely not the source rocks of the Winterburn Group in that area.

The Duvernay petroleum system was thought to be the source of the oil and bitumen in the Winterburn Group (Creaney et al. 1994) until Shuqing et al. (2008) found that most of the oil and bitumen in the Devonian rocks of northern Alberta came from the Devonian-Mississippian Exshaw Formation. Adams (2008) also found that the Duvernay petroleum system was not a significant source of oil and bitumen in northeastern Alberta and suggested that the potential source rocks included the Exshaw Formation, the Triassic Doig Formation, the Triassic Montney Formation and the Jurassic Gordondale Member. Ranger and Gingras (2006) and Higley et al. (2009) found that the oil and bitumen found in the Devonian rocks in northern Alberta were sourced from the Jurassic Fernie Group rocks, specifically, the Gordondale Member and Poker Chip A Shale Member. Ranger and Gingras (2006) and Higley et al. (2009) performed the most comprehensive study of the Devonian strata in northern Alberta and it is likely that their model is the most applicable to the rocks of the Graminia Formation in the Germain Field.

Understanding the timing of bitumen migration is important in order to understand the timeframe in which most of the diagenesis occurred. Assuming that the source rocks of the Graminia Formation in the Germain Field were the Jurassic Fernie Group rocks (as per Ranger and Gingras 2006, and Higley et al. 2009), hydrocarbon migration is thought to have occurred from 40 to 90 million years ago in the WCSB, with most of the migration occurring 50 and 70 million years ago, during the late Cretaceous to the Eocene (Ranger and Gingras 2006; Higley et al. 2009). Radiometric studies suggested that hydrocarbons may have migrated as early as 118 to 108 million years ago during the early Cretaceous in the WCSB (Selby and Creaser 2005). Thus, most of the diagenetic alteration must have occurred prior to the Cretaceous.

Facies F

The dolomite powders of Facies F are very similar to the 'powdered dolomite' described from the Buda Hills of Hungary (Poros et al. 2013), 'powdered dolomite' or 'dolofudge' in the Grosmont Formation, Alberta, Canada (Machel et al. 2012); the 'chalky' or "porous, friable" dolomite in the Winnipegosis Formation, Saskatchewan, Canada (Fu et al. 2004; 2008), and the 'flour dolomite' in the Yunnan-Guizhou Plateau, China (Ji et al. 2004a; b). The dolomite in Facies F also bears a striking resemblance to the pulverulite or 'spongy dolomite' of the Edwards Formation in Texas, USA (Blank and Tynes 1965; Fisher and Rodda 1969; Rose 1972; Chafetz and Butler 1980) and the pulverulite of the Lockport Dolomite found at Rocky Ridge, Ohio, USA (Kahle 2011). The dolomite in Facies F also shares many similarities with the 'dolomitic sand' of the Upper-Cambrian to Lower-Ordovician Knox Group rocks from near Knoxville, Tennessee, USA and the 'disaggregated dolomite' or 'sanded dolomite' from the Muschelkalk sequence of the Cracow-Silesian region, in Poland (Bogacz et al. 1973).

Despite extensive study of powder dolostones (Table 4.1), their formation is poorly understood. To date, the four models proposed for their formation are: (1) "cryogenic powderization" (Poros et al. 2013), (2) hydrothermal-related formation (Kendall 1960; Bogacz et al. 1973), (3) recent weathering-induced formation (Blank and Tynes 1965; Fisher and Rodda 1969; Rose 1972; Chafetz and Butler 1980; Kahle 2011), and (4) karst/exposure-related formation (Fu et al. 2004a, b; Machel et al. 2012).

Poros et al. (2013) suggested that the powdered dolomite found in Triassic dolostones of the Buda Hills, Hungary was formed through a process called "cryogenic powderization." This model suggests that the dolostones disintegrated into powdered dolomite after they had been saturated with water and then subject to subaerial exposure in a cold climate (Poros et al. 2013). The dolostones were pervasively fractured forming a vast network which drastically improved permeability and allowed for the near complete saturation of the intercrystalline space in the dolostone to become saturated with water. Once this saturated unit was exposed to cold climatic conditions, the water froze, physically forcing the dolomite crystals apart and powdering the dolostone (Poros et al. 2013).

While this model may provide a reasonable explanation for the dolostones in Hungary, it is unlikely that it could account for Facies F in the Graminia Formation in the Germain Field. There is no evidence of any subaerial exposure of the rocks that would have been consistent with multiple episodes of exposure needed to form the beds and laminae of Facies F through cryogenic powderization. Also, the paleogeography in the Devonian indicates that the Germain Field was located close to the equator, where the climate would not be conducive to cold conditions needed to drive the process.

Reference	Terminology	Location	Age	Rock Description	Possible Formation
Poros et al. 2013	Powdered dolomite	Buda Hills, Hungary	Triassic	Fine grained dolomite crystals ranging in 100 to 300 μm in diameter. The powder has a flour-like appearance. Commonly contains come breccia clasts that are a few cm in diameter. There is variable degree of powderization; some areas are completely powdered and others are more intact.	Cryogenic powderization – dolostones were pervasively fractured forming a vast network which drastically improved permeability and allowed for the near complete saturation of the intercrystalline space in the dolostone to become saturated with water. Once this saturated unit was subaerially exposed into cold climate conditions, the water froze, physically forcing the dolomite crystals apart and functionally powdering the dolostone. Previous studies propose the following models for how the powdered dolomite formed, but have been largely disproven: Hydrothermal-related formation, weathering-induced formation and karst/exposure-related formation (here, the exposure is related to the Pre-Tertiary unconformity).
Machel et al. 2012	Powdered dolomite or dolofudge	Grosmont Formation, Alberta, WCSB	Devonian	Nearly white to grey dolomite powder – bitumen matrix/cement.	Karst/exposure-related – gypsum and anhydrite layers contained floating dolomite crystals and when these sulphate minerals were dissolved during a period of karstification and exposure, the dolomite crystals remained, leaving a dolomite powder.

Table 4.1: Summary of the instances of powdered dolomite in the literature and its suggested origins.

Kendall 1960	Dolomitic Sand	Jefferson City Mine, outside Knoxville, Tennessee (USA)	Upper Cambrian - Lower Ordovician	Light gray to white and yellowish, dolomite with sphalerite powder; considered to be detrital. Grain size ranges from sand-sized grains to dolomite fragments several inches long. Appears in laminae (tenths of an inch thick) to beds (not exceeding 1 ft. thick); these are parallel with strike and dip of the rock and fills vugs to caves/caverns.	Hydrothermal-related formation – the dolomitic sands were thought to be the product of formation of "grain-by-grain release of dolomite particles that were capable of some intergranular solution" in the presence of hydrothermal fluids (Kendall 1960). The dolomitic material was thought to be held in suspension by the hydrothermal fluids until the waters released and it was deposited as now observed. The hydrothermal fluids were also thought to emplace the sphalerite that is present with the dolomitic sands observed under similar conditions.

Table 4.1 Continued.

Bogacz et al. 1973	Disaggregated dolomite or sanded dolomite	Muschelkalk Sequence, Cracow-Silesian Region, Poland	Triassic	The dolomite is described as a weakly cemented, porous mass of dolomite crystals and grains, typically consisting of very fine-grained crystals that can also occur as large, angular rock fragments. It is light-gray to almost white, sometimes with a dark tint if galena or other sulphides are present and sometimes yellowish (due to secondary oxidation) in color.	Hydrothermal-related formation – the dolomites are thought to be detrital and formed from the ore-bearing dolomites in the area via solution disaggregation which "sanded" parts of the ore-bearing dolomite rocks. This "sanding" process dissolutes the crystal edges with hydrothermal fluids. It is thought that the disaggregation and galena emplacement are penecontemporaneous and that the ore-mineralization is occurring separately from the disaggregation (i.e. the two are separate and un-related processes). They note that there is no evidence of surficial weathering in these rocks.
Fu et al. 2004; 2008	Chalky dolomite and "porous, friable dolomite"	Winnipegosis Formation, Saskatchewan, WCSB	Devonian	Greyish white to cream-coloured, porous, friable and slightly indurated silt-sized particles composed of single dolomite crystals or aggregates of crystals. Sand-sized breccia fragments are present.	Karst/Exposure-related – the smaller-scale powdered dolomite "chalky horizon" was interpreted to be pedogenic in nature and was essentially just part of calcrete profile (Fu et al. 2004). The larger bed-size occurrences were thought to be due to local dedolomitization and/or dissolution of dolomite (Fu et al. 2008).

Table 4.1 Continued.

Ji et al. 2004a, b	Flour dolomite	Yunnan Guizhou Plateau, China	Triassic	The flour dolomite is described as being part of a weathering bedrock horizon, which is subdivided into a flour dolomite layer, a cracked dolomite layer and primary dolomite layer The flour dolomite layer was found to be enriched in rare earth elements compared to the cracked dolomite and intact or primary dolomite layers.	Karst/Exposure-related – the whole area has been subjected to massive chemical weathering and karstification; Ji et al. (2004 a, b) do not outright suggest a model of formation for this flour dolomite layer as the focus of their study is the geochemistry of the rocks.
Blank and Tynes 1965; Rose 1972; Chafetz and Butler 1980	Chalky dolomite or pulverulite	Edwards Formation, Texas (USA)	Cretaceous	Soft, friable, porous mass of rounded dolomite crystals. The powdery nature of this dolomite is actually due to the hollow dolomite rhombs.	Weathering-induced powderization – product of partial dissolution of host limestone or dolomite brought about by near surface Pleistocene-Holocene weathering. It is believed that this phenomenon only occurs several meters into the face of the exposed outcrop and is not present within the unexposed sections.

Table 4.1 Continued.

Kahle 2011	Pulverulite	Lockport Dolomite, Rocky Ridge, Ohio (USA)	Silurian	Porous, crumbly, soft and powdery, subrounded to rounded masses of dolomite; dolomite crystals range in 5 to 20 μm in diameter. It forms in bedding perpendicular pipes. (Unlike the Edwards Formation pulverulite, there are no hollow dolomite crystals).	Weathering-Induced Powderization – resulted from downward percolation of very acidic groundwater leading to chemical and mechanic weathering which produced the powdered. The very acidic ground water was thought to be caused by the interaction of the tree roots and ground water.

Table 4.1 Continued.

Machel et al. (2012) suggested that cryogenic powderization is a potential mode of formation for the powdered dolomites found in the Grosmont Formation in Alberta, Canada. They suggested that if the migration of bitumen into the Grosmont Formation was very late, the dolostones in the formation could have been subject to cryogenic powderization during the Pleistocene. This would imply that the bitumen migrated after the period of glaciation during the Pleistocene to allow the dolomites to be saturated with water then frozen and powdered. Higley et al. (2009) showed, however, that the bitumen migrated into the Grosmont Formation during the late Cretaceous to Eocene, at about the same time as the Graminia Formation. This implies that rocks of both the Grosmont Formation and Graminia Formation were saturated with bitumen prior to the Pleistocene. Thus, it is not likely that cryogenic powderization formed the powdered dolomites of the Grosmont Formation or the dolomites of Facies F in the Graminia Formation.

Kendall (1960) described a light-gray to whitish yellow 'dolomitic sand' in the Upper Cambrian to Lower Ordovician Knox Group rocks, outside Knoxville, Tennessee. Kendall (1960) also found sphalerite in the dolomites, which is what gives them their yellowish hue. This dolomitic sand was found filling vugs, caves, and caverns. He thought that the 'dolomitic sand' must have been formed during the same time as the sphalerite and that its formation had to be related to the same hydrothermal fluids that produced the dolomite. Kendall (1960) argued that the vugs, caves, and caverns were formed prior to the hydrothermal fluid influx through separate processes, possibly karst. Kendall (1960) proposed that these 'dolomitic sands' were the product of "grain-by-grain release of dolomite particles" into suspension in the hydrothermal fluid, which settled out once the water receded. Kendall (1960) did not suggest the precise mechanism of how the dolomite grains were released.

Bogacz et al. (1973) also proposed a hydrothermal-related method of formation for the 'disaggregated dolomite' or 'sanded dolomite' found in the Muschelkalk Sequence in the Cracow-Silesian Region of Poland. Similar to the 'dolomitic sand' described by Kendall (1960), this dolomite contains hydrothermal minerals, including galena and some sphalerite and was also found in vugs, caves, and caverns in the rock. Bogacz et al. (1973) argued that the dolomite was formed through solution disaggregation or a process referred to as "sanding," while the vugs, caves, and caverns were formed earlier, likely through karstification. The "sanding" or solution disaggregation process is where hydrothermal fluids cause the dissolution of dolomite crystal separating them from the original rock and forming anything from a very finely grained, crystalline powder to large, angular rock fragments. Bogacz et al. (1973) also argued that while the emplacement of the galena and other hydrothermal minerals was penecontemporaneous with the formation of the disaggregated dolomite, the mineralization and disaggregation occurred independently of each other in the same hydrothermal fluid.

The presence of sphalerite, galena, and other hydrothermal minerals in the dolomite powder found in the rocks of Tennessee (Kendall 1960) and Poland (Bogacz et al. 1973) fits the hydrothermal-related model of formation. This model, as proposed, cannot account for the occurrence of Facies F in the Graminia Formation in the Germain Field as there is no evidence to suggest any hydrothermal alteration of those rocks. Also, there is a lack of hydrothermal minerals present, even in trace amounts.

Chafetz and Butler (1980), Rose (1972), and Blank and Tynes (1965) proposed that the pulverulite that they found in the Edwards Formation along road-cut out crops in Texas, USA was the product of partial dissolution of the host limestone or dolomite associated with near surface Pleistocene-Holocene weathering. Chafetz and Butler (1980) argued that this phenomenon only occurs several meters into the face of the exposed outcrop and is not present within the unexposed sections. Rose (1972) found that the pulverulite in the Edwards Formation is comprised of hollow dolomite rhombs, which may account for the powder-like nature of the dolomite.

Kahle (2011) described a variety of pulverulite, found in the Lockport Dolomite, near Rocky Ridge, Ohio, USA, as “porous, crumbly, soft and powdery” dolomite. According to Kahle (2011), these powdery dolomites did not have hollow rhombs like those in the Edwards Formation. This dolomite is, however, similar to the powdered dolomite in Facies F of the Graminia Formation. Kahle (2011), like Chafetz and Butler (1980), Rose (1972), and Blank and Tynes (1965), attributed formation of this dolomite to recent weathering and thought the term pulverulite was appropriate. Kahle (2011) suggested that the powdered dolomite formed via the downward percolation of acidic groundwater which led to chemical and mechanical weathering. The acidic ground water was attributed to the interaction of the tree roots and ground water.

The recent weathering model is also applicable to the examples given in Texas and in Ohio, but cannot explain the powdered dolomite found in the Graminia Formation. Facies F occurs randomly throughout the entire formation and does not seem to be directly related to any weathering surfaces. Similarly, if Facies F was the product of weathering, there would be horizons that would correlate between wells from when the intact dolostones were exposed to weathering; however, Facies F cannot be correlated between any wells in the Germain Field (Fig. 4.1, 4.2).

Fu et al. (2004, 2008) proposed a karst/exposure-related origin for chalky dolomite found in the Winnipegosis Formation in Saskatchewan, Canada. Fu et al. (2004) suggested that the 'chalky horizon' of dolomite is pedogenic in origin and hence part of a calcrete profile. The thicker horizons in the Winnipegosis Formation were also thought to be related to the karstification and were attributed to local dedolomitization and/or dissolution of dolomite (Fu et al. 2008).

Machel et al. (2012) went into more detail with respect to the karst/exposure model. They suggested that there were gypsum and anhydrite layers in the Grosmont Formation that contained floating dolomite crystals and at some point, the gypsum and anhydrite were dissolved during a period of exposure and karstification. This process left the dolomite crystals without cement or matrix and as a result, they remained as a powder. After bitumen migration, this powder became saturated with the bitumen, just like the powdered dolomite seen in the Graminia Formation. Machel et al. (2012) also mentioned that the powdered dolomite could have been formed through syn-depositional calcite or dolomite dissolution or syn-depositional evaporate dissolution but did not elaborate on these alternatives.

The origin of the powdered dolomite in the Graminia Formation remains an enigma. Among the models proposed, the karst/exposure model seems the most probable. Machel et al. (2012) and Fu et al. (2004, 2008) both agreed that karst/exposure led to the formation of powdered dolomite, but the precise mechanism involved in its formation is not known. The Graminia Formation underwent a period of subaerial exposure and was potentially subject to some karstification which formed the paleosol between the Carboniferous and Cretaceous although beyond the paleosol, there is no evidence of such process occurring. In the model proposed by Machel et al. (2012), the presence of sulphate minerals like gypsum and anhydrite are critical for the formation of powdered dolomite and while the Graminia Formation is known to have contained sulphate minerals (Meijer Drees et al. 1998), there are no reported instances of powdered dolomite when these minerals are present in the formation. Conversely, in the Germain Field, there are no sulphate minerals present and yet there is powdered dolomite in the rocks.

Another problem arises when applying the karst/exposure model to Facies F of the Graminia Formation in the Germain Field. If Facies F was formed as a result of subaerial exposure and karstification, some correlation of the horizons of Facies F representing paleoexposure surfaces should be expected. There is, however, a lack of any correlation of Facies F across the Germain Field (Fig. 4.1, 4.2). The karst/exposure model could still apply if the occurrence of the Facies F was due to the facies acting as a cave or cavern fill. This would explain the lack of correlation across the Germain Field as the level of well control in this study would not provide a small enough scale to determine this.

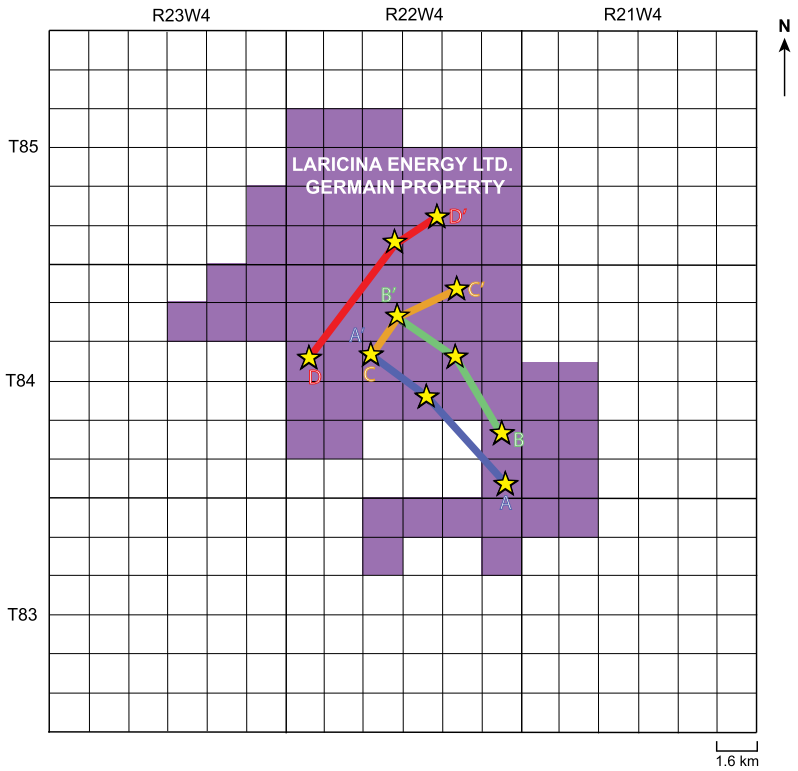

Figure 4.1: Index Map illustrating the cross-sections that show the changes in porosity and permeability laterally over the Germain Field.

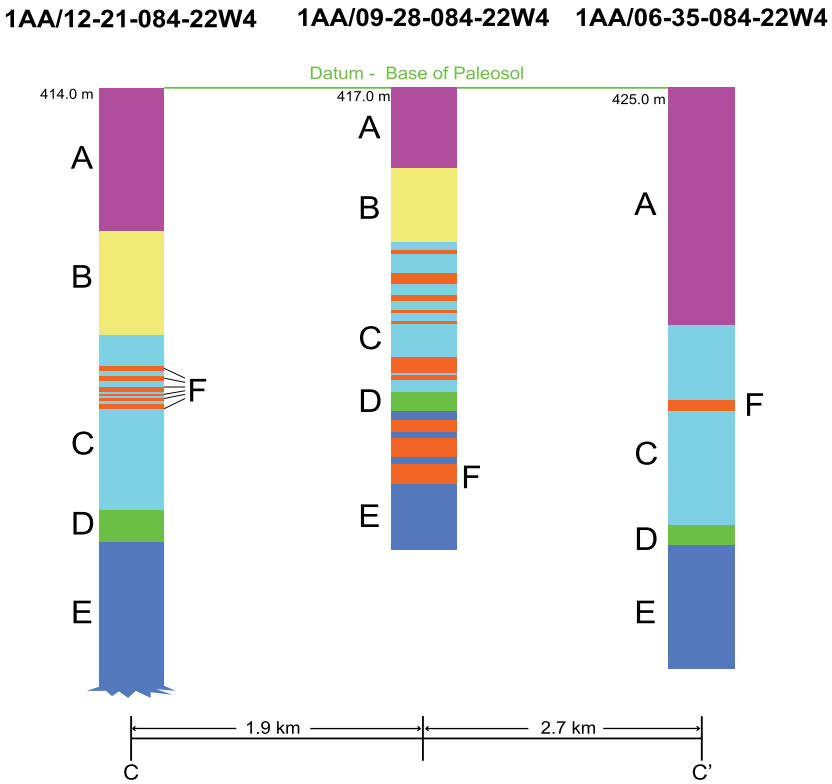

Figure 4.2: Cross Section C-C' showing the lack of correlation of Facies F in the Graminia Formation across the Germain Field.

It is evident that there are issues with how the karst/exposure model applies to the rocks of the Graminia Formation. Perhaps the bitumen that saturates the powdered dolomites of the Grosmont Formation Facies F of the Graminia Formation is related to its formation within rocks of the WCSB. Often the dolomite in these formations is not known to be powdered until the bitumen is extracted. The powdered dolomites in the WCSB could possibly be formed by an interaction of the parent rock with some compound in the bitumen. This compound in the bitumen is causing the dolomites to chemically disaggregate. Both the Graminia Formation and Grosmont Formation are thought to have been sourced by the same source rocks (Higley et al. 2009), so this compound could be exclusive to this petroleum system, which is why not all of the dolomitic rocks in the basin demonstrate this phenomenon. Also, some types of dolomite in Facies C and E might be more susceptible to this chemical alteration which forms Facies F, which is why Facies F is not pervasively found.

Porosity and Permeability in the Germain Field

Porosity

There are three types of porosity in the rocks of the Graminia Formation; intergranular/ intercrystalline, vuggy, and fracture. The average porosity values range from 10 to 37% and vary across the six facies, with the lowest in Facies D and the highest in Facies F.

The dominant porosity type in the Graminia Formation is intergranular/intercrystalline porosity. Intergranular porosity dominates Facies A and B, where the quartz content exceeds the dolomite content, whereas intercrystalline porosity dominates Facies C, E and F where the dolomite content is higher than the quartz content. The size and shapes of the intergranular and intercrystalline spaces vary between the facies due to differences in grain and crystal size, shape, and packing.

The intergranular pores in Facies A and B are most influenced by the presence of quartz grains. The average quartz grain size ranges from 25 to 50μm. The grains are typically subangular to subrounded and tend to be moderately (Facies A) to sparsely packed (Facies B). This results in irregularly shaped, oblate to circular pores that average 10 μm in width and 50 μm in length (Facies A), and 50 μm in width and 80 μm in length (Facies B).

The intercrystalline porosity in Facies C, E, and F is controlled largely by the dolomite crystals. The lengths of the dolomite crystals range from about 10 to 200 μm and range in width from about 10 to 150 μm. The crystals vary from anhedral to euhedral and are most commonly closely packed. This results in very little pore space and typically imperfect polygonal shaped

(rhombic, rectangular or square-like) pores. These pores average 5 μm in width to 10 μm in length (Facies C), and 20 μm in width to 30 μm in length (Facies E). The pore spaces in Facies F vary widely based on the degree of cementation, from 5 μm in cemented samples to over 1 mm in uncemented samples. The intercrystalline space is considerably smaller and more regularly shaped than the intergranular pore space in Facies A and B, excluding Facies F, which can vary widely.

Vuggy porosity includes ovate vugs 0.5 to 6 mm in diameter, in Facies E, and spherical vugs, 10 to 20 mm in diameter, in Facies A. In Facies C and, to a lesser degree in Facies E, the vuggy porosity is largely moldic. These molds mimic the shape of the leached ooids, peloids, brachiopod fragments, and gastropod fragments. The vugs are variably filled with micritic to sparry calcite cement. In Facies A, C, and E, the calcite cement is commonly zoned. The vugs in Facies C and E are commonly lined with finely crystalline dolomitic cement. The overall porosity of the vugs may be decreased depending on the degree of cementation. Some vugs in Facies A are 20 mm in diameter but cementation of the vug only results in 2 mm of actual pore space.

Fracture porosity contributes substantially to the porosity of Facies E. There is some minor fracture porosity present in Facies A. The fractures in Facies E, which are 2 to 15 cm long and 2 to 10 mm wide, form an interconnected network. Many of the fractures are partially filled (20 to 50%) with low-ferroan equant, sparry calcite. The fractures in Facies A, up to 20 mm long and 0.2 mm wide, are commonly occluded by low-ferroan, sparry equant calcite.

Porosity Trends and Architecture

There is no readily apparent correlation between porosity and depth from the Cretaceous unconformity (Fig. 4.3A, 4.3B, 4.3C). The porosity values increase and decrease with no identifiable pattern. Similarly, the average porosity does not increase or decrease predictably across the Germain Field (Fig. 4.1, 4.4, 4.5, 4.6 and 4.7).

The mineralogical composition does not affect the average porosity values (Table 4.2). Facies F, with the highest average porosity (37%), is comprised largely of dolomite (99%) and has the lowest quartz content (1%) while the facies with the lowest average porosity (Facies E; 17%) has an average dolomite content of greater than 90% and an average of 5% quartz.

There does not appear to be any correlation between porosity and the average grain/ crystal size (Table 4.2). For example, both Facies A and Facies C have an average porosity of 21%; Facies A has an average quartz grain size of 35 μm and an average dolomite crystal size

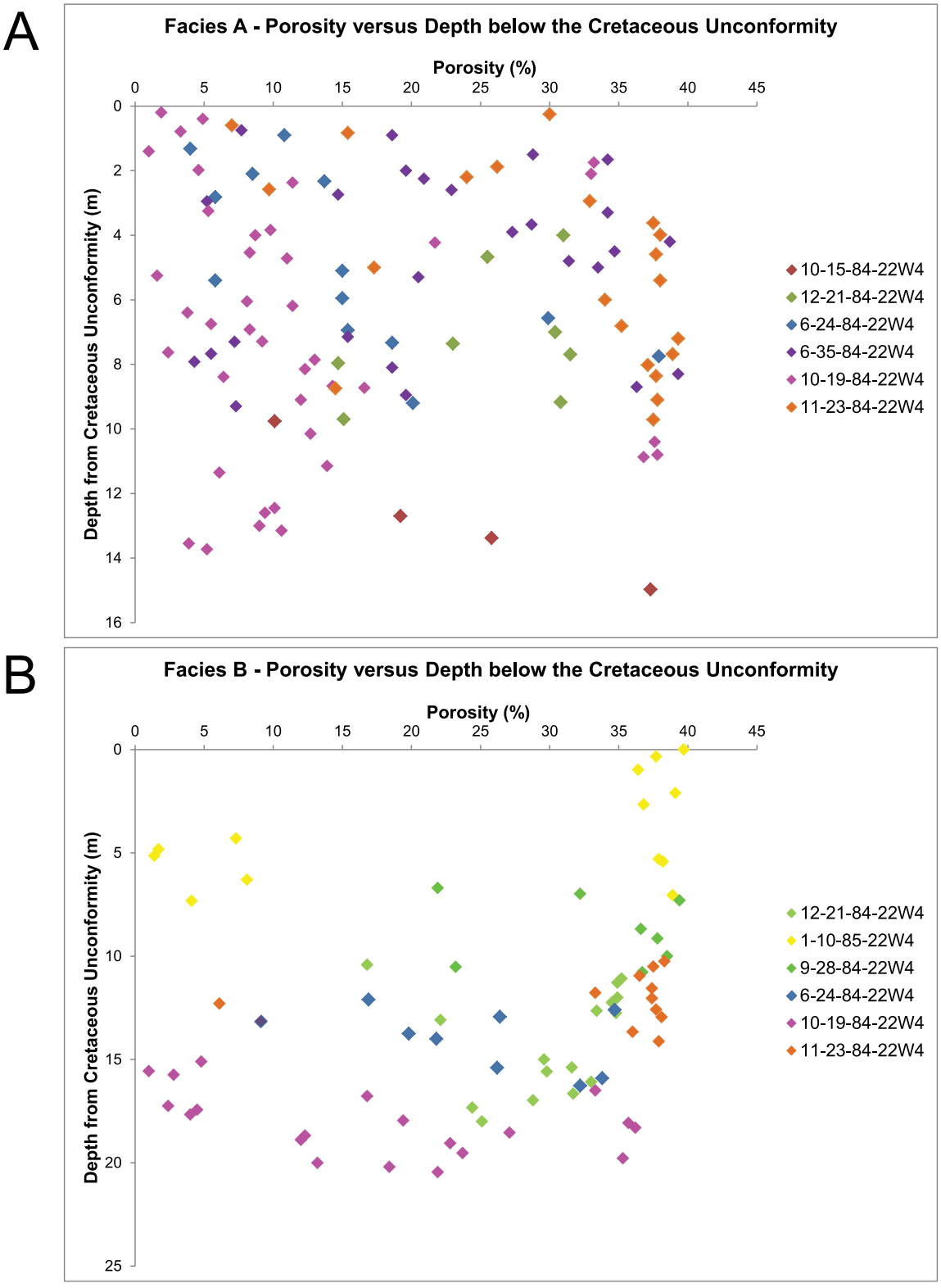

Figure 4.3A: A) Porosity values plotted versus depth from the Cretaceous unconformity for Facies A of the Graminia Formation. B) Porosity values plotted versus depth from the Cretaceous unconformity for Facies B of the Graminia Formation.

A

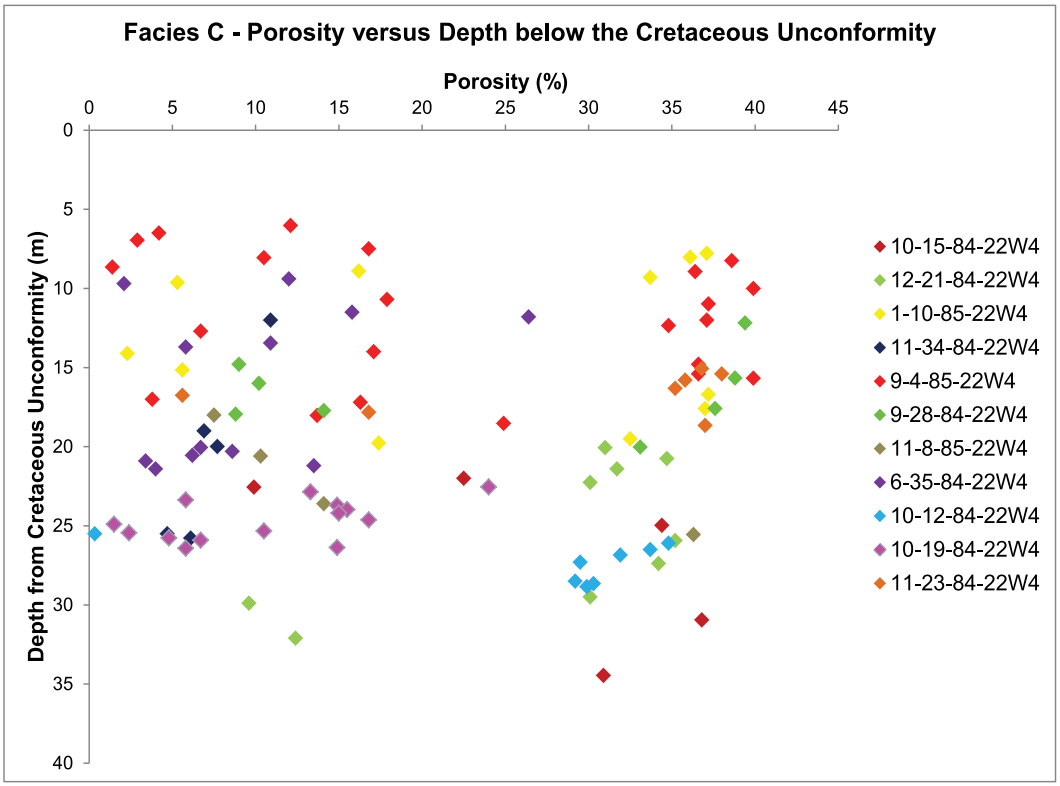

B

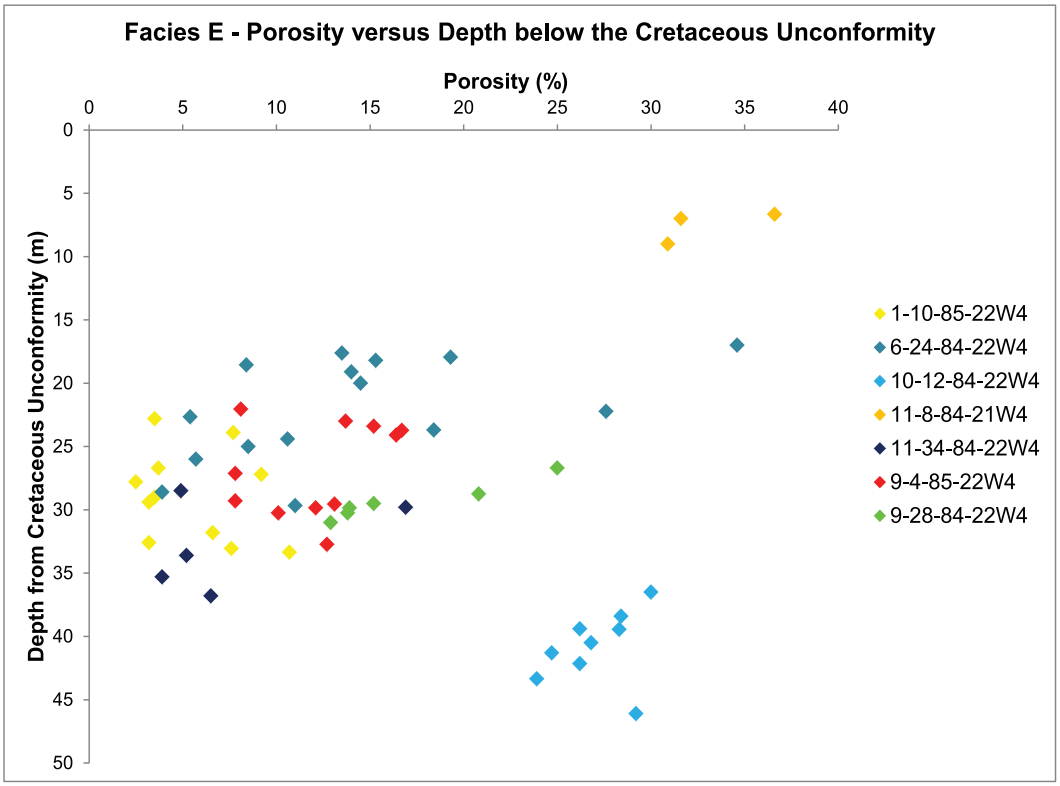

Figure 4.3B: A) Porosity values plotted versus depth from the Cretaceous unconformity for Facies C of the Graminia Formation. B) Porosity values plotted versus depth from the Cretaceous unconformity for Facies E of the Graminia Formation.

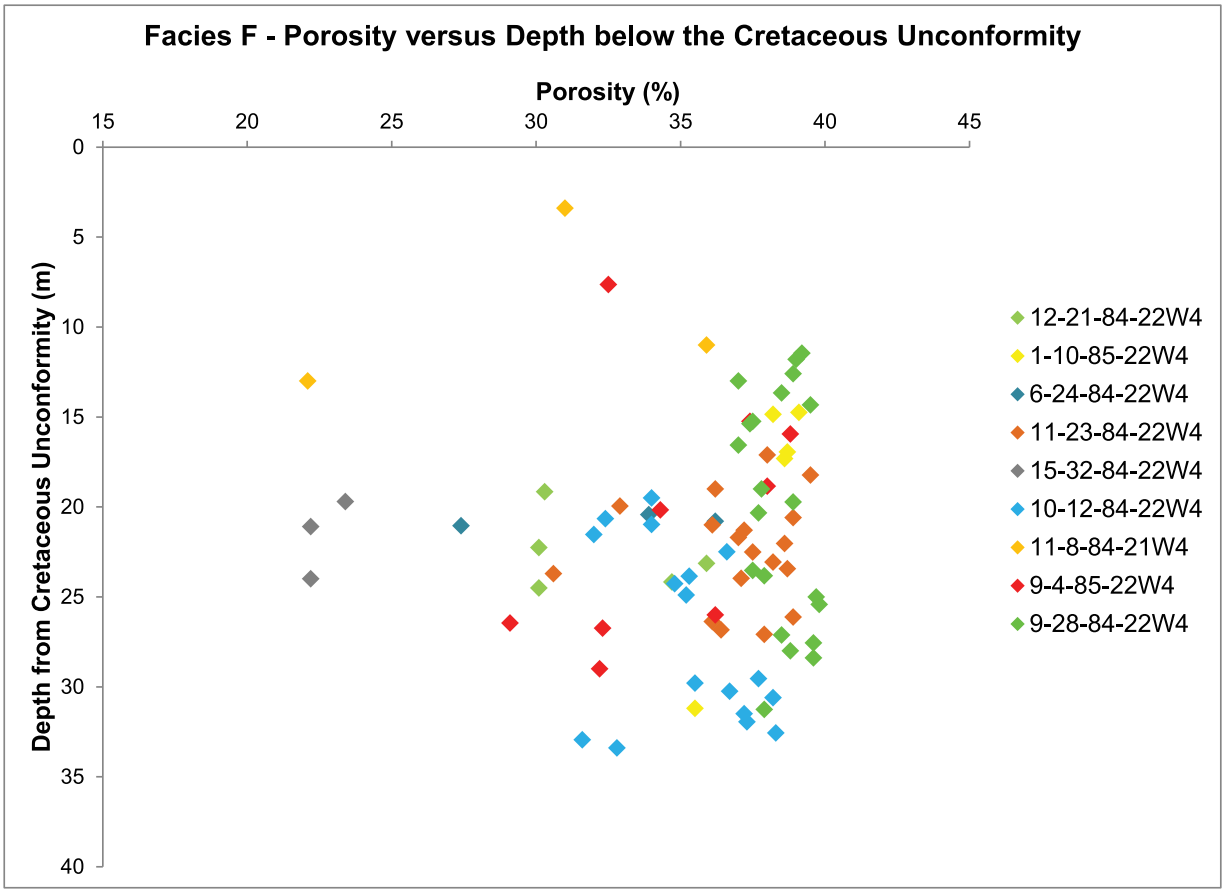

Figure 4.3C: Porosity values plotted versus depth from the Cretaceous unconformity for Facies F of the Graminia Formation.

Facies	Average Porosity (%)	Average Permeability (md)	Average Quartz Grain Size (µm)	Average Dolomite Crystal Size (µm)	Average Modal Percentage of Dolomite (%)	Average Modal Percentage of Quartz (%)
A	21	315	35	105	50-80	20-50
B	27	450	30	110	50-65	35-50
C	21	275	25	30	45-70	40-70
E	17	200	30	30	>90	5
F	37	425	50	50	99	<1

Table 4.2: The average porosity and permeability values, average quartz grains, average dolomite crystal sizes, average modal percentage of dolomite and average modal percentage of quartz of each of the facies of the Graminia Formation.

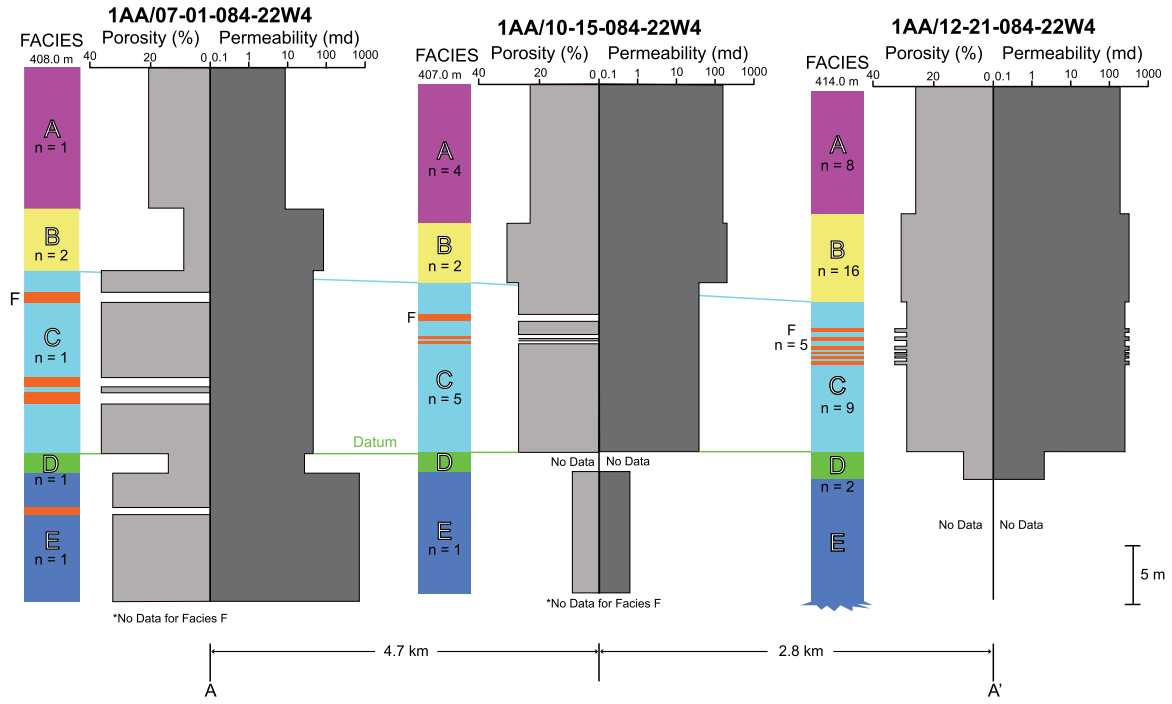

Figure 4.4: Cross-section A-A' showing the variability of the porosity and permeability of the facies in the Graminia Formation across the Germain Field.

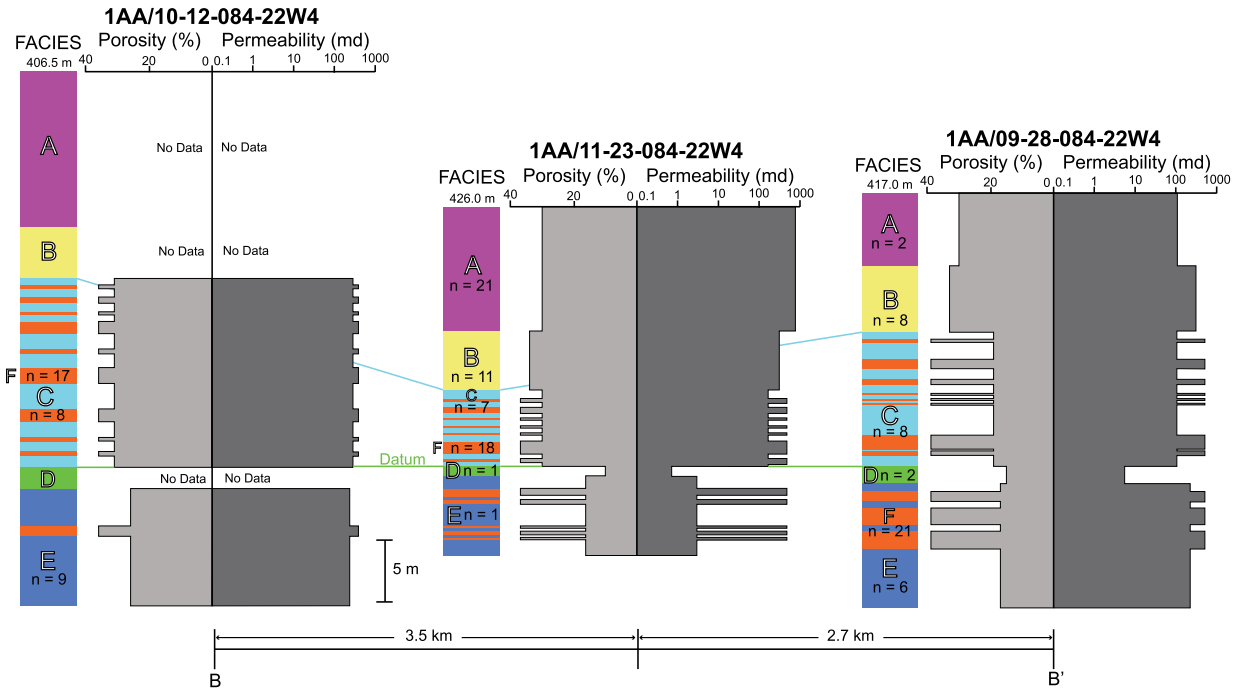

Figure 4.5: Cross-section B-B' showing the variability of the porosity and permeability of the facies in the Graminia Formation across the Germain Field.

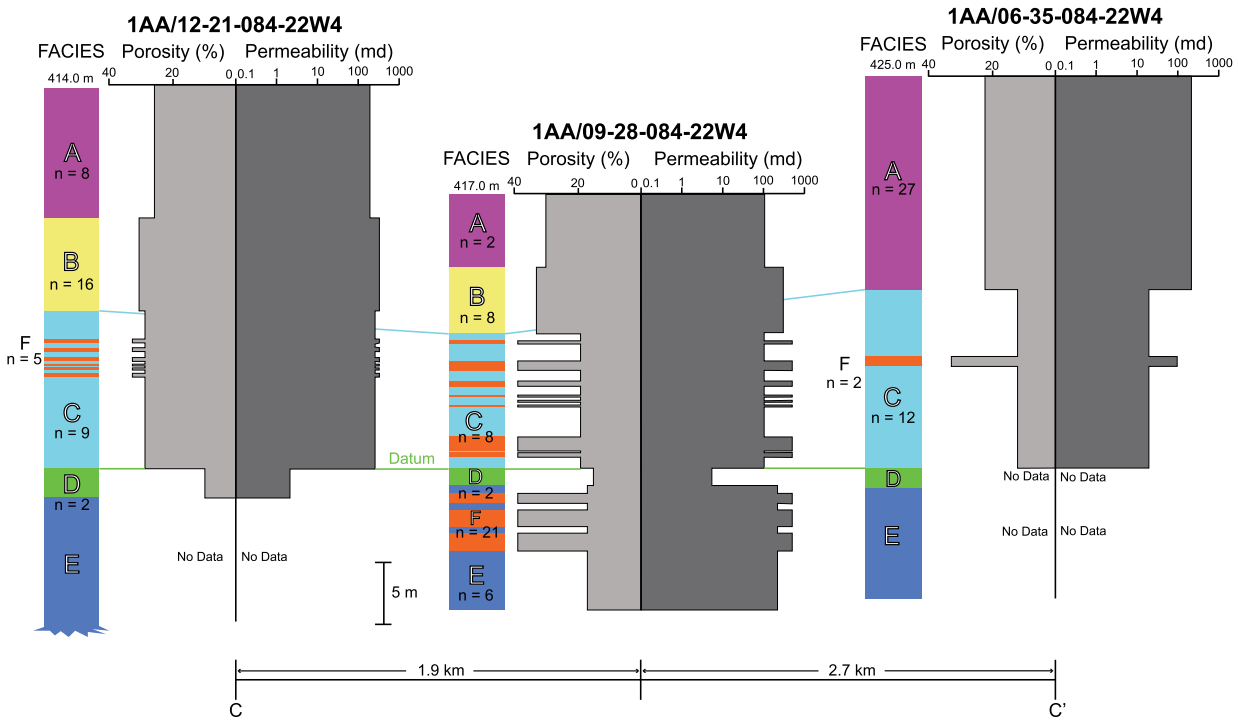

Figure 4.6: Cross-section C-C' showing the variability of the porosity and permeability of the facies in the Graminia Formation across the Germain Field.

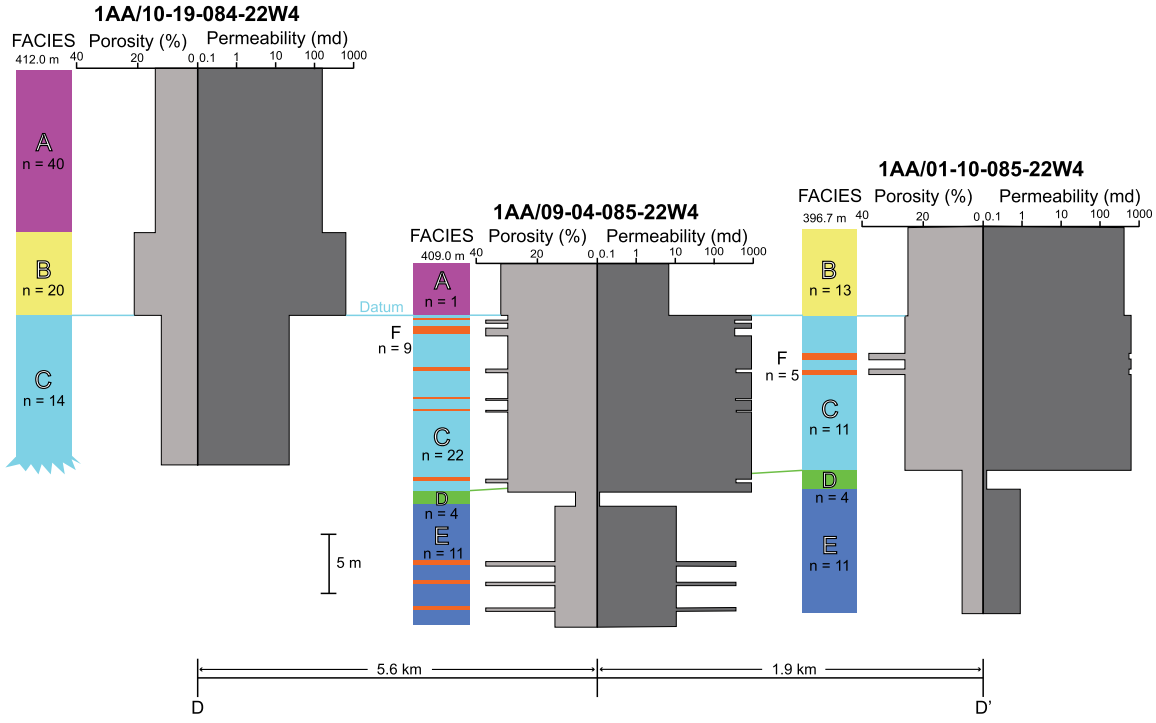

Figure 4.7: Cross-section D-D' showing the variability of the porosity and permeability of the facies in the Graminia Formation across the Germain Field.

of 105 μm whereas Facies C has an average quartz grain size of 25 μm and an average dolomite crystal size of 30 μm. Also, the facies with the highest average porosity (Facies F; 37%) has an average quartz grain and dolomite crystal size of 30 μm. Facies B has the second highest average porosity (27%) and has an average quartz grain size of 35 μm and also has the largest average dolomite crystal size of 110 μm.

Permeability

Permeability in the Graminia Formation is limited to the permeability resulting from the intergranular/intercrystalline porosity, and the fracture permeability. The average permeability values of these rocks ranges from 5 md (Facies D) to 450 md (Facies B). Overall, the permeability throughout the Graminia Formation is high.

The main permeability present in the rocks is due to the intergranular (Facies A and B, have the highest clastic content) and intercrystalline (Facies C, E and F, which have the highest dolomite content) spaces.

Factures also increase permeability, especially in Facies A and E; however, these fractures can be completely filled with calcite cement, which decreases the overall permeability drastically. The facies with the highest permeability values (Facies B) is not fractured.

Permeability Trends and Architecture

There are no readily apparent trends between permeability and depth below the Cretaceous unconformity (Fig. 4.8A, 4.8B, 4.8C). The permeability values increase and decrease in no particular pattern as depth from the Cretaceous unconformity varies. Similarly, the average permeability does not increase or decrease predictably across the Germain Field (Fig. 4.1, 4.4, 4.5, 4.6 and 4.7), nor does it vary in any recognizable pattern.

The average permeability values were also not affected by the mineralogical composition of the rocks in the facies (Table 4.2). Facies E has the lowest average permeability (200 md) and is comprised of greater than 90% dolomite with 5% quartz content, whereas Facies F has the highest average permeability (425 md) and is comprised of 99% dolomite with less than 1% quartz.

Investigation of the relation of the average grain/crystal size to the average permeability values revealed no correlation between these two factors (Table 4.2). For example, Facies B and F have very close average permeability values of 450 md and 425 md, respectively; Facies B

has an average quartz grain size of 30 μm and an average dolomite crystal size of 110 μm, while Facies F has an average crystal size of 50 μm and an average dolomite crystal size of 50 μm. Also, Facies A has very similar average quartz grain and average dolomite crystal sizes to Facies B (35 μm and 105 μm in Facies A, respectively, and 30 μm and 110 μm, respectively) but they have very different average permeabilities; 315 md in Facies A and 450 md in Facies B.

A

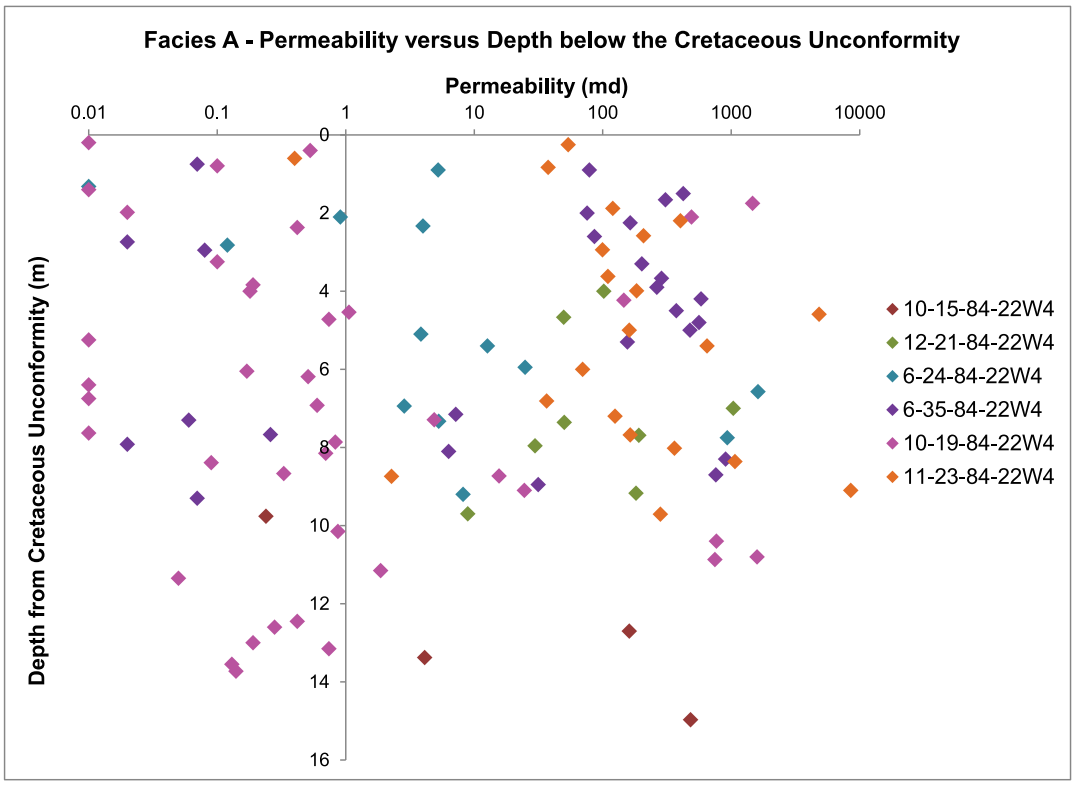

B

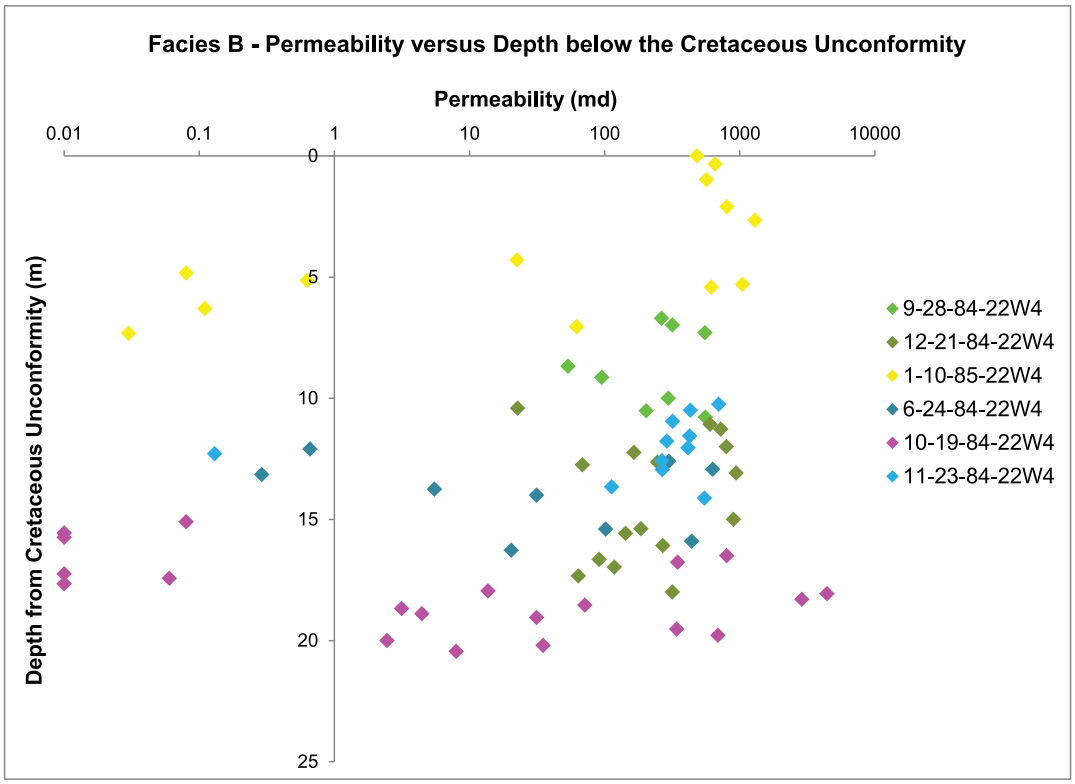

Figure 4.8A: A) Permeability values plotted versus depth from the Cretaceous unconformity for Facies A of the Graminia Formation. B) Permeability values plotted versus depth from the Cretaceous unconformity for Facies B of the Graminia Formation.

A

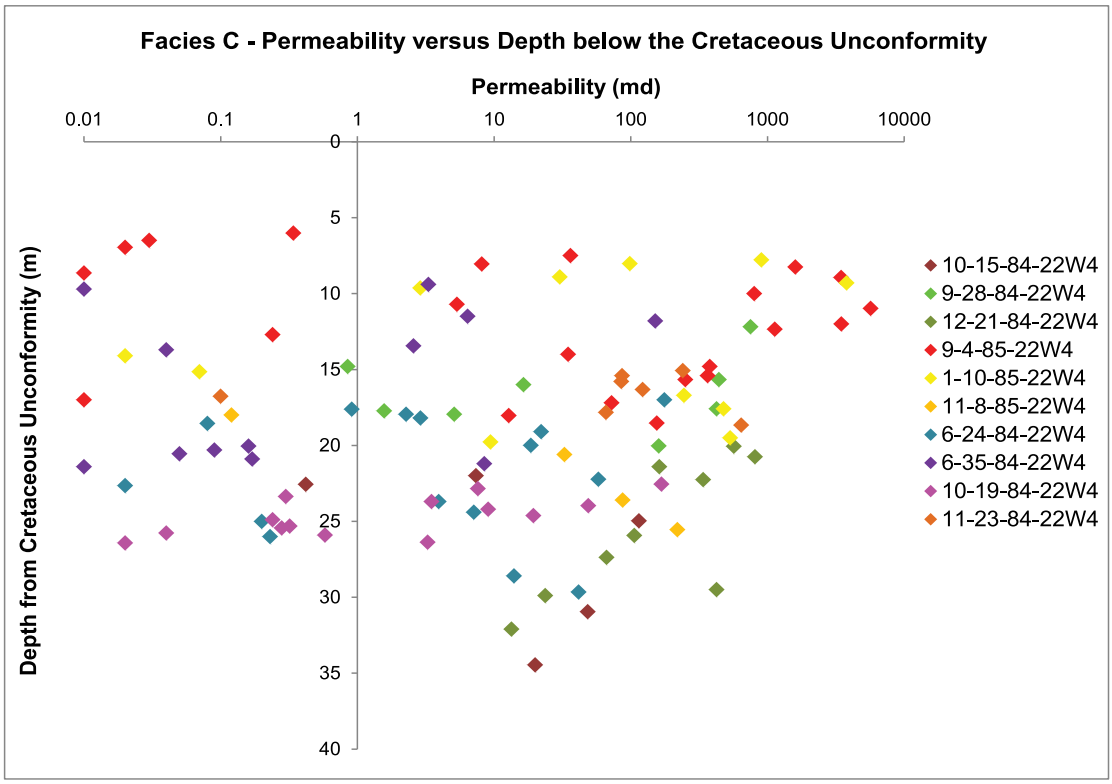

B

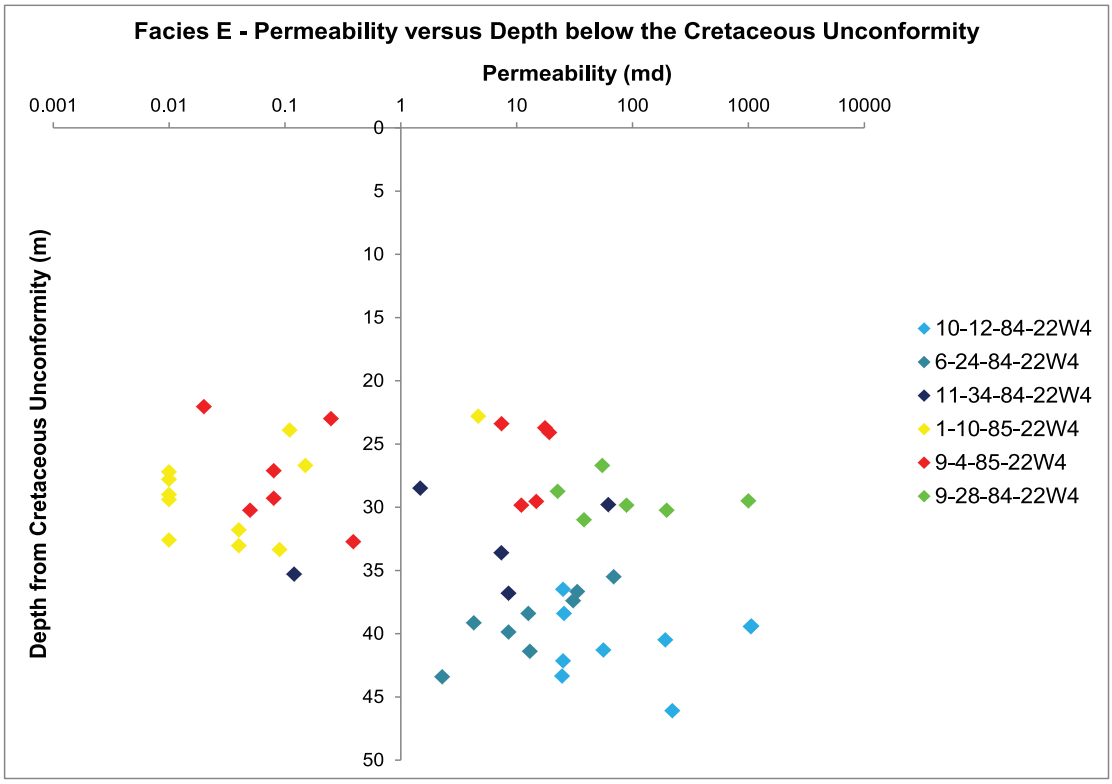

Figure 4.8B: A) Permeability values plotted versus depth from the Cretaceous unconformity for Facies C of the Graminia Formation. B) Permeability values plotted versus depth from the Cretaceous unconformity for Facies E of the Graminia Formation.

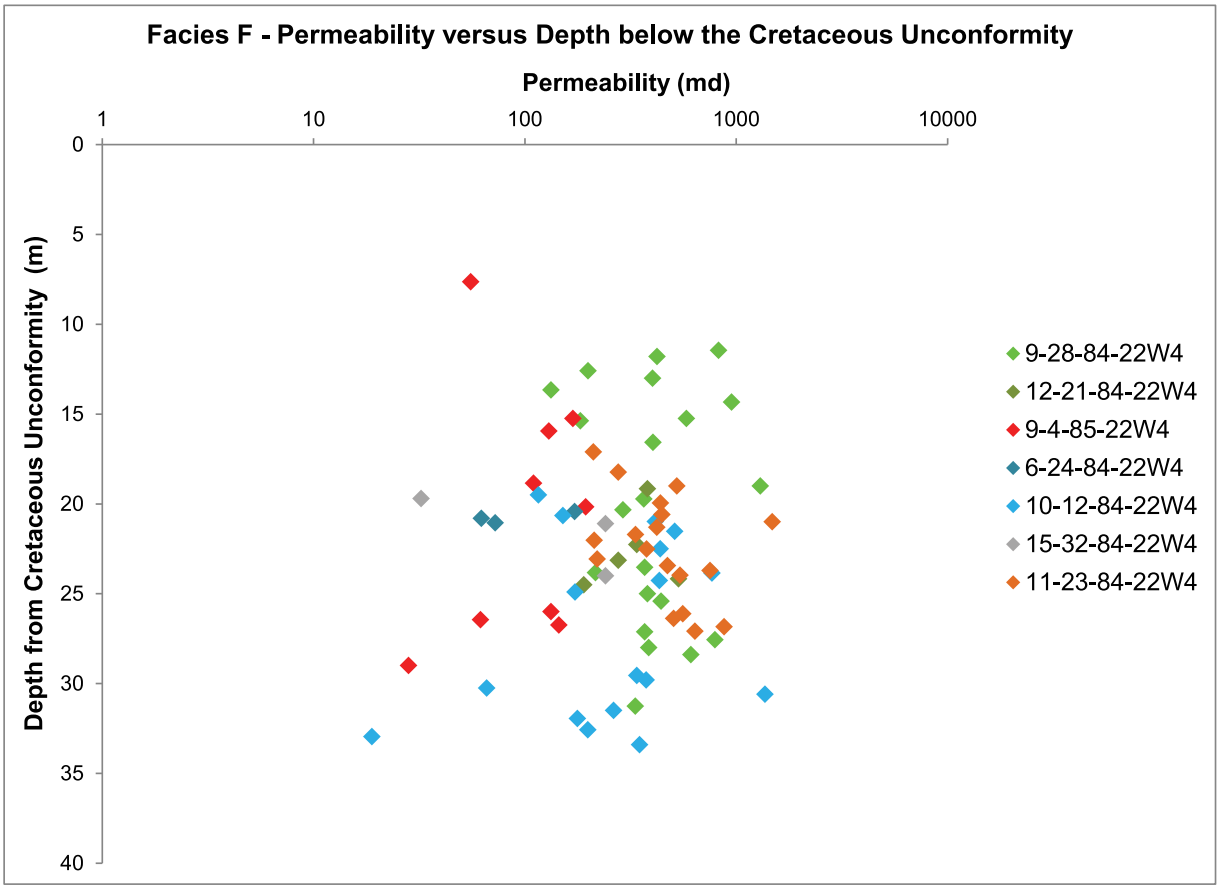

Figure 4.8C: Permeability values plotted versus depth from the Cretaceous unconformity for Facies F of the Graminia Formation.

CHAPTER 5: CONCLUSIONS

1. The Graminia Formation is divided into six facies (A, B, C, D, E and F) based on mineralogy, fabric and cement types observed in the core samples. The Graminia Formation is bitumen-bearing.

    a. Facies A is formed of very finely to finely crystalline dolomitic siltstone to silty dolostone that is interlaminated/mottled (respectively) with silty shale. This facies can appear brecciated or disrupted. Found in the upper part of Upper Graminia Member, this facies has porosities ranging from 3 to 39% with an average of 21% and an average permeability of 315 md. It is moderately bitumen saturated.

    b. Facies B is a very finely crystalline dolomitic siltstone to silty dolostone that is easily identifiable on borehole logs by its high gamma ray signature. Found in the lower part of the Upper Graminia Member, it lacks the silty shale laminae that are found in Facies A. Facies B has porosities of 2 to 40% with an average of 27% with an average permeability of 450 md. It is also saturated with bitumen, but less so than Facies F

    c. Facies C is a very finely crystalline silty dolostone that is variably mottled and/or interlaminated with silty shale with a bioturbated aspect. It is found in the upper part of the Blueridge Member. Porosities range from 4 to 38% with an average of 21% and an average permeability of 275 md. It is moderately bitumen saturated.

    d. Facies D is a green-gray laminated shale bed, 1 to 2 m thick that is found in the middle of the Blueridge Member, between Facies C and E. Facies D has porosity values that range from 4 to 16% with an average of 10% and an average permeability of 5 md. It has no bitumen saturation.

    e. Facies E is a highly fractured, very finely crystalline, variably silty dolostone, typically found in the lower half of the Blueridge Member. Facies E has porosities that range from of 4 to 37% with an average of 17% and an average permeability of 200 md. It has moderate to low bitumen saturation.

    f. Facies F is very finely crystalline, poorly cemented dolostone that is cemented by bitumen. When the bitumen is removed, the rock becomes a dolomite powder, white-gray in colour with a flour-like the texture. This facies is found in beds up to 20 cm thick interbedded with Facies C and E. This facies differs from Facies B because it is formed entirely of dolomite. Facies F has porosities of 30 to 40%

with an average of 37% with an average permeability of 425 md. It is always saturated with bitumen.

2. The facies always occur in order throughout the study area; A, B, C, D and E (from the top, down) with F occurring randomly, but always in association with Facies C and E. All wells have Facies C, D and E while not all wells have Facies A, B or F. The facies all thicken to the north (variable towards the north-northeast and north-northwest) and are thinner or missing in the southeast. Exceptions are Facies D, which is approximately the same thickness throughout, and Facies F which is randomly present and randomly thins and thickens.

3. The sediments of the Blueridge Member were deposited during a third order regression in an inner-ramp setting. The overlying sediments of the Upper Graminia Member were deposited during a fall in sea level which caused the ramp to shallow into a peritidal to supratidal zone. There is no evidence of a disconformity between the Blueridge Member and Upper Graminia Member in the Germain Field and thus belongs to the Winterburn megasequence and not the Wabamun megasequence as originally proposed for these strata in other areas of the basin.

4. Despite the destruction of much of the original depositional fabric by dolomitization, there is still some evidence remaining that allows for the understanding of the diagenetic evolution of the rocks. These aspects include the vugs (very common), dolomitic cement (common), fractures (rare), calcite cements (very common), stylolites (very rare), the paleosol, and pervasive dolomitization. The precise timing and formation of dolomite is not known, but is thought to perhaps be sabhka related based on the depositional framework.

5. It is not known exactly how and when Facies F was formed. There are four theories as to how Facies F could have been formed: (1) “cryogenic powderization” (Poros et al. 2013), (2) hydrothermal-related formation (Kendall 1960; Bogacz et al. 1973), (3) recent weathering-induced formation (Blank and Tynes 1965; Fisher and Rodda 1969; Rose 1972; Chafetz and Butler 1980; Kahle 2011), and (4) karst/exposure-related formation (Fu et al. 2004a, b; Machel et al. 2012). It is most likely that Facies F was formed through karst/exposure which also formed the paleosol that overlies the Upper Graminia Member.

6. The main types of porosity in the Graminia Formation are intergranular/intercrystalline (very common), vuggy (common), and fracture (rare). The permeability is controlled by the intergranular/intercrystalline spaces and fractures.

7. The porosity and permeability values have no correlation with depth below the Cretaceous unconformity, i.e. they neither increase or decrease with increasing or decreasing depth from the Cretaceous unconformity. They also do not display any predicatble with respect to depth below the Cretaceous unconformity. The mineralogical composition does not affect the porosity or the permeability; i.e. more dolomite or quartz does not translate into higher or lower porosity or permeability, respectively. There is no correlation between porosity or permeability and average grain/crystal size.

References:

ADAMS, J. J., 2008, The impact of geological and microbiological processes on oil composition and fluid property variations in heavy oil and bitumen reservoirs: University of Calgary, Calgary, 786 pp.

ALLAN, J., CREANEY, S., 1991, Oil families of the Western Canada Basin: Bulletin of Canadian Petroleum Geology, v. 39, p. 107-122.

ANDRICHUK, J.M., WONFOR, J.S., 1953, Late Devonian geologic history in Stettler Area, Alberta, Canada: Bulletin of Canadian Petroleum Geology, v. 1, p. 3-5.

ANDRICHUK, J.M., WONFOR, J. S., 1954, Late Devonian geologic history in Stettler Area, Alberta, Canada: American Association of Petroleum Geology Bulletin, v. 38, p. 2500-2536.

BATHURST, R.G.C., 1975, Developments in Sedimentology: Carbonate sediments and their diagenesis: Amsterdam, Elsevier, 660 pp.

BELYEA, H.R., 1954a, Cross-sections through the Devonian system of the Alberta plains: Alberta Society of Petroleum Geology News Bulletin, v. 2, p. 2-5.

BELYEA, H.R., 1954b, Further discussion on the use of the term Nisku: Bulletin of Canadian Petroleum Geology, v. 2, p. 3-4.

BELYEA, H.R., 1955, Correlations in Devonian of southern Alberta: Bulletin of Canadian Petroleum Geology, v. 3, p. 151-156.

BELYEA, H.R., MCLAREN, D.J., 1957, Upper Devonian nomenclature in southern Alberta: Bulletin of Canadian Petroleum Geology, v. 5, p. 166-182.

BLANK, H.R., TYNES, E.W., 1965, Formation of caliche *in situ*: Geological Society of America Bulletin, v. 76, p. 1387-1392.

BOGACZ, K.D., DZULYNSKI, S., HARANCZYK, C., 1973, Caves filled with clastic dolomite and galena mineralization in disaggregated dolomites: Rocznik Polskiego Towarzystwa Geologicznego - Annales de la Societe Geologique de Pologne, v. 43, p. 59-72.

BOND, D.P.G., WIGNALL, P.B., 2008, The role of sea-level change and marine anoxia in the Frasnian-Famennian (Late Devonian) mass extinction: Palaeogeography, Palaeoclimatology, Palaeoecology, v. 263, p. 107-118.

BURROWES, O.G., KRAUSE, F. F., 1987, Overview of the Devonian system: subsurface of Western Canada Basin, *in* Krause, F.F., Burrowes, O.G., eds., Devonian lithofacies and reservoir styles in Alberta, 13th Canadian Society of Petroleum Geologists Core Conference and Display Handbook: Calgary, Canadian Society of Petroleum Geologists, p. 1-20.

CHAFETZ, H.S., BUTLER, J. C., 1980, Petrology of recent caliche pisolites, spherulites, and speleothem deposits from central Texas: Sedimentology, v. 27, p. 497-518.

CHOQUETTE, A.L., 1955, The Blue Ridge Member of the Graminia Formation: Alberta Society of Petroleum Geologists, v. 3, p. 70-73.

CREANEY, S., ALLAN, J., COLE, K.S., FOWLER, M.G., BROOKS, P.W., OSADETZ, K.G., MACQUEEN, R.W., SNOWDON, L.R., RIEDIGER, C.L., 1994, Petroleum generation and migration in the Western Canada Sedimentary Basin, *in* Mossop, G.D., Shetsen, I., eds., Geological Atlas of the Western Canada Sedimentary Basin: Calgary, Canadian Society of Petroleum Geologists and Alberta Research Council, p. 455-468.

DICKSON, J.A.D., 1966, Carbonate identification and genesis as revealed by staining: Journal of Sedimentary Petrology, v. 36, p. 491-505.

DIX, G.R., 1990, Stages of platform development in the upper Devonian (Frasnian) Leduc Formation, Peach River Arch, Alberta: Bulletin of Canadian Petroleum Geology, v. 38, p. 66-92.

DUNHAM, R.J., 1962, Classification of carbonate rocks according to depositional texture, *in* Ham, W., ed., Classification of carbonate rocks – Memoir 1: Tulsa, American Association of Petroleum Geologists, p. 108-221.

DUNN, C.E., 1975, The Upper Devonian Duperow Formation in southeastern Saskatchewan - Geological Report 179: Regina, Saskatchewan Department of Mineral Resources, 149 pp.

EMBRY, A., 1988, Middle-upper Devonian sedimentation in the Canadian arctic islands and Ellesmerian Orogeny, *in* McMillan, N.J., Embry, A.F., Glass, D.J., eds., Devonian of the World; Proceedings of the Second International symposium on the Devonian System – Memoir 14: Calgary, Canadian Society of Petroleum Geologists, v. 2, p. 15-28.

EXPLORATION AND PRODUCTION DEPARTMENT, AMERICAN PETROLEUM INSTITUTE, 1998, Recommended practices for core analysis – Recommended Practice 40: Washington, D.C., American Petroleum Institute, 236 pp.

EXPLORATION STAFF, CHEVRON STANDARD LIMITED, 1979, The geology, geophysics and significance of the Nisku reef discoveries, west Pembina Area, Alberta, Canada: Bulletin of Canadian Petroleum Geology, v. 27, p. 326-359.

FISHER, W.L., RODDA, P.U., 1969, Edwards Formation (Lower Cretaceous), Texas: Dolomitization in a carbonate platform system: American Association of Petroleum Geologists Bulletin, v. 53, p. 55-72.

FOLK, R.L., 1965, Some aspects of recrystallization in ancient limestones, *in* Pray, L.C., Murray, R.C., eds., Dolomitization and Limestone Diagenesis - Special Publication 35: Tulsa, Society of Economic Paleontologists and Mineralogists, v.13, p. 14-48.

FOWLER, M.G., STASIUK, L.D., HEARN, M., OBERMAJER, M., 2001, Devonian hydrocarbon source rocks and their derived oils in the Western Canada Sedimentary Basin: Bulletin of Canadian Petroleum Geology, v. 49, p. 117-118.

FRIEDMAN, G.M., 1965, Terminology of crystallization textures and fabrics in sedimentary rocks: Journal of Sedimentary Petrology, v. 35, p. 643-655.

FU, Q., QING, H., BERGMAN, K.M., 2004, Dolomitization calcrete in the Middle Devonian Winnipegosis carbonate mounds, subsurface: Sedimentary Geology, v. 168, p. 46-69.

FU, Q., QING, H., BERGMAN, K.M., YANG, C., 2008, Dedolomitization and calcite cementation in the Middle Devonian Winnipegosis Formation in central Saskatchewan, Canada: Sedimentology, v. 55, p. 1623-1642.

GELDSETZER, H.H.J., 1988, Ancient wall reef complex, Frasnian age, Alberta, *in* Geldsetzer, H.H.J., James, N.P., Tebbutt, G.E., eds., Reefs, Canada and adjacent area – Memoir 13: Calgary, Canadian Society of Petroleum Geologists, p. 431-439.

GELDSETZER, H.H.J., GOODFELLOW, W.D., MCLAREN, D.J., 1993, The Frasnian-Famennian extinction event in a stable cratonic shelf setting; Trout River, Northwest Territories, Canada, *in* Geldsetzer, H.H.J., Nowlan, G.S. , eds., Event Markers in Earth History: Amsterdam, Elsevier, p. 81-95.

GEOLOGICAL STAFF OF IMPERIAL OIL LIMITED, WESTERN DIVISION, 1950, Devonian nomenclature in Edmonton Area, Alberta, Canada: American Association of Petroleum Geologists Bulletin, v. 34, p. 1807-1825.

GOODFELLOW, W.D., GELDSETZER, D.J., MCLAREN, M.J., ORCHARD, M.J., KLAPPER, G., 1989, Geochemical and isotopic anomalies associated with the Frasnian-Famennian extinction: Historical Biology: International Journal of Paleobiology, v. 2, p. 51-72.

HAQ, B.U., SCHUTTER, S.R., 2008, A chronology of Paleozoic sea-level changes: Science, v. 322, p. 64-68.

HIGLEY, D.K., LEWAN, M.D., ROBERTS, L.N.R., HENRY, M., 2009, Timing and petroleum sources for the Lower Cretaceous Mannville Group oil sands of northern Alberta based on 4-D modeling: American Association of Petroleum Geologists Bulletin, v. 93, p. 203-230.

JI, H., WANG, S., OUYANG, Z., ZHANG, S., SUN, C., LIU, X., ZHOU, D., 2004a, Geochemistry of red residua underlying dolomites in karst terrains of Yunnan-Guizhou Plateau I. The formation of Pingba profile: Chemical Geology, v. 203, p. 1-27.

JI, H., WANG, S., OUYANG, Z., ZHANG, S., SUN, C., LIU, X., ZHOU, D., 2004b, Geochemistry of red residua underlying dolomites in karst terrains of Yunnan-Guizhou Plateau II. The mobility of rare earth elements during weathering: Chemical Geology, v. 203, p. 29-50.

JOHN, E.H., WIGNALL, P.B., NEWTON, R.J., BOTTRELL, S.H., 2010, $\delta^{34}S_{CAS}$ and $\delta^{18}S_{CAS}$ records during the Frasnian-Famennian (Late Devonian) transition and their bearing on mass extinction models: Chemical Geology, v. 275, p. 221-234.

JOHNSON, J.G., KLAPPER, G., SANDBERG, C.A., 1985, Devonian eustatic fluctuations in Euramerica: Geological Society of America Bulletin, v. 96, p. 567-587.

KAHLE, C.F., 2011, Scanning electron microscopy of pulverulite in Silurian Lockport dolomite near Rocky Ridge, OH: Carbonates Evaporites, v. 27, p. 3-8.

KATZ, A., 1971, Zoned dolomite crystals: Journal of Geology, v. 79, p. 38-51.

KENDALL, D.L., 1960, Ore deposits and sedimentary features, Jefferson City Mine, Tennessee: Economic Geology, v. 55, p. 985-1003.

KENT, D.M., 1968, The Geology of the Upper Devonian Saskatchewan Group and equivalent rocks in western Saskatchewan and adjacent areas – Geological Report 179: Regina, Saskatchewan Department of Mineral Resources, 221 pp.

KENT, D.M., 1969, Potential hydrocarbon reservoir rocks in the upper Devonian Saskatchewan Group of western Saskatchewan, Twentieth Annual Conference: Eastern Montana Symposium: The Economic Geology of Eastern Montana and Adjacent areas: Billings, Montana Geological Society, p. 55-68.

KENT, D.M., 1984, Carbonate and associated rocks of the Williston Basin, Short Course Notes: Denver, Rocky Mountain Section of the Society for Economic Paleontologists and Mineralogists, 137 pp.

KENT, D.M., 1994, Paleogeographic evolution of the cratonic platform; Cambrian to Triassic, *in* Mossop, G., Shetsen, I., eds., Geological Atlas of the Western Canada Sedimentary Basin: Calgary, Canadian Society of Petroleum Geologists - Alberta Research Council, p. 68-86.

MACHEL, H.G., BORRERO, M.L., DEMBICKI, E., HUEBSCHER, H., PING, L., ZHAO, Y., 2012, The Grosmont: the world's largest unconventional oil reservoir hosted in carbonate rocks: Geological Society of London Special Publications, v. 370, p. 49-81.

MCLAREN, D.J., MOUNTJOY, E.W., 1962, Alexo equivalents in the Jasper region, Alberta – GSC Paper 62-23: Edmonton, Geological Survey of Canada, 36 pp.

MCLEAN, R.A., KLAPPER, G., 1998, Biostratigraphy of Frasnian (Upper Devonian) strata in western Canada, based on conodonts and rugose corals: Bulletin of Canadian Petroleum Geology, v. 43, p. 515-563.

MEIJER DREES, N.C., JOHNSTON, D.I., FOWLER, M.G., 1998, Lithology, biostratigraphy and geochemistry of the upper Devonian Graminia Formation, central Alberta: Bulletin of Canadian Petroleum Geology, v. 48, p. 148-165.

MOORE, P.F., 1988, Devonian reefs in Canada and some adjacent areas, *in* Geldsetzer, H.H.J., James, N.P., Tebbutt, G.E., eds., Reefs, Canada and adjacent area – Memoir 13: Calgary, Canadian Society of Petroleum Geologists, p. 367-390.

MORROW, D.G., GELDSETZER, H.H.J., 1988, Devonian of eastern Canadian Cordillera, *in* McMillan, N.J., Embry, A.F., Glass, D.J., eds., Devonian of the World; Proceedings of the Second International symposium on the Devonian System – Memoir 14: Calgary, Canadian Society of Petroleum Geologists, v. 1, p. 85-121.

ORCHARD, M.J., 1988, Conodonts from the Frasnian-Famennian boundary in Western Canada, *in* McMillan, N.J., Embry, A.F., Glass, D.J., eds., Devonian of the World; Proceedings of the Second International symposium on the Devonian System – Memoir 14: Calgary, Canadian Society of Petroleum Geologists, v. 3, p. 35-52.

POROS, Z., MACHEL, H.G. MINDSZENTY, A., MOLNAR, F., 2013, Cryogenic powderization of Triassic dolostones in the Buda Hills, Hungary: International Journal of Earth Science, v. 102, p. 1513-1539.

POTMA, K., WEISSENBERGER, J. A. W., WONG, P. K., GILHOOLY, M. G., 2001, Toward a seequence stratigraphic framework for the Frasnian of the Western Canada Sedimentary Basin: Bulletin of Canadian Petroleum Geology, v. 49, p. 37-85.

RANGER, M. J., GINGRAS, M. K., 2006, Geology of the Athabasca Oil Sands - Field guide and overview: Edmonton, Department of Earth and Atmospheric Sciences, University of Alberta, 119 pp.

RICHARDS, B.C., 1989, Upper Kaskaskia sequence - uppermost Devonian and lower Carboniferous, *in* Ricketts, B.D., ed., Western Canada Sedimentary Basin, a case history: Calgary, Canadian Society of Petroleum Geologists, p. 165-201.

ROSE, P.R., 1972, Edwards Group, surface and subsurface, central Texas - Report of investigations 74: Austin, University of Texas at Austin - Bureau of Economic Geology, 198 pp.

SCHOLLE, P.A., ULMER-SCHOLLE, D. S., 2003, A color guide to the petrography of carbonate rocks: grains, textures, porosity, diagenesis: Tulsa, American Association of Petroleum Geologists, 474 p.

SCOTESE, C.R., VAN DER VOO, R., BARRETT, S. F., 1985, Silurian and Devonian base maps: Philosophical Transactions Royal Society of London, v. 309, p. 57-77.

SELBY, D., CREASER, R.A., 2005, Direct radiometric dating of the Devonian-Mississippian time-scale boundary using the Re-Os black shale geochronometer: Geology, v. 33, p. 545-548.

SHEILDS, M.J., GELDSETZER, H.H.J., 1992, The Mackenzie margin, Southesk-Carin carbonate complex: depositional history, stratal geometry and comparison with other Late Devonian Platform-margins: Bulletin of Canadian Petroleum Geology, v. 60, p. 274-293.

SHUQING, Z., HAIPING, H., YUMING, L., 2008, Biodegradation and origin of oil sands in the Western Canada Sedimentary Basin: Petroleum Science, v. 5, p. 87-94.

SLOSS, L.L., 1963, Sequences in the cratonic interior of North America: Geological Society of America Bulletin, v. 72, p. 93-113.

SLOSS, L.L., 1988, Tectonic evolution of the craton in Phanerozoic Time, *in* Sloss, L.L., ed., The Geology of North America: Denver, American Geological Society, p. 25-51.

Sorauf, J.E., Pedder, A.E.H., 1986, Late Devonian rugose corals and the Frasnian-Famennian crisis: Canadian Journal of Earth Sciences, v. 23, p. 1265-1287.

Stasiuk, L.D., Fowler, M.G., 2004, Organic facies in Devonian-Mississippian strata of Western Canada Sedimentary Basin: relation to kerogen type, paleoenvironment, and paleogeography: Bulletin of Canadian Petroleum Geology, v. 52, p. 234-255.

Stearn, C.W., 1987, Effect of the Frasnian-Famennian extinction event on the stromatoporoids: Geology, v. 15, p. 677-679.

Stoakes, F.A., 1992, Winterburn megasequence, *in* Wendte, J.C., Stoakes, F.A., Campbell, C.V., eds., Devonian-Early Mississippian Carbonates of the Western Canada Sedimentary Basin: A Sequence Stratigraphic Framework: Tulsa, Society of Sedimentary Geology, p. 207-224.

Storey, T.P., 1953, Some regional Devonian correlation in Alberta, Canada: Bulletin of Canadian Petroleum Geology, v. 1, p. 3-6.

Switzer, S.B., Holland, W.G., Christie, D.S., Graf, G.C., Hedinger, A.S., McAuley, R.J., Wierzbicki, R.A., Packard, J.J., 1994, Devonian Woodbend-Winterburn strata of the Western Canada Sedimentary Basin, *in* Mossop, G., Shetsen, I., eds., Geological Atlas of the Western Canada Sedimentary Basin: Calgary, Canadian Society of Petroleum Geologists - Alberta Research Council, p. 165-202.

Tucker, M.E., Wright, V.P., 1990, Carbonate sedimentology: Oxford, Blackwell Science Ltd., 482 pp.

Warren, P.S. Stelck, C.R., 1954, The Stratigraphic Significance of the Devonian coral reefs of Western Canada: Stratigraphy, *in* Clark, L.M., ed., Western Canada Sedimentary Basin: Tulsa, American Association of Petroleum Geologists Bulletin, p. 214-218.

Weissenberger, J.A.W., 1994, Frasnian reef and basinal strata of West Central Alberta: a combined sedimentological and biostratigraphic analysis: Bulletin of Canadian Petroleum Geology, v. 42, p. 1-25.

Wendte, J.C., 1992a, Overview of the Devonian of the Western Canada Sedimentary Basin, *in* Wendte, J.C., Stoakes, F.A., Campbell, C.V., eds., Devonian – Early Mississippian carbonates of the Western Canada Sedimentary Basin: A Sequence Stratigraphic Framework: Tulsa, Society for Sedimentary Geology, p. 1-24.

Wendte, J.C., 1992b, Cyclicity of Devonian strata in the Western Canada Sedimentary Basin, *in* Wendte, J.C., Stoakes, F.A., Campbell, C.V., eds., Devonian-Early Mississippian Carbonates of the Western Canada Sedimentary Basin: A Sequence Stratigraphic Framework: Tulsa, Society for Sedimentary Geology, p. 25-39.

Witzke, B.J., Heckel, P.H., 1988, Paleoclimatic indicators and inferred Devonian paleolattitudes of Euramerica, *in* McMillan, N.J., Embry, A.F., Glass, D.J., eds., Devonian of the World; Proceedings of the Second International symposium on the Devonian System – Memoir 14: Calgary, Canadian Society of Petroleum Geologists, v. 1, p. 49-63.

WONFOR, J.S., ANDRICHUK, J. M., 1953, Upper Devonian in the Stettler Area, Alberta, Canada: Bulletin of Canadian Petroleum Geology, v. 1, p. 3-6.

WORKMAN, L.E., 1954, Clastic content of the Winterburn northwest of Edmonton: Bulletin of Canadian Petroleum Geology, v. 2, p. 8-9.

WRIGHT, V.P., 1992, Paleosol recognition: a guide to early diagenesis in terrestrial settings, *in* Wolf, K.H., Chilingarian, G.V., eds., Diagenesis III - Developments in Sedimentology: Devonian Sedimentology: Amsterdam, Elsevier Science, p. 591-619.

WRIGHT, G.N., MCMECHAN, M.E., POTTER, D.E.G., 1994, Structure and architecture of the Western Canada Sedimentary Basin, *in* Mossop, G.D., Shetsen, I., eds., Geological Atlas of the Western Canada Sedimentary Basin: Calgary, Canadian Society of Petroleum Geologists and Alberta Research Council, p. 25-40.

ZIEGLER, P.A., 1988, Laurussia - the Old Red Continent, *in* McMillan, N.J., Embry, A.F., Glass, D.J., eds., Devonian of the World; Proceedings of the Second International symposium on the Devonian System – Memoir 14: Calgary, Canadian Society of Petroleum Geologists, v. 1, p. 15-48.

Appendix:

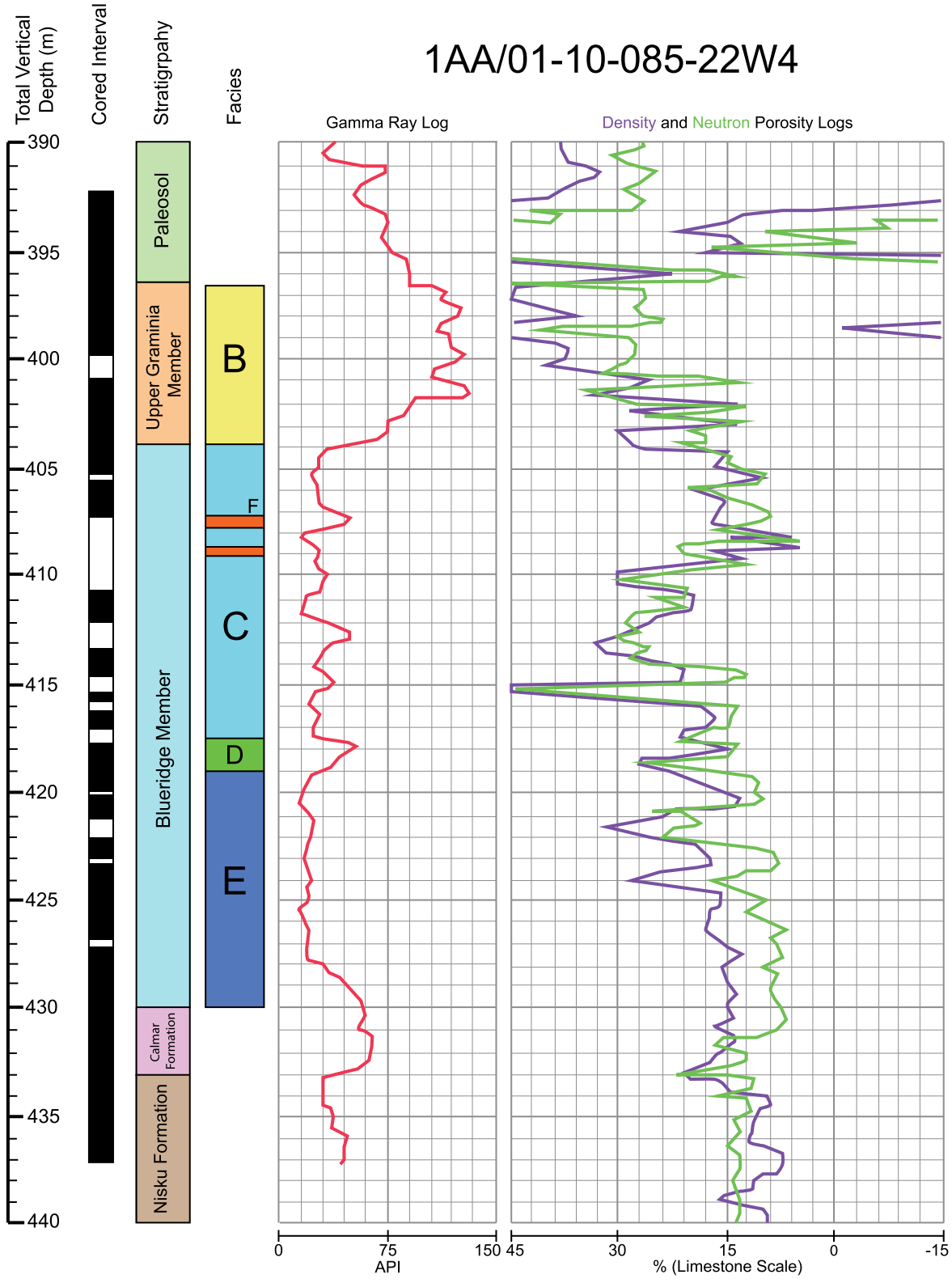

Appendix Figure 1: Well logs, cored intervals, stratigraphy and facies of 1AA/01-10-085-22W4.

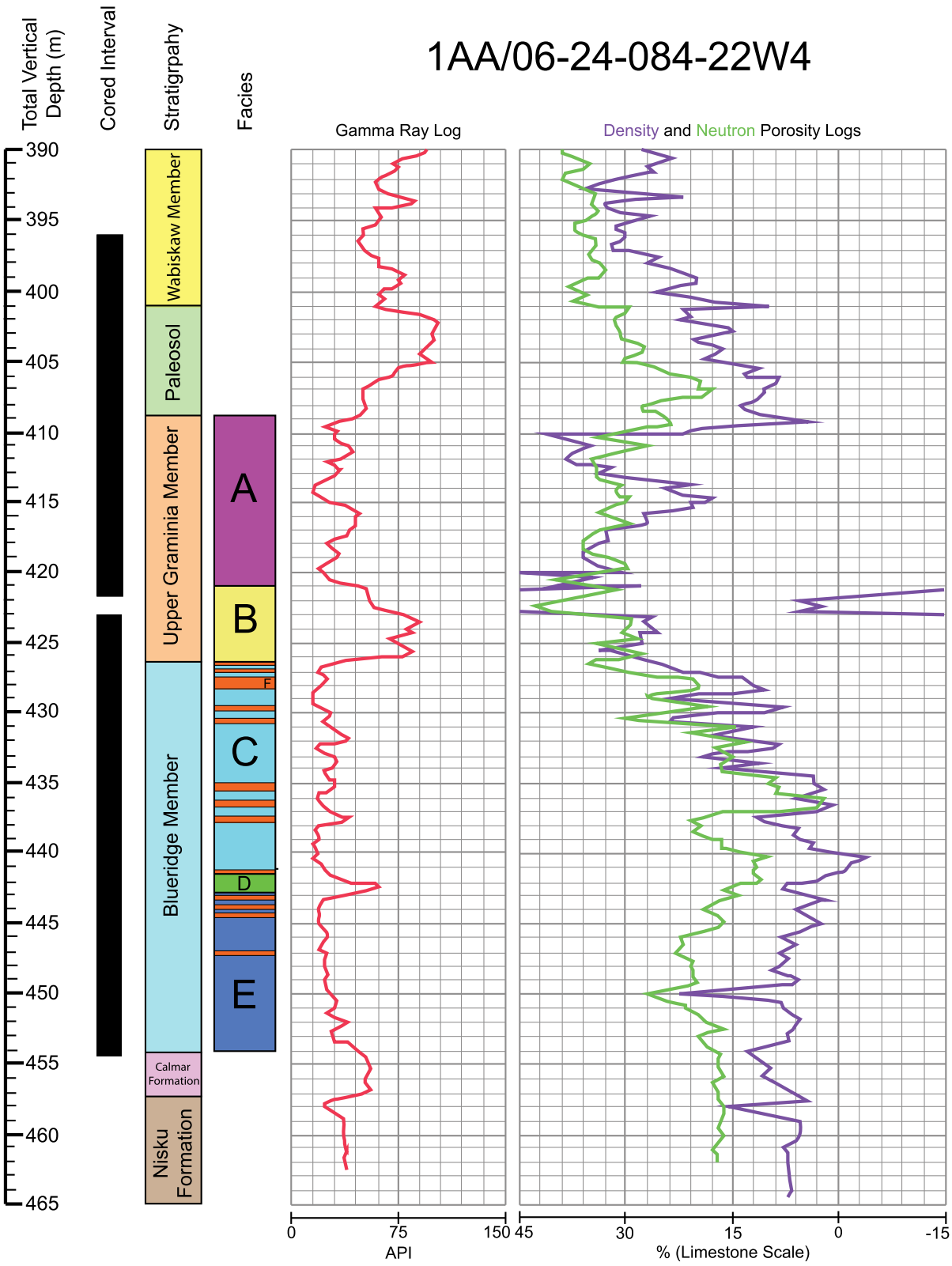

Appendix Figure 2: Well logs, cored intervals, stratigraphy and facies of 1AA/06-24-084-22W4.

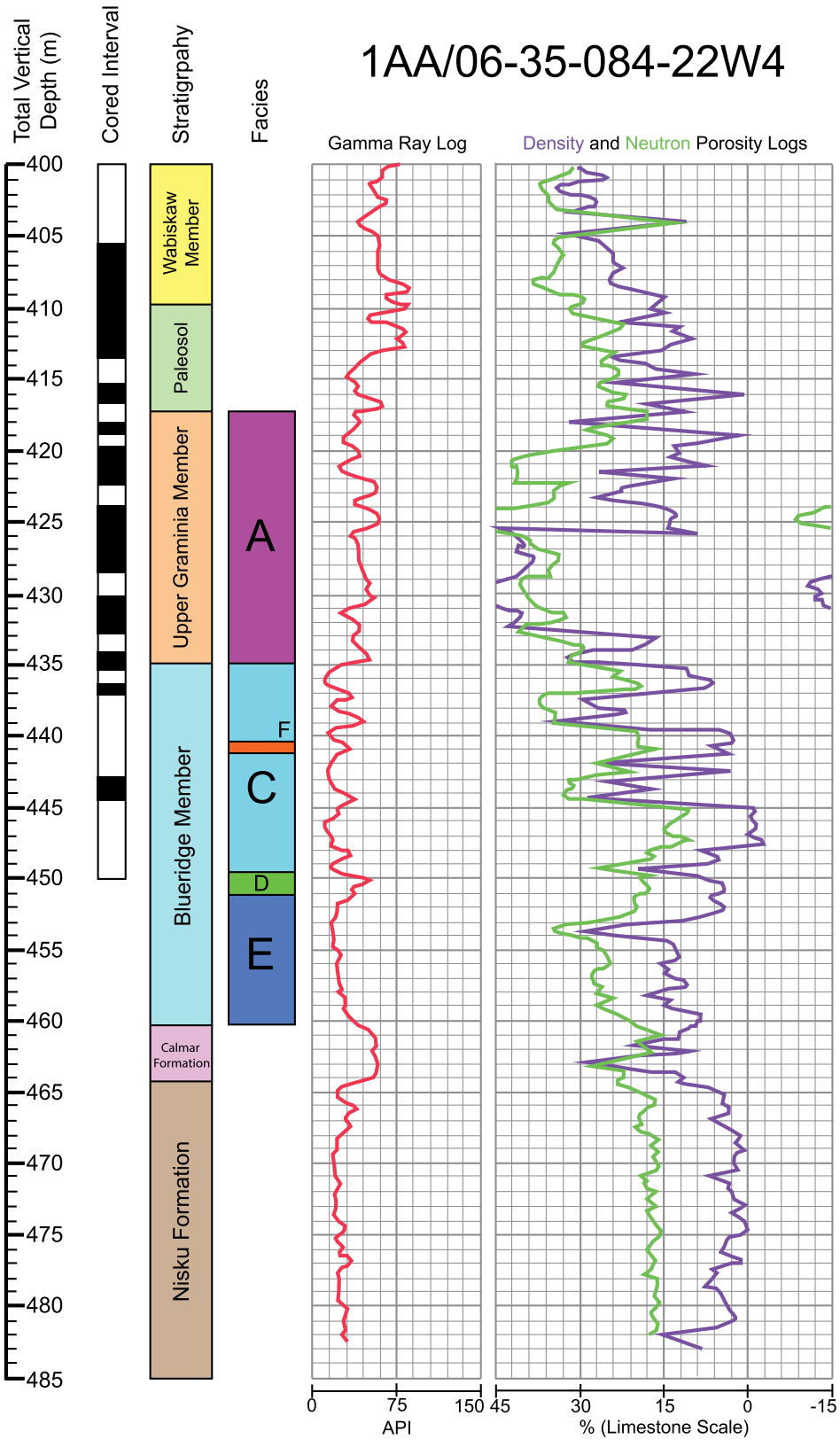

Appendix Figure 3: Well logs, cored intervals, stratigraphy and facies of 1AA/06-35-084-22W4.

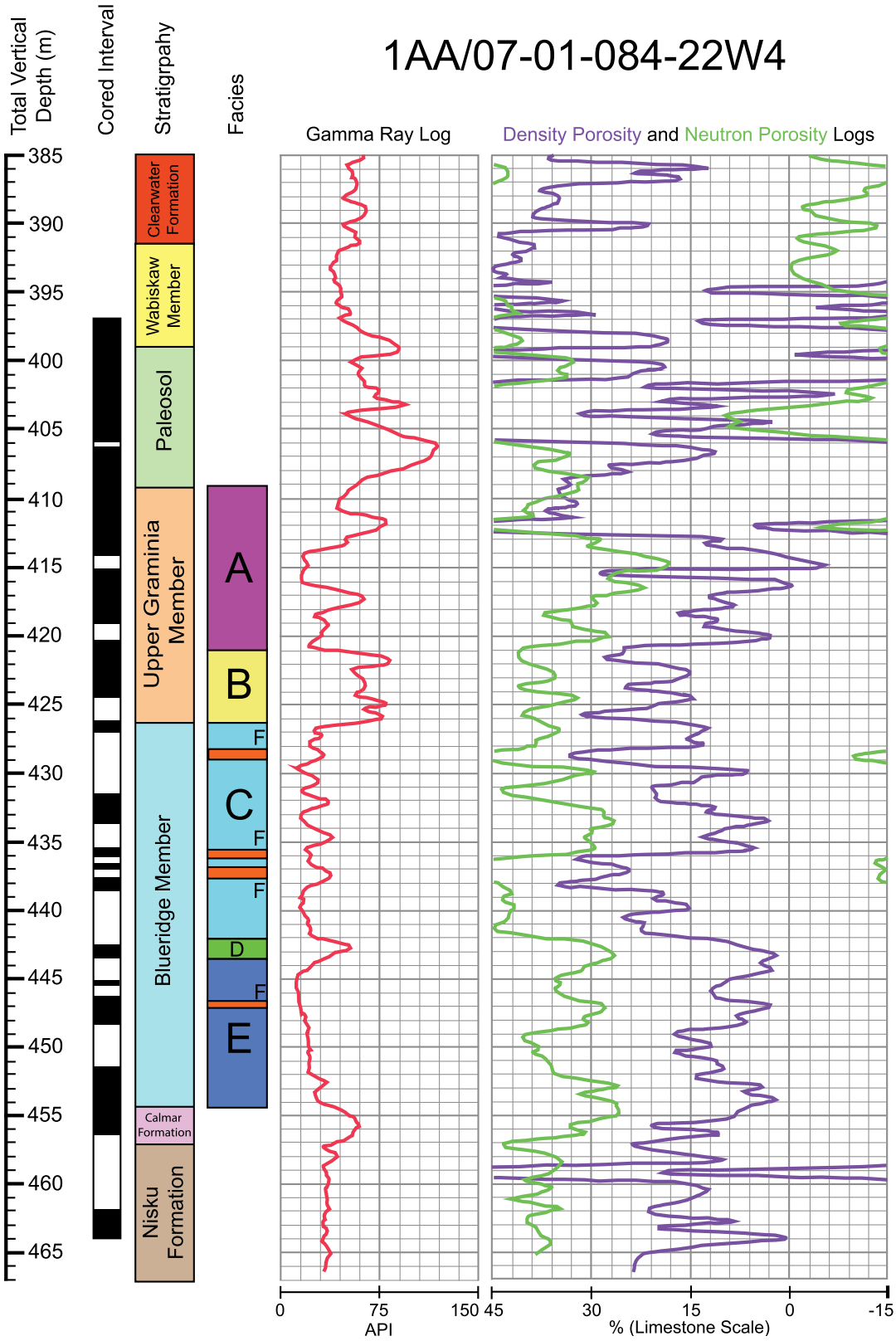

Appendix Figure 4: Well logs, cored intervals, stratigraphy and facies of 1AA/07-01-084-22W4.

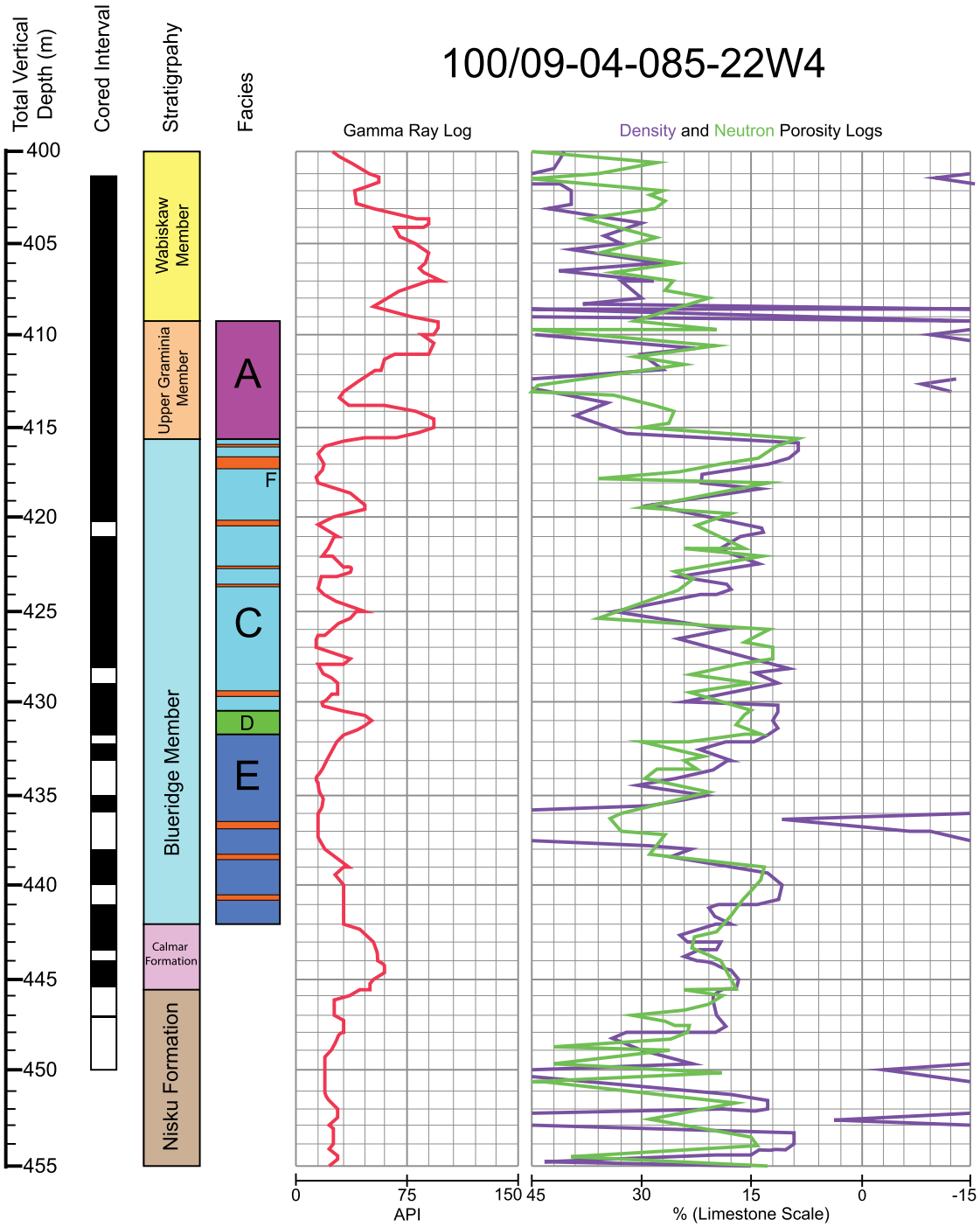

Appendix Figure 5: Well logs, cored intervals, stratigraphy and facies of 100/09-04-085-22W4.

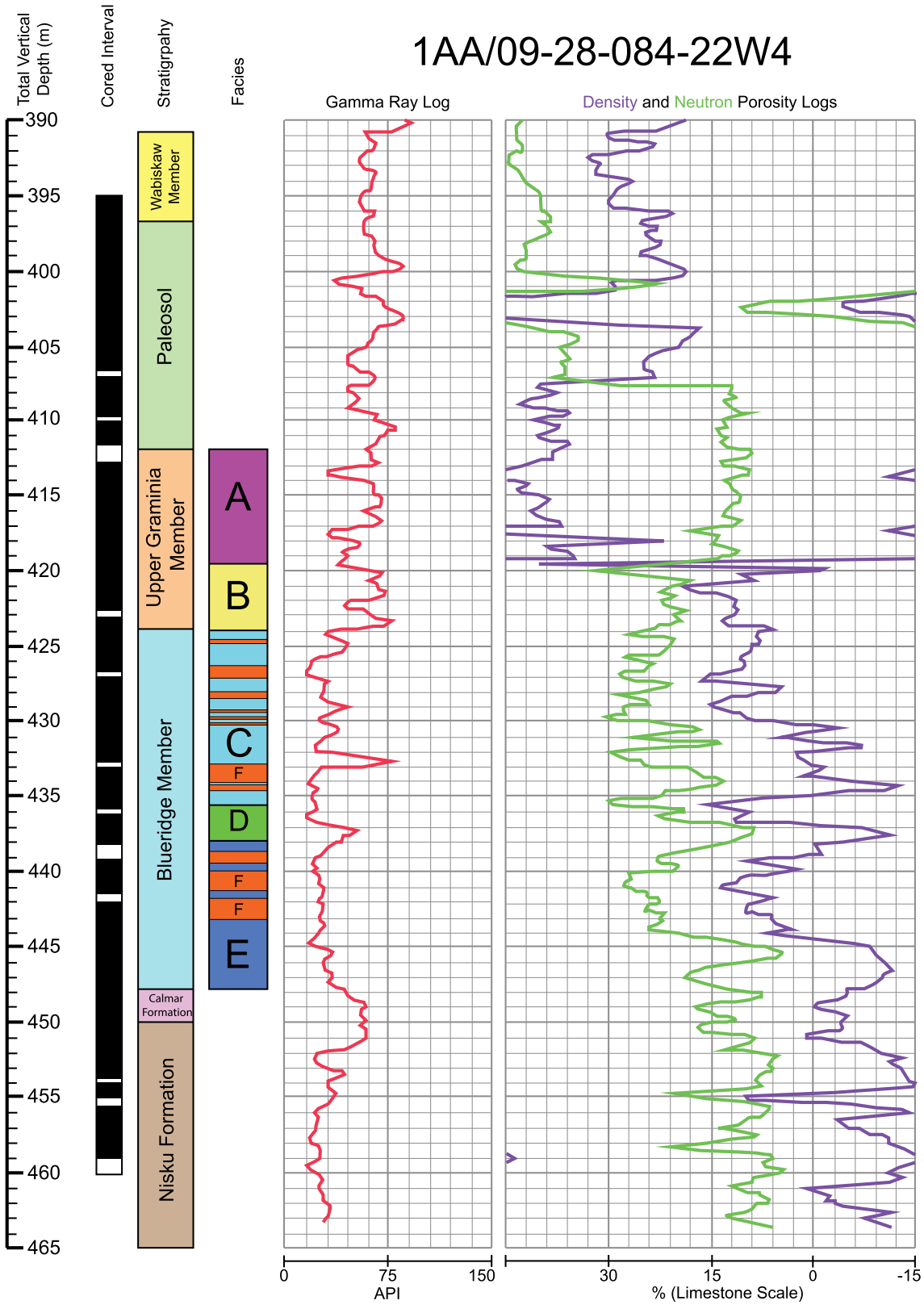

Appendix Figure 6: Well logs, cored intervals, stratigraphy and facies of 1AA/09-28-084-22W4.

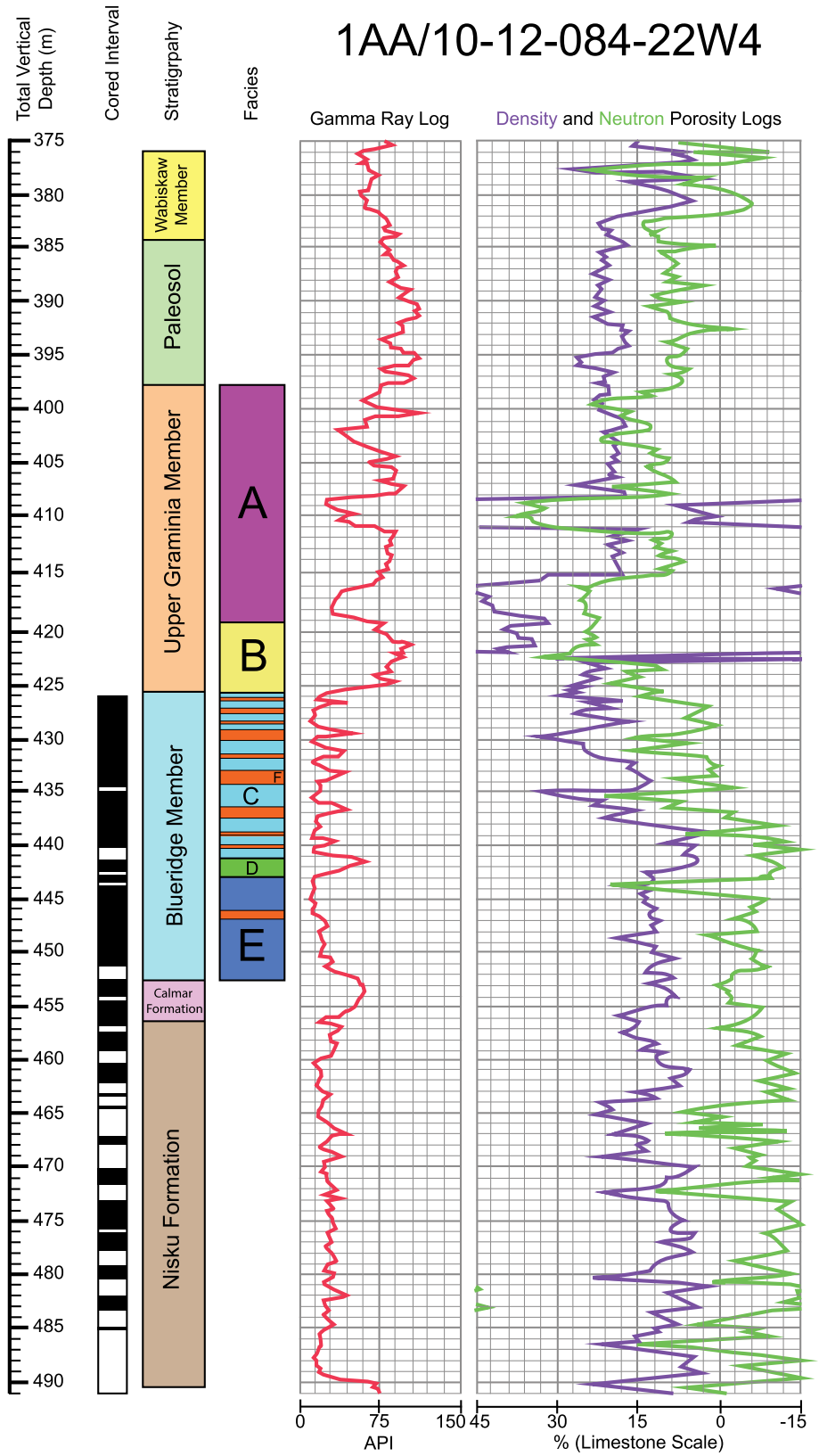

Appendix Figure 7: Well logs, cored intervals, stratigraphy and facies of 1AA/10-12-084-22W4.

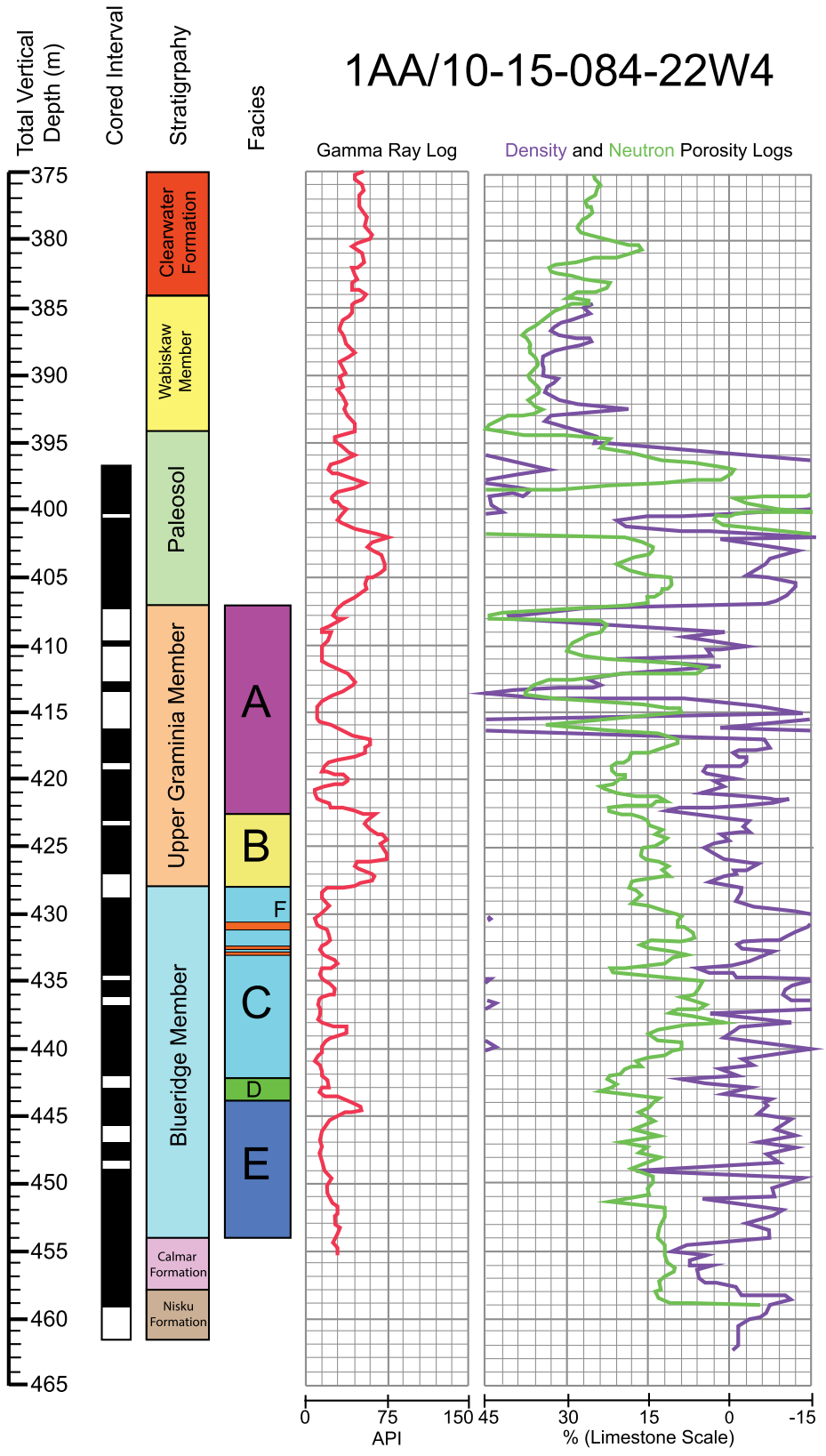

Appendix Figure 8: Well logs, cored intervals, stratigraphy and facies of 1AA/10-15-084-22W4.

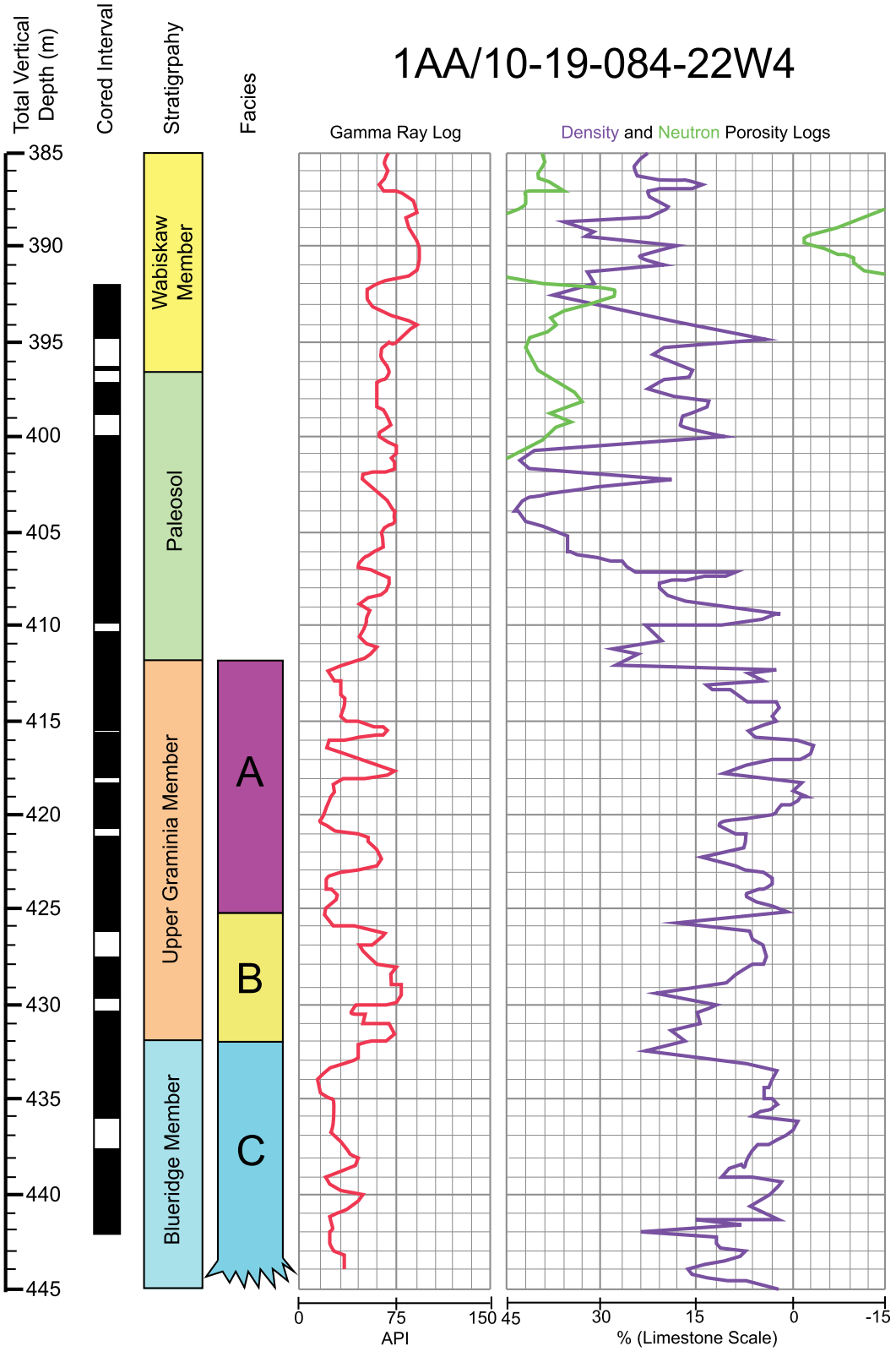

Appendix Figure 9: Well logs, cored intervals, stratigraphy and facies of 1AA/10-19-084-22W4.

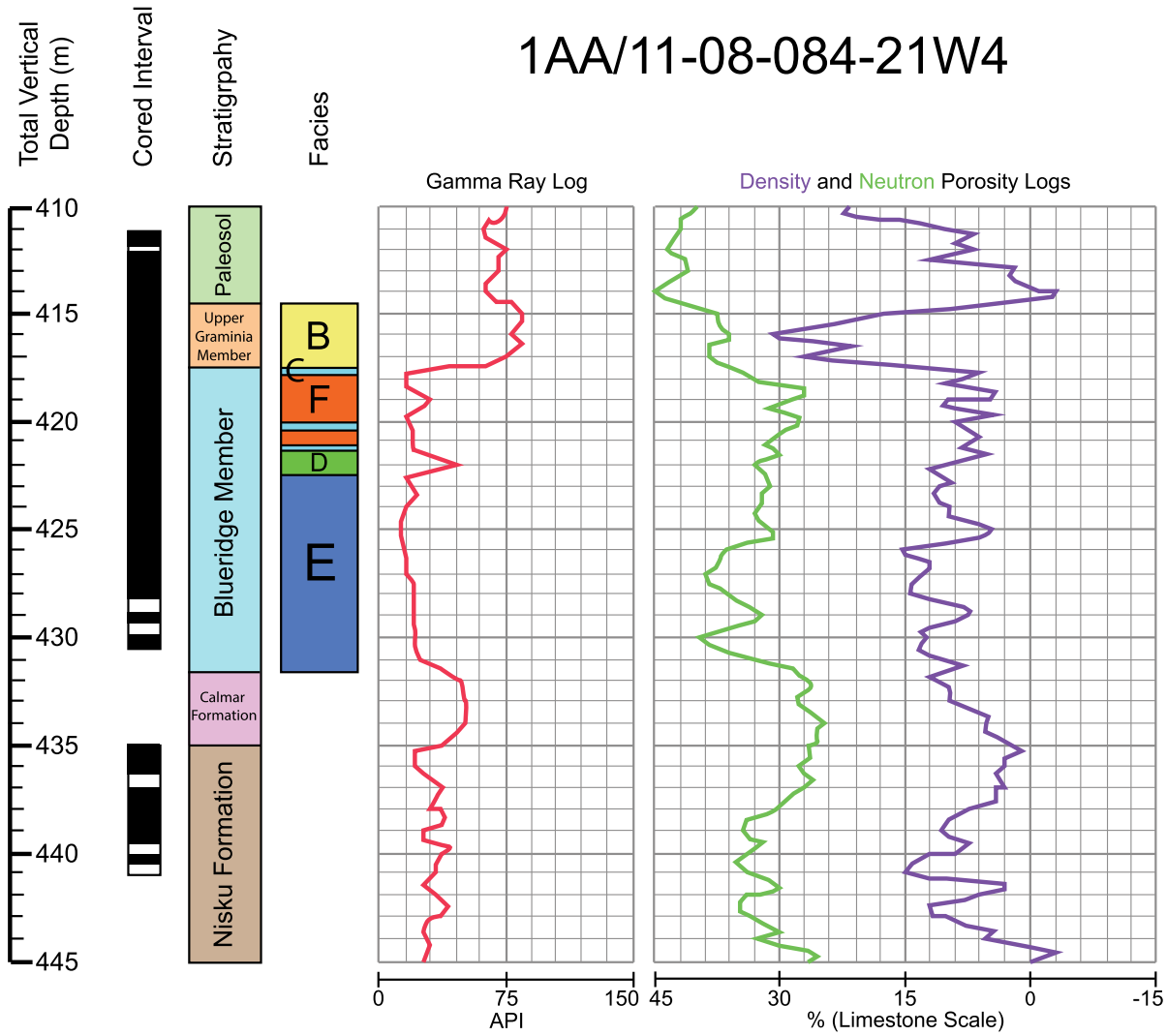

Appendix Figure 10: Well logs, cored intervals, stratigraphy and facies of 1AA/11-08-084-21W4.

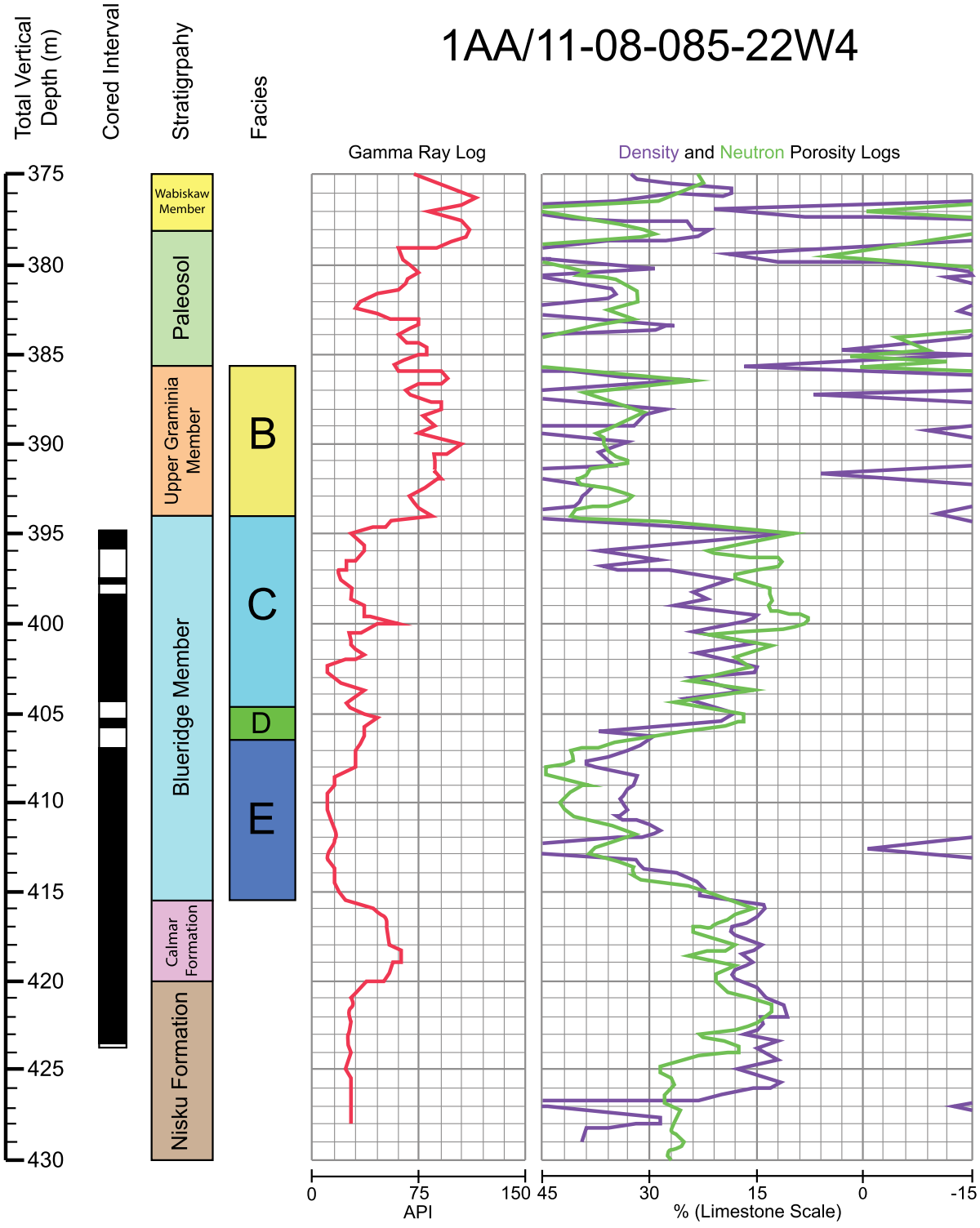

Appendix Figure 11: Well logs, cored intervals, stratigraphy and facies of 1AA/11-08-085-22W4.

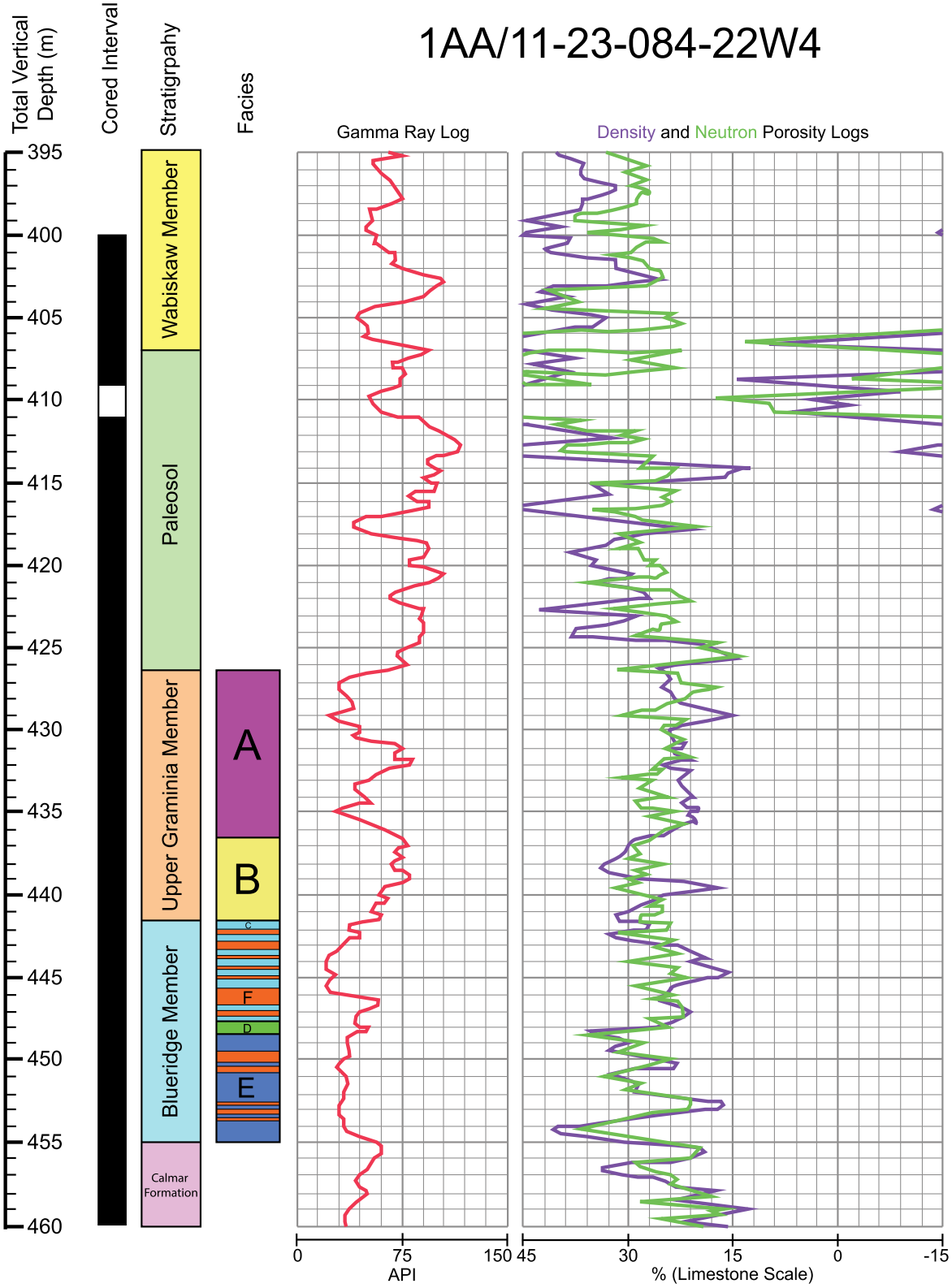

Appendix Figure 12: Well logs, cored intervals, stratigraphy and facies of 1AA/11-23-084-22W4.

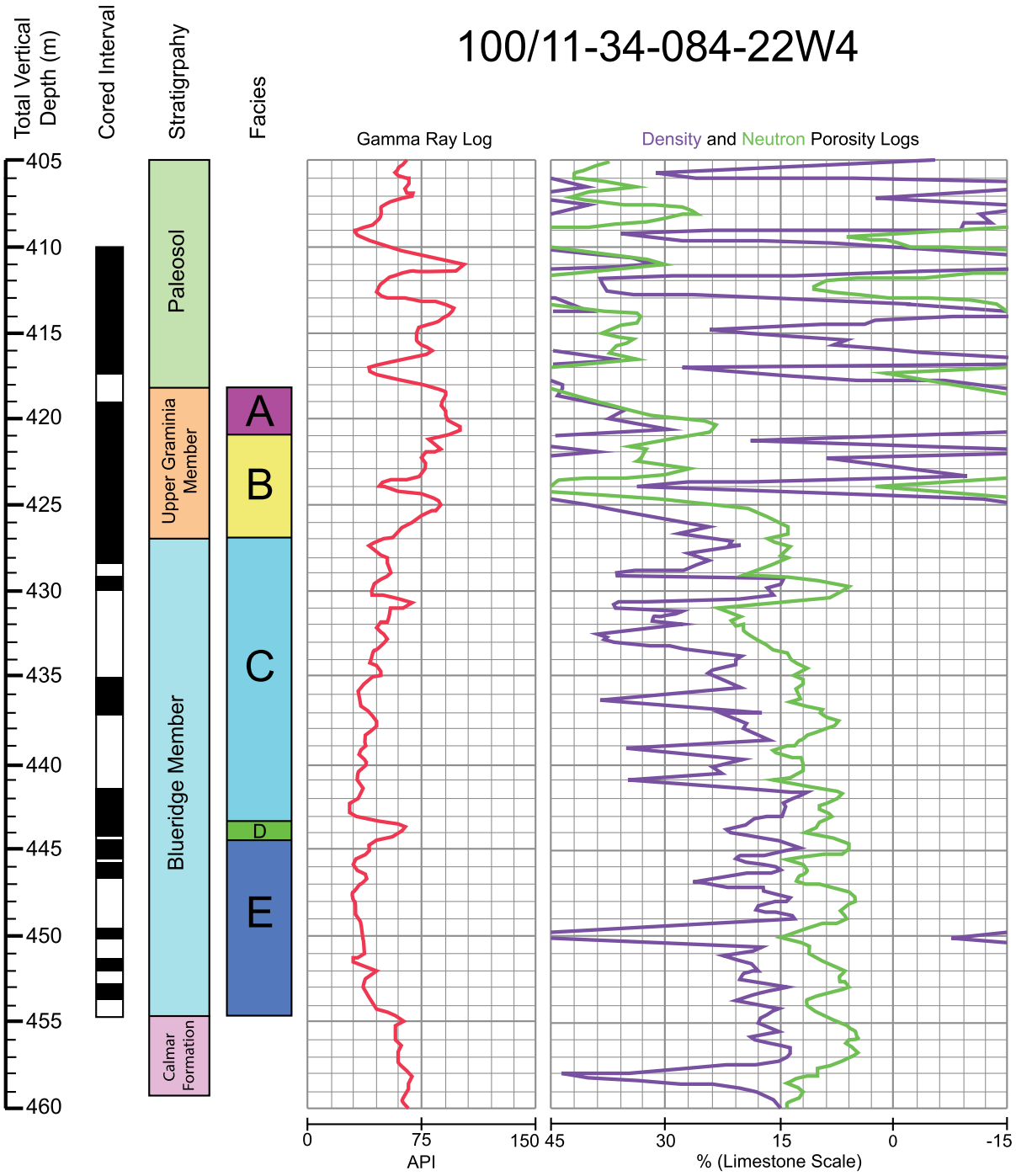

Appendix Figure 13: Well logs, cored intervals, stratigraphy and facies of 100/11-34-084-22W4.

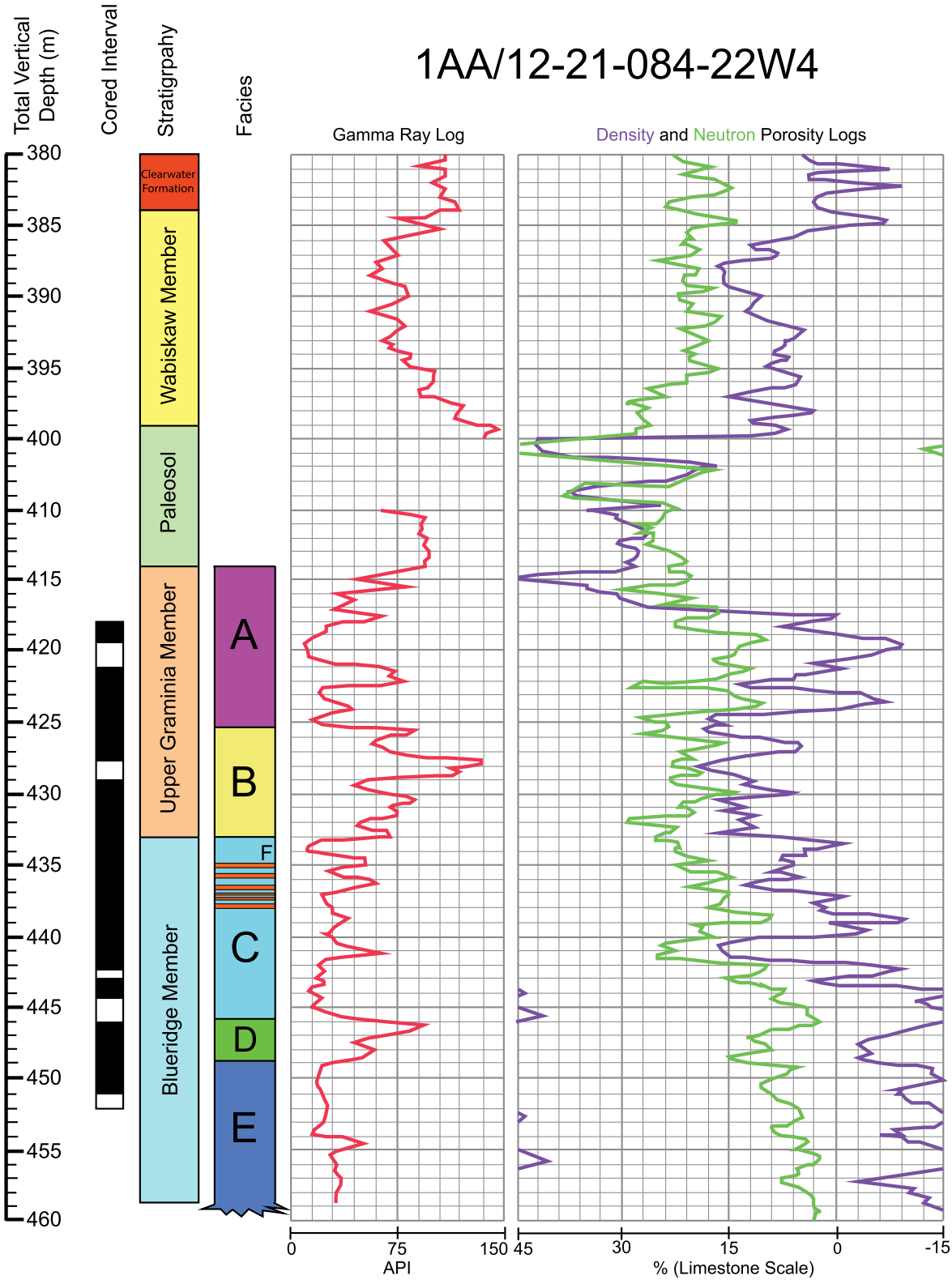

Appendix Figure 14: Well logs, cored intervals, stratigraphy and facies of 1AA/12-21-084-22W4.

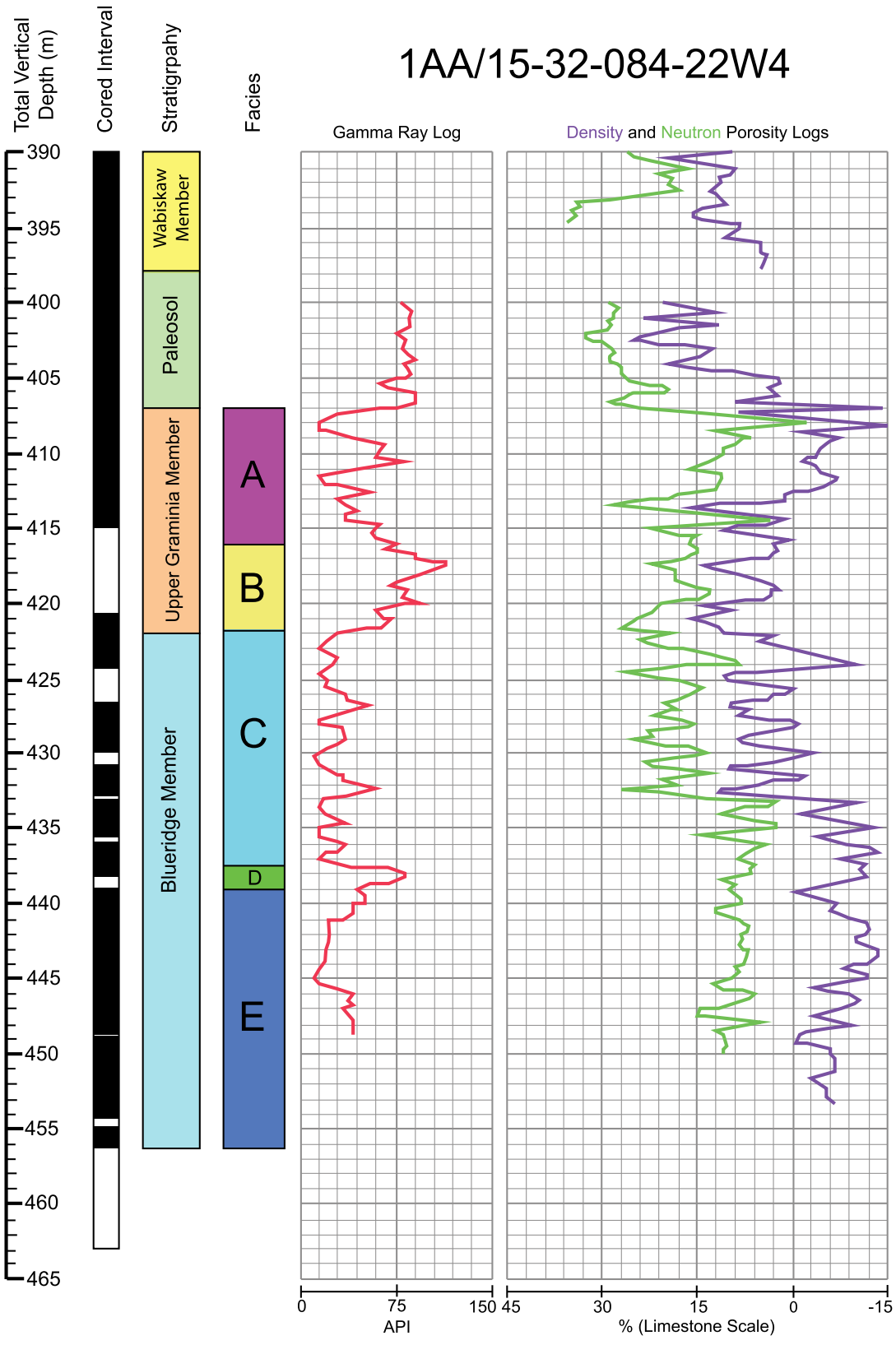

Appendix Figure 15: Well logs, cored intervals, stratigraphy and facies of 1AA/15-32-084-22W4.